Doctoral Dissertation

Fouling mitigation in membrane bioreactors by nanobubble-assisted backwashing

ナノバブルを用いた逆洗による膜分離活性汚泥法のファウリング抑制

HELMANO DAVID GALVÃO FERNANDES

Division of Environmental Engineering
Graduate School of Engineering
Hokkaido University

Fouling mitigation in membrane bioreactors by nanobubble-assisted backwashing

Advisor: Professor Katsuki Kimura

By

Helmano David Galvão Fernandes

Division of Environmental Engineering
Graduate School of Engineering
Hokkaido University

ACKNOWLEDGEMENTS

This research could not have been done without the help, support, and assistance I received from several people. I want to thank them and dedicate this dissertation to them.

To the Japanese Government, represented by the Ministry of Education, Culture, Sports, Science and Technology (MEXT), and the Cape Verdean Government. For the opportunity to study in Japan under a Scholarship.

To my supervisor, Dr. Katsuki Kimura, for the opportunity to research under him, believing in me, and always encouraging me to continue and work harder.

To Prof. Dr. Satoshi Okabe and Hisashi Satoh, for being part of the evaluation process and all the insights and advice given.

To Prof. Dr. Akira Hafuka and Takayuki Kakuda, for all the insights and advice given.

To Mr. Kudo, Matsuo and Uesugi for all the technical support that I received from him.

To Ms. Kikuchi, Goto and Tsuru who gave us administrative support.

To all my lab-mates for providing a healthy, delightful, and professional environment.

To the e3 staff and community for working hard for us and making our stay more enjoyable.

To my wife, Débora for all the support.

To all my relatives, friends, and family who believed, supported, and encouraged me.

ABSTRACT

Membrane bioreactors (MBRs) are a relatively new wastewater treatment technology that applies efficient solid-liquid separation via membrane filtration, integrated with a biological process. Since their first introduction in a 1989 paper by Japanese and Thai engineers, the use of submerged membrane bioreactors (SMBRs) has been increasing. MBR technology has significant advantages over conventional activated sludge (CAS) processes including higher quality effluent, smaller footprint, complete removal of bacteria, and ease of operation. Nevertheless, the widespread application of MBRs still faces a major obstacle: membrane fouling. The accumulation of foulants on the membrane surface and inside its pores requires periodic cleaning, which increases operational and maintenance costs and reduces the membrane's lifetime and initial permeability. Several measures have been presented to mitigate membrane fouling, including intensive aeration, granular material scouring, antifouling membranes, optimization of operating conditions, coagulation, and diverse cleaning protocols. The application of ceramic membranes is also increasing. Ceramic membranes are compact, can withstand heat and high pressures, have a long life, and are resistant to chemical/physical damage. It has been shown that granular scouring is effective in controlling membrane fouling. Intensive physical cleaning with granular materials was possible due to the high resistance of ceramic membranes. An increasingly prevalent measure for the mitigation of membrane fouling in MBRs by enhancing the efficiency of membrane cleaning is chemically enhanced backwashing (CEB). The combination of mechanical scouring using granular material and CEB with sodium hypochlorite (NaClO) has been demonstrated to efficiently control fouling in MBRs. Although these countermeasures are effective to some extent, it was observed that a dense gel layer was still formed on the surface of membranes used in MBRs even with such intensive cleaning. In addition, the environmental impact of the use of chemicals is a concern. Therefore, further improvements in cleaning efficiency are still necessary to promote the widespread installation of MBRs and bring impactful changes to wastewater treatment systems. On the other hand, Nanobubbles (NBs), also

called ultrafine bubbles (UFB), are environmentally friendly and have been shown to possess cleaning properties. Therefore, a novel approach to mitigate fouling in MBRs, nanobubble-assisted backwashing (NBB), is presented in this study. NBs generated in this study had an average diameter of about 150 nm, and some of the nanobubbles could pass through microfiltration (MF) membranes used for MBRs. Therefore, nanobubbles introduced from the permeate side during backwashing might exhibit cleaning effects for membranes since applications of nanobubbles for cleaning various materials such as protein-coated gold electrodes and stainless steel have been reported. The effectiveness of NBB was compared with that of tap water backwashing (TWB) and CEB using 50 ppm NaClO. Experiments were carried out by using three bench-scale MBRs installed at a local wastewater treatment plant. The three MBRs were operated in parallel with identical operating conditions except for backwashing conditions. Polyethylene glycol (PEG) granular materials were inserted in each membrane tank to scour the membrane surface. Regardless of the variation of the feed, NBB always exhibited better cleaning performance than TWB, and the cleaning efficiency of NBB was sometimes comparable to that of CEB. The degree of reversible fouling observed with TWB was 424 % higher than that with NBB, indicating that NBB is much more effective than TWB for the control of reversible fouling. It was also found that NBB could mitigate irreversible fouling even in the absence of a thick protective layer on the surface of the membrane. It was attempted to reveal the mechanism by which NBB enhances the cleaning effect by carrying out a comprehensive analysis of the distribution of filtration resistance, mixed liquor suspension, and the fouling layer. Significant changes in the microbial activity of the mixed liquor suspension and sludge properties in the MBRs were not observed when NBB was carried out. The results of the analysis suggested that NBB made the structure of the fouling layer more porous, possibly facilitating the removal of the fouling layer from the membrane. The use of high-concentration nanobubble (HC-NB) water can be beneficial for the cleaning efficiency of NBB. However, further studies are needed to elucidate the optimal concentration of NBs. Further improvements in the cleaning efficiency of NBB can be achieved. It was attempted to improve the cleaning efficiency of NBB by adding a small amount of NaClO to NB water used for backwashing. The cleaning efficiency of NBB was improved by the synergetic effect of NaClO and NBs working in different ways when they were co-present in the

backwash solution. It was suggested that NBs made the structures of the fouling layer looser and more porous, whereas NaClO chemically degraded the components of the fouling layer. The importance of pH (4, 8.5, and 12) in NBB combined with NaClO was shown in this study. The cleaning efficiency was found to be high at pH 4, followed by 8.5 and 12. This difference was mainly attributed to differences in the sizes of NBs under different pH. Thus, the synergetic effects of NBB combined with NaClO were mostly enhanced under acidic conditions. An assessment of the costs of backwashing showed that, except for tap water, the NB water is the cheapest among all the backwashing solutions used in this study, while HC-NB water is the most expensive. Although the mixture of NBs and NaClO is more expensive than each solution separately, the synergy of NBs and NaClO at acidic conditions (pH 4) is so positive that it becomes significantly more cost-effective, due to considerable improvements in the degree of fouling mitigation. The synergy of NBs and other chemicals can be further investigated in future studies. The application of NBB has still been rarely investigated and this study showed for the first time that NBs can be used for fouling mitigation in MBRs. In addition, the efficiency of NBB could be further improved by mixing NB with chemical reagents. This can lead to a new method for alleviating membrane fouling in MBRs.

Keywords: MBRs, fouling, Nanobubble backwashing, CEB, Synergy, ceramic membranes.

LIST OF PUBLICATIONS

Peer-reviewed journal articles

- **H. Fernandes**, S. Kiuchi, T. Kakuda, A. Hafuka, T. Tsuchiya, Y. Matsui, K. Kimura, Synergistic effects of nanobubbles and chemicals on backwashing for submerged MBRs treating municipal wastewater, Journal of Water Process Engineering 63 (2024) 105541. https://doi.org/10.1016/j.jwpe.2024.105541.
- **H. Fernandes**, S. Kiuchi, T. Kakuda, A. Hafuka, T. Tsuchiya, Y. Matsui, K. Kimura, Fouling mitigation in membrane bioreactors by nanobubble-assisted backwashing, Journal of Water Process Engineering 53 (2023) 103860. https://doi.org/10.1016/J.JWPE.2023.103860.

Peer-reviewed conference articles

- **Fernandes, H**., Hafuka, A., Tsuchiya, T., Kimura, K. “Synergistic effects of nanobubbles and chemicals on backwashing for submerged MBRs treating municipal wastewater” 13th International Congress on Membranes and Membrane Process, Chiba, July 2023.

Conferences articles

- **Fernandes, H**., Kiuchi, S., Hafuka, A., Tsuchiya, T., Kimura, K. "Fouling mitigation in submerged MBRs by the synergistic effect of nanobubbles and chemicals" The 60th Annual Technical Conference on Sewerage, Sapporo, August 2023.
- **Fernandes, H**., Kiuchi, S., Hafuka, A., Kimura, K. “Application of Nanobubble Backwashing for Membrane Fouling Mitigation in Submerged MBRs” 55th Annual Conference of Japan Society on Water Environment, on-line, March 2021.

Additional publications

- Nakagawa, H., **Fernandes, H**., Hafuka, A., Tsuchiya, T., Kimura, K. " Effective backwashing of MBRs by a combination of nanobubbles and surfactants" The 61st Annual Technical Conference on Sewerage, Tokyo, August 2024.

- NAKAGAWA, H., KIUCHI, S., **FERNANDES, H**., HAFUKA, A., & KIMURA, K. (2022). OPTIMIZATION OF NANOBUBBLE ASSISTED BACKWASHING OF MEMBRANES. Journal of Japan Society of Civil Engineers, Ser. G (Environmental Research), 78(7), III_143-III_148. https://doi.org/10.2208/jscejer.78.7_III_143.
- KIUCHI, S., **FERNANDES, H**., HAFUKA, A., & KIMURA, K. (2020). CLEANING OF FOULED MEMBRANES USED FOR MBRS BY USING MICROBUBLLES AND NANOBULLES. Journal of Japan Society of Civil Engineers, Ser. G (Environmental Research), 76(7), III_149-III_155. https://doi.org/10.2208/jscejer.76.7_iii_149.

TABLE OF CONTENTS

LIST OF TABLES

LIST OF FIGURES

LIST OF ABBREVIATIONS

AFM	Atomic force microscopy
APF	Aminophenyl fluorescein
BSA	Bovine serum albumin
CAS	Conventional activated sludge
CB	Coarse bubble
CEB	Chemically enhanced backwashing
CIP	Cleaning in place
CP	Concentration polarization
COD	Chemical Oxygen Demand
CST	Capillary suction time
DO	Dissolved oxygen
DOC	Dissolved organic carbon
DOM	Dissolved organic matter
EEM	Excitation emission matrix
EPS	Extracellular polymeric substance
FO	Forward osmosis
FT-IR	Fourier-transform infra-red
HA	Humic acid
HC-NBW	High concentration nanobubble water
HRT	Hydraulic retention time
HS	Humic substances
JPY	Japanese yen

LC-OCD	Liquid chromatography organic carbon detector
LMH	Liter per hour per square meter
MBR	Membrane bioreactor
MD	Membrane distillation
MF	Microfiltration
MLSS	Mixed liquor suspended solids
MLVSS	Mixed liquor volatile suspended solids
MNB	Micro-nanobubbles
NB	Nanobubble
NBB	Nanobubble-assisted Backwashing
NBW	Nanobubble water
NTA	Nanoparticle tracking analysis
OECD	Organization for Economic Co-operation and Development
ONB	Ozone nanobubble
ORP	Oxidation reduction potential
OUR	Oxygen uptake rate
PEG	Polyethylene glycol
PTFE	Polytetrafluoroethylene
PVDF	Polyvinylidene fluoride
RO	Reverse osmosis
ROS	Reactive oxygen species
SDG	Sustainable Development Goal
SDS	Sodium dodecyl sulfate
SEM	Scanning electron microscopy
SMBR	Submerged membrane bioreactor

SMP	Soluble microbial products
SOUR	Specific oxygen uptake rate
SRT	Solids retention time
TMP	Transmembrane pressure
TP	Disodium terephthalate
TPOH	2-hydroxyterephthalate
TOC	Total organic carbon
TW	Tap-water
TWB	Tap-water backwashing
UFB	Ultrafine bubbles
UV	Ultra-violet
WWTP	Wastewater treatment plant

CHAPTER 1: INTRODUCTION

The current state of worldwide water availability is not desirable. Cheap, environmentally friendly, and high-quality water-producing technologies are needed. Membrane bioreactors (MBRs) are a relatively new wastewater treatment technology integrating solid-liquid separation by membrane filtration and biological treatment. Since their first introduction in a 1989 paper by Japanese and Thai engineers, the use of submerged membrane bioreactors (SMBRs) has been increasing [1]. MBR technology has significant advantages over conventional activated sludge (CAS) processes including complete removal of bacteria and ease of operation. In the CAS system, solid-liquid separation is carried out by gravity sedimentation, whereas MBRs apply membrane filtration for solid-liquid separation, leading to the production of stable and high-quality effluent water [2]. The application of membrane filtration also enables a high biomass concentration in MBRs, significantly reducing their footprint and creating favorable conditions for the thriving of slow-growth-rate bacteria [3]. These bacteria might play a key role in the removal of persistent components. In addition, higher biomass concentrations lead to a reduction in sludge production. A significant drawback of the CAS system is sludge bulking; however, MBRs circumvent this issue by eliminating the need for sludge gravity sedimentation. Furthermore, MBRs are highly adaptable to compact satellite systems or upgrading existing wastewater treatment plants [4]. Nevertheless, the widespread application of MBRs still faces a major obstacle: membrane fouling. The accumulation of foulants on the membrane surface and inside its pores requires periodic cleaning, which increases operational and maintenance costs

and reduces membrane's lifetime and initial permeability [5,6]. Solving the issue of membrane fouling would ease the widespread application of MBRs and significantly contribute to the great problem of water scarcity. There are two approaches to combat the issue of membrane fouling in MBRs: improving the filterability of sludge and enhancing the efficiency of membrane cleaning. As for the former approach, sludge granulation [7] and detailed characterization of sludge [8] have been investigated recently. In this dissertation, the latter approach was focused on. When it comes to enhancing the efficiency of membrane cleaning, several measures have been presented, including intensive aeration, granular material scouring, antifouling membranes, optimization of operating conditions, coagulation, and diverse cleaning protocols [9–12]. The application of ceramic membranes is also increasing. Ceramic membranes are compact, can withstand heat and high pressures, have a long life and are resistant to chemical/physical damage. Therefore, ceramic membranes can be used with intensive cleaning without collapsing [13,14]. Kimura et al. showed that granular scouring was effective for controlling membrane fouling [15]. Intensive physical cleaning with granular materials was possible due to the high resistance of ceramic membranes. An increasingly prevalent measure for the mitigation of membrane fouling in MBRs by enhancing the efficiency of membrane cleaning is chemically enhanced backwashing (CEB) [16]. In previous studies, we demonstrated that a combination of mechanical scouring using granular material and CEB with sodium hypochlorite (NaClO) could efficiently control fouling in MBRs [14,15]. Although these countermeasures are effective to some extent, it was observed that a dense gel layer was still formed on the surface of membranes used in MBRs even with such intensive cleaning [14]. Therefore, further improvements in cleaning efficiency are still necessary to promote the widespread installation of MBRs and bring impactful changes to wastewater treatment systems.

Nanobubbles (NBs), also called ultrafine bubbles, are defined as fine bubbles with a volume equivalent diameter smaller than 1 μm [17]. NBs have unique characteristics including high stability/durability, large surface area per unit volume, and a negative surface charge [18,19]. Recently, the use of NBs for various cleaning applications has

been investigated and their cleaning efficiencies have been reported. The mechanisms for their high cleaning efficiencies are still being investigated. Also, applications of NBs for cleaning membranes used for water and wastewater treatment have recently been investigated. Ghadimkhani et al. investigated the cleaning of flat-sheet ceramic membranes that were completely clogged with humic acid (HA) by air NBs [20]. In their study, membrane cleaning was performed by flushing the surface of the fouled membranes with water containing NBs. After continuously flushing for 6 h, the permeate flux was almost completely recovered. They suggested that the cleaning effect was attributed to reactive oxygen species (ROS) generated during the collapse of NBs. Dayarathne et al. applied micro-nano bubbles (MNB) (size range of 150 nm to 250 nm) for cleaning reverse osmosis (RO) membranes. MNBs were added to saline water (NaCl: 35 g/L) and were circulated in the feed water channel to clean the surfaces of fouled RO membranes. They observed that MNBs could completely restore the water permeability of the membranes by disrupting the concentration polarization layer formed on the membrane surface [21]. The same research group conducted another study using MNBs for chemical-free scale inhibition and compared them with commercially available antiscalants. They concluded that introducing MNBs in the feed solutions of RO systems was more effective for maintaining permeability than using commercially available antiscalants. The mechanism of the high anti-scaling effect of MNBs was explained by their stimulation of a turbulent flow and their physicochemical properties including adsorption capacity and negative zeta potential [22]. Farid et al. used water containing NBs to clean membranes used in a forward osmosis (FO) system treating aquaculture wastewater [23]. Adding NBs into the feed water reduced the accumulation of foulants on the membrane surface. They hypothesized that reactive radicals and shock/pressure waves were produced when introduced NBs collapsed, and subsequentially hydrodynamic flow conditions in the feed stream could be improved. In a later study, they investigated the effects of introducing NBs into the feed of membrane distillation (MD) systems treating high-salinity brine [24]. Severe membrane scaling occurred on the surface of the membrane tested without NBs, while little salt deposition was observed on the surface of the membrane in the presence of NBs. They attributed it to

two mechanisms: high surface shear forces caused by flow turbulence generated by NBs and adsorption of ions onto the NB surface by the negative zeta potential of NBs.

The results of those studies in which NBs were used for cleaning membranes and the difficulties in cleaning them, as mentioned before, motivated the use NBs for cleaning membranes used in MBRs. To the best of our knowledge, the application of NBs for fouling mitigation in MBRs has not been reported in the literature. In addition, the lack of studies on the use of NBs for membrane backwashing brings novelty to our study. As it was already verified that NBs could pass through the pores of microfiltration (MF) membranes [25], it was thought that backwashing using water-containing NBs (nanobubble backwashing (NBB)) could effectively clean MF membranes used for MBRs. Therefore, in this study, the effectiveness of NBB was compared with that of tap water backwashing (TWB) and CEB with NaClO on the basis of multiple experiments in which three bench-scale MBRs installed at a local wastewater treatment plant were operated in parallel with different backwashing solutions.

Our study also encompassed the enhancement of NBB by the tentative synergy between NBs and sodium hypochlorite (NaClO), a well-known oxidizing agent. We attempted the combination of NBB and CEB: a small amount of NaClO was added to NB water and this mixture was used for backwashing to control fouling in MBRs.

1.1 Objective and outline

1.1.1 Problem

As stated before, the current prospect of water availability is not desirable. Wastewater treatment technologies such as MBRs should be widely encouraged and applied to aid the mitigation of water scarcity. However, membrane fouling needs to be addressed before MBRs can be established as the major water reclamation technology. Besides, chemical cleaning, which is widely applied in fouling mitigation, has several drawbacks. Thus, it is desirable to cease or at least reduce the use of chemicals. On the other hand, NBs are promising but could also negatively affect the microbial community in MBRs,

due to their oxidative effect, and could be cost-ineffective. In this context, four problems were identified.

1. Membrane fouling is an obstacle for the widespread use of MBRs, and calls for novel fouling mitigation methods;
2. CEB with NaClO negatively impacts MBR performance and microbial activity in MBRs;
3. The efficiency of NBB might be limited;
4. NBs-based solutions for membrane backwashing in MBRs might be cost-ineffective.

1.1.2 Objective

The main objective of this study was to mitigate membrane fouling in MBRs using effective and, as much as possible, chemical-free methods. This objective was aimed at by establishing four specific goals. Goal number 1 looks forward to tackle problem number 1, while goal number 2 addresses problems number 2. Finally, goals number 3 and 4 serve to investigate problems number 3 and 4, respectively, as shown below:

1. To mitigate membrane fouling in MBR by the application of nanobubble-assisted backwashing (NBB) (Chapter 4);
2. To assess the effect of NBs on the microbial activity in MBRs (Chapter 5);
3. To enhance the efficiency of NBB by the synergy with NaClO (Chapter 6);
4. To assess the cost-effectiveness of the use on NB-based backwashing (Chapter 7).

1.1.3 Outline

Chapter 1 makes a brief introduction to this dissertation.

Chapter 2 is a literature review providing the grounds for this dissertation. A brief background of the state of water scarcity and wastewater treatment technologies is

presented. The review focuses on CAS and MBRs, showing the disadvantages of the former and how MBRs are superior. The drawbacks of MBRs are also discussed, as well as several solutions. Membrane cleaning is addressed, in particular the prospects of a novel application, presented by the first time by this work.

Chapter 3 presents basic concepts of MBRs, including different configurations, operating parameters and membrane cleaning methods. An introduction to nanobubbles, their properties and generation methods is also made.

Chapter 4 introduces the experimental section of this dissertation. A comparative study on the efficiencies of NBB, TWB and CEB on fouling mitigation is presented. Materials and methods are explained and results discussions are discussed. The effect of the concentration of NBs is also considered.

Chapter 5 presents the assessment of the impact of NBB on the performance of MBRs and the microbial activity.

Chapter 6 continues the experimental section. The synergy between NBs and NaClO is investigated and discussed. Fouling mitigation by backwashing of membrane used for MBRs with a mixture of NBs and NaClO under different pH conditions is investigated. This chapter also consists of methods, results and discussion.

Chapter 7 makes an assessment of the costs related to NBB, HC-NB and all the backwashing solutions used in this study.

Chapter 8 summarizes and draws the most important conclusion of this dissertation. Suggestions for future works are presented.

REFERENCES

[1] K. Yamamoto, M. Hiasa, T. Mahmood, T. Matsuo, Direct solid-liquid separation using hollow fiber membrane in an activated sludge aeration tank, 1989. https://doi.org/10.1016/B978-1-4832-8439-2.50009-2.

[2] P. Côté, H. Buisson, C. Pound, G. Arakaki, Immersed membrane activated sludge for the reuse of municipal wastewater, Desalination 113 (1997) 189–196. https://doi.org/10.1016/S0011-9164(97)00128-8.

[3] S. Rosenberger, U. Krüger, R. Witzig, W. Manz, U. Szewzyk, M. Kraume, Performance of a bioreactor with submerged membranes for aerobic treatment of municipal waste water, Water Res 36 (2002) 413–420. https://doi.org/10.1016/S0043-1354(01)00223-8.

[4] W.J. Davies, M.S. Le, C.R. Heath, Intensified activated sludge process with submerged membrane microfiltration, Water Science and Technology 38 (1998) 421–428. https://doi.org/https://doi.org/10.1016/S0273-1223(98)00541-1.

[5] M. Bagheri, S.A. Mirbagheri, Critical review of fouling mitigation strategies in membrane bioreactors treating water and wastewater, Bioresour Technol 258 (2018) 318–334. https://doi.org/10.1016/J.BIORTECH.2018.03.026.

[6] X. Yang, D. Li, Z. Yu, Y. Meng, X. Zheng, S. Zhao, F. Meng, Biochemical characteristics and membrane fouling behaviors of soluble microbial products during the lifecycle of

Escherichia coli, Water Res 192 (2021) 116835. https://doi.org/10.1016/j.watres.2021.116835.

[7] W. Zhang, W. Liang, Z. Zhang, T. Hao, Aerobic granular sludge (AGS) scouring to mitigate membrane fouling: Performance, hydrodynamic mechanism and contribution quantification model, Water Res 188 (2021). https://doi.org/10.1016/j.watres.2020.116518.

[8] T. Kakuda, R. Naito, A. Suzuki, A. Hafuka, K. Kimura, Quantitative and qualitative variations of biopolymers in a pilot-scale membrane bioreactor treating municipal wastewater throughout 3 years of operation, J Environ Manage 328 (2023). https://doi.org/10.1016/j.jenvman.2022.116863.

[9] Z. Wang, J. Ma, C.Y. Tang, K. Kimura, Q. Wang, X. Han, Membrane cleaning in membrane bioreactors: A review, J Memb Sci 468 (2014) 276–307. https://doi.org/10.1016/J.MEMSCI.2014.05.060.

[10] T. Kurita, K. Kimura, Y. Watanabe, The influence of granular materials on the operation and membrane fouling characteristics of submerged MBRs, J Memb Sci 469 (2014) 292–299. https://doi.org/10.1016/j.memsci.2014.05.057.

[11] W. Fu, X. Wang, J. Zheng, M. Liu, Z. Wang, Antifouling performance and mechanisms in an electrochemical ceramic membrane reactor for wastewater treatment, J Memb Sci 570–571 (2019) 355–361. https://doi.org/10.1016/j.memsci.2018.10.077.

[12] S. Wang, J.W. Chew, Y. Liu, An environmentally sustainable approach for online chemical cleaning of MBR with activated peroxymonosulfate, J Memb Sci 600 (2020) 117872. https://doi.org/10.1016/j.memsci.2020.117872.

[13] K. Hashimoto, A. Onzuka, W. Nishijima, M. Yamazaki, M. Aoki, T. Sao, Effect of fine bubbles for washing of monolith type porous ceramic membranes treating oil-in-water emulsions, Chemosphere 305 (2022) 135487. https://doi.org/10.1016/J.CHEMOSPHERE.2022.135487.

[14] Y. Ninomiya, K. Kimura, T. Sato, T. Kakuda, M. Kaneda, A. Hafuka, T. Tsuchiya, High-flux operation of MBRs with ceramic flat-sheet membranes made possible by intensive membrane cleaning: Tests with real domestic wastewater under low-temperature conditions, Water Res 181 (2020) 115881. https://doi.org/10.1016/j.watres.2020.115881.

[15] K. Kimura, H. Uchida, Intensive membrane cleaning for MBRs equipped with flat-sheet ceramic membranes: Controlling negative effects of chemical reagents used for membrane cleaning, Water Res 150 (2019) 21–28. https://doi.org/10.1016/j.watres.2018.11.030.

[16] F. Meng, S. Zhang, Y. Oh, Z. Zhou, H.-S. Shin, S.-R. Chae, Fouling in membrane bioreactors: An updated review, Water Res 114 (2017) 151–180. https://doi.org/10.1016/J.WATRES.2017.02.006.

[17] International Organization for Standardization, Fine bubble technology — General principles for usage and measurement of fine bubbles — Part 1: Terminology, ISO 20480-1:2017 (2017).

[18] A.J. Atkinson, O.G. Apul, O. Schneider, S. Garcia-Segura, P. Westerhoff, Nanobubble Technologies Offer Opportunities to Improve Water Treatment, Acc Chem Res 52 (2019) 1196–1205. https://doi.org/10.1021/acs.accounts.8b00606.

[19] S.M.A. Movahed, A.K. Sarmah, Global trends and characteristics of nano- and micro-bubbles research in environmental engineering over the past two decades: A scientometric analysis, Science of the Total Environment 785 (2021) 147362. https://doi.org/10.1016/j.scitotenv.2021.147362.

[20] A. Ghadimkhani, W. Zhang, T. Marhaba, Ceramic membrane defouling (cleaning) by air Nano Bubbles, Chemosphere 146 (2016) 379–384. https://doi.org/10.1016/J.CHEMOSPHERE.2015.12.023.

[21] H.N.P. Dayarathne, J. Choi, A. Jang, Enhancement of cleaning-in-place (CIP) of a reverse osmosis desalination process with air micro-nano bubbles, Desalination 422 (2017) 1–4. https://doi.org/10.1016/j.desal.2017.08.002.

[22] H.N.P. Dayarathne, S. Jeong, A. Jang, Chemical-free scale inhibition method for seawater reverse osmosis membrane process: Air micro-nano bubbles, (2019). https://doi.org/10.1016/j.desal.2019.03.008.

[23] M.U. Farid, P.J. Choi, J.A. Kharraz, J.Y. Lao, S. St-Hilaire, Y. Ruan, P.K.S. Lam, A.K. An, Hybrid nanobubble-forward osmosis system for aquaculture wastewater treatment and reuse, Chemical Engineering Journal 435 (2022) 135164. https://doi.org/10.1016/J.CEJ.2022.135164.

[24] M.U. Farid, J.A. Kharraz, C.H. Lee, J.K.H. Fang, S. St-Hilaire, A.K. An, Nanobubble-assisted scaling inhibition in membrane distillation for the treatment of high-salinity brine, Water Res 209 (2022) 117954. https://doi.org/10.1016/J.WATRES.2021.117954.

[25] S. Kiuchi, H. Fernandes, A. Hafuka, K. Kimura, Cleaning of fouled membranes used for MBRs by using microbubbles and nanobubbles, J. JSCE G 76(7) (2020) 149–155.

CHAPTER 2: LITERATURE REVIEW

2.1 Background

Life cannot be sustained without water. All forms of life and nature itself depend on this natural resource to thrive. Animals need water for consumption and to perform their body functions and plants use it to transport nutrients. It is a necessary resource to preserve ecosystems and life forms that depend on their stable functioning. Additionally, humans use water for basic needs, including domestic and potable purposes, and extend its use for industrial and recreational ends. "The human right to water is indispensable for leading a healthy life in dignity. It is a pre-requisite to the realization of all other human rights"[1]. On the other hand, freshwater accounts for only 2.5% of all the water on earth, and less than 1% is usable and available for humans and ecosystems [2]. This problem could be further aggravated by increasing populational growth, which brings an unbalance between the available amount of fresh water and water demand for consumption and human activity. According to a United Nations Water's (UN-Water) report, by 2025, 1 800 million people worldwide will be affected by absolute water scarcity. Also, two-thirds of the population could be living under stressful conditions [3]. The organization looks forward to increasing freshwater availability by its sixth Sustainable Development Goal (SDG). SDG's target 6.3 deals with water quality improvement, wastewater treatment, and safe reuse [4]. Their 2007 report states that water scarcity hangs on various conditions such as climate change, droughts, population growth, and economic development. Some of the solutions to these issues have been

implemented, including a call for efficient water use, better resource management measures, measures to reduce water losses, policies aiming to increase water reclamation and reuse, development of better technologies, and so forth. This dissertation results from a research effort to contribute to the major water issue in the world.

2.2 Conventional activate sludge

Conventional Activated Sludge (CAS) is the most commonly applied technology for wastewater treatment. It is based on organic matter degradation by aerobic microorganisms that convert carbonaceous and other constituents to gases and cell tissue[5]. It is a centennial invention that has been improved over time. A typical CAS process is based on three steps, as shown in Figure 2.2-1: the primary clarifier, the aeration basin, and the secondary clarifier. The primary clarifier or primary treatment receives sewage from the preliminary treatment which removes dust, coarse solids, and excess scum. In the primary clarifier, the sewage is settled to separate coarse and heavy solids from finer ones. Floating matter and scum are also removed from the top of the basin, while the rest goes to the secondary treatment. The next two steps compose the secondary treatment divided into the aeration tank and the secondary clarifier. The

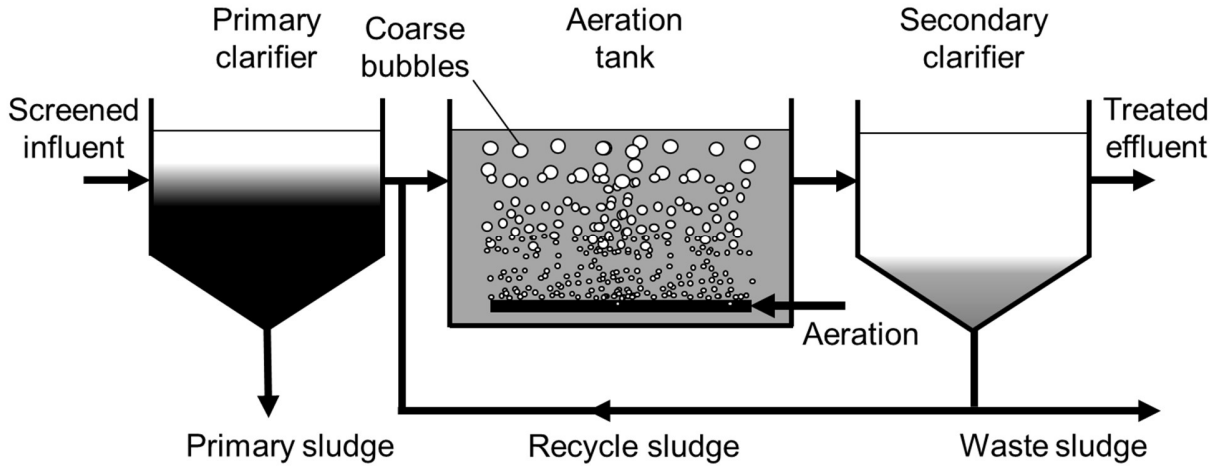

Figure 2.2-1: Typical activated sludge process flow.

aeration basin receives primary sewage free of thick sludge and gives initiation to a biological process. Aerobic bacteria kept in suspension by coarse bubble aeration degrade organic matter transforming it into gases and cell tissue. The sewage is then kept in a secondary clarifier to further the removal of particles. In this stage, a certain amount of sludge is returned to the aeration basin to keep the microbial suspension stable or activated; thus, the name activated sludge. The remaining sludge is also collected and submitted to treatment in a sludge processing facility. Depending on the final use intended for the treated secondary effluent, disposal in the environment or further treatment can occur. Although not part of the typical CAS process, tertiary treatment is sometimes required. Since the secondary effluent is not free from contaminants such as viruses and bacteria, further treatment, including disinfection via chlorination or ultra-violet (UV) light is necessary. In other cases, CAS processes can be upgraded by membrane filtration systems.

2.3 Membrane bioreactors

Membrane bioreactor (MBR) is a relatively new wastewater treatment technology that applies efficient solid-liquid separation via membrane filtration, integrated with a

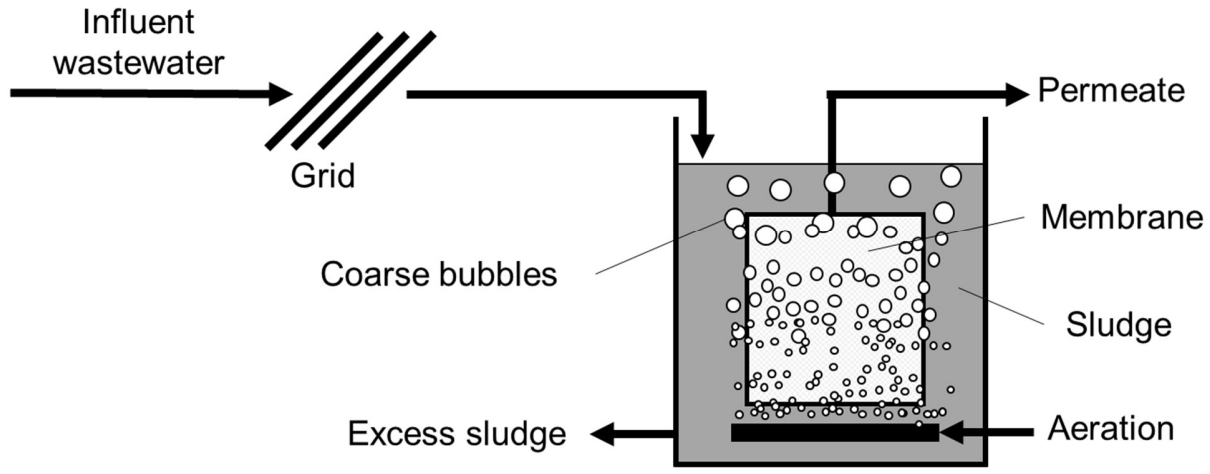

Figure 2.3-1: Basic arrangement of a membrane bioreactor.

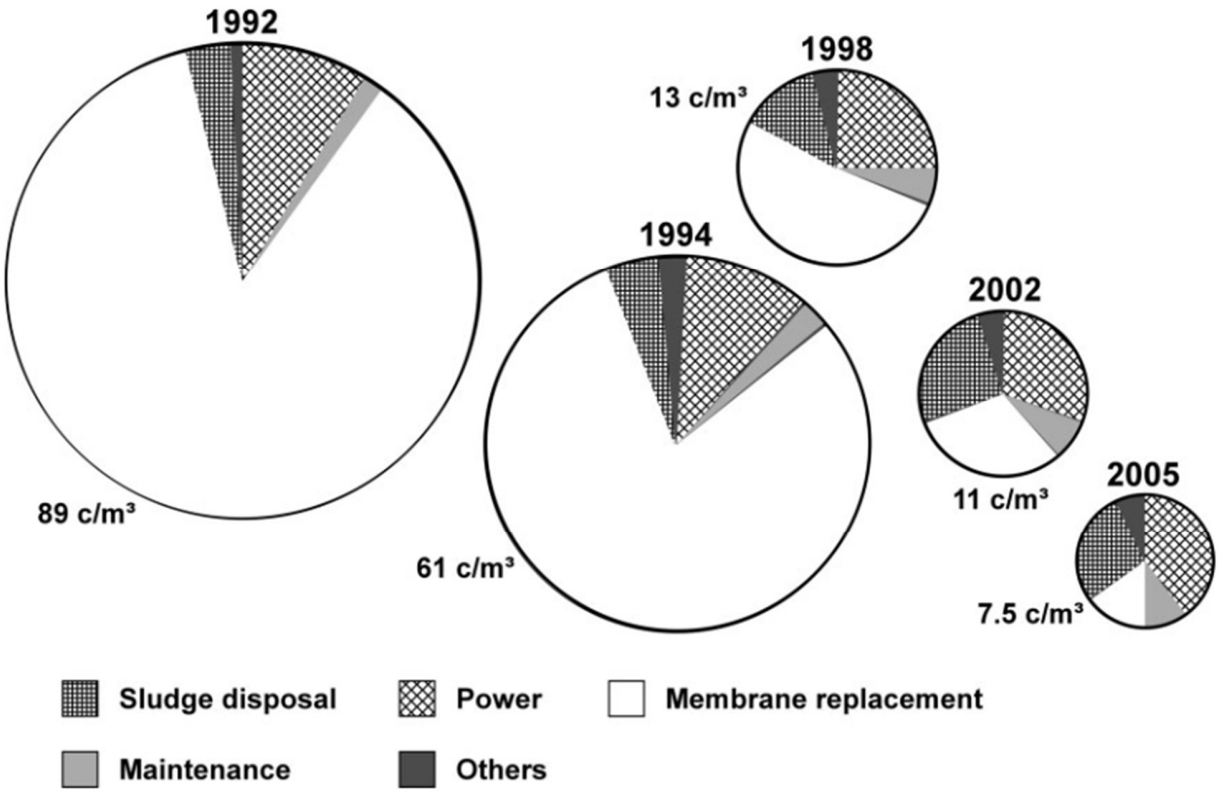

Figure 2.3-2: Operating and maintenance costs of MBRs over time.

biological process within a reactor [6] (Figure 2.3-1). The first report on MBRs was a 1969 publication in the Proceedings of the 24th Industrial Waste Conference, in which solid-liquid separation of activated sludge was said to be achieved by membranes [7]. Their goal was the develop a new compact wastewater treatment technology producing high-quality treated water and that didn't depend on separation by gravity. They used an ultrafiltration membrane to separate solids from wastewater sludge. While, initially, the cost of membranes was high, which hindered the commercial availability of MBRs, after several years, the application and research on MBRs has significantly increased. Although not as widely used as CAS, MBRs have several advantages over its counterpart. In CAS, liquid-solid separation is conducted by huge sedimentation tanks. MBRs, on the other hand, apply membrane filtration to separate solids, which provides stable and high-quality effluent water [8]. Membrane filtration also allows a high biomass concentration within the bioreactor, which substantially reduces its physical footprint

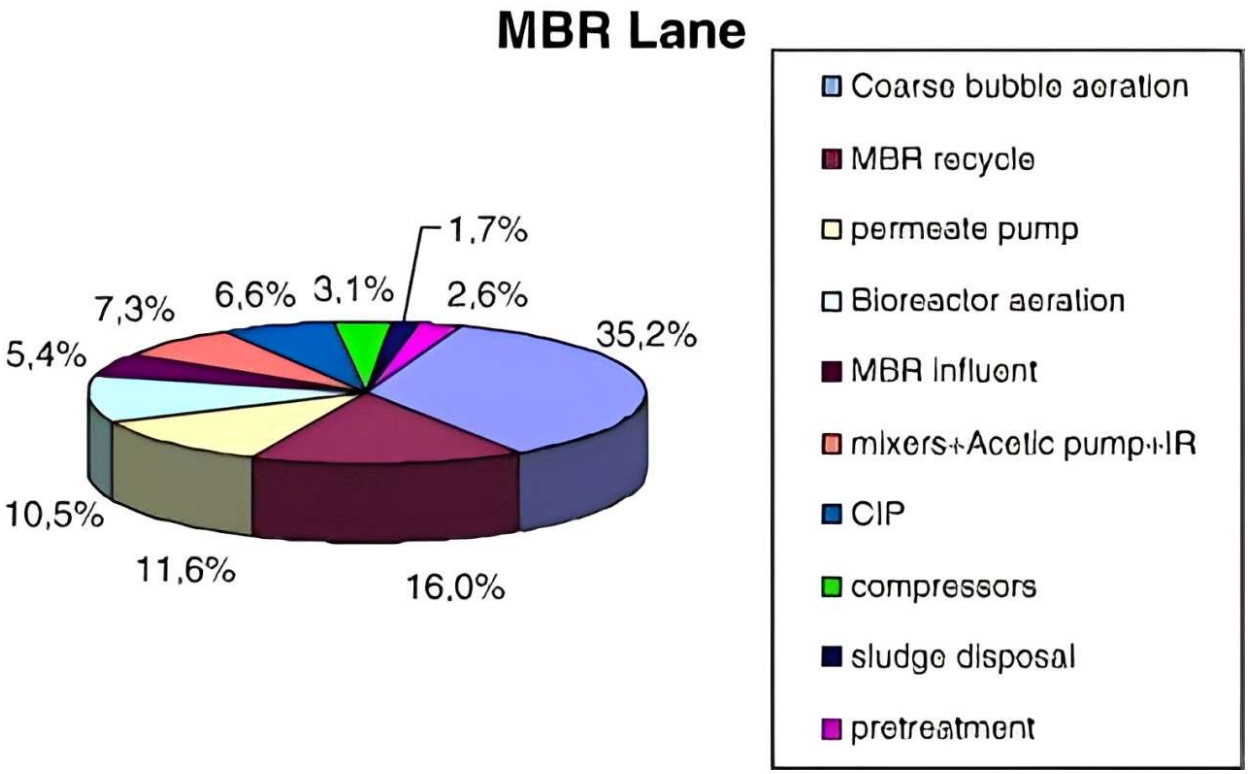

Figure 2.3-3: Energy contributions of the different devices in MBRs.

and provides suitable conditions for slow growth rate bacteria to be stablished [9]. These bacteria can further remove persistent components. A high biomass concentration also reduces sludge production and costs related to sludge treatment. A significant disadvantage of CAS processes is sludge bulking. In MBRs, however, Sludge bulking is not a problem since sedimentation is not needed. MBRs are also very suitable as compact satellite systems or even as an upgrade to existing wastewater treatment plants [10].

2.3.1 Obstacles to the widespread application of MBRs

Despite having several advantages over CAS processes, the worldwide industrial application of MBRs is still not a reality. One of the main reasons for the limited application of MBRs is the high-cost of operation/maintenance, which is higher than that of CAS [11]. Figure 2.3-2 shows changes in the operational and maintenance costs of MBRs [12]. In the 1990s, the cost of membrane replacement accounted for the larger portion of MBR's operational costs. However, with the decline in membrane prices in the

2000s, the costs decreased to less than one-tenth. In recent years, the costs of energy consumption in MBR operation have come to account for most of the whole operational costs. Fenu reported that 0.3 kW m^{-2} of energy is required for CAS processes, while MBRs requires more than double (0.8-1.2 kW m^{-2}) [13]. The major factor for the high operational costs increases in MBRs, is coarse bubble aeration for the mitigation of membrane fouling [12]. In Figure 2.3-3 a breakdown of full-scale MBRs power consumption is shown [13]. In a common MBR, aeration is conducted to mitigate membrane fouling and to degrade organic matters by biodegradation. As shown in Figure 2.3-3, aeration for mitigating membrane fouling consumes more than twice the energy required for biodegradation. Accordingly, a reduction in aeration rate is a good approach to reduce the cost of MBR operation.

2.3.2 Membrane fouling

Although MBRs have several advantages over CAS processes, their widespread application still faces a major obstacle: membrane fouling. Membrane fouling is the deposition of particles on the membrane surface or inside its pores (section3.1.7), increasing the transmembrane pressure and decreasing membrane permeability. Because of that, there is a need to continually clean the membranes, which increases operational and maintenance costs and reduces membrane lifetime [14,15]. Several solutions to mitigate membrane fouling, including antifouling membranes, optimization of operating conditions, and membrane cleaning[16], have been presented. Other studies have reported the use of chemical cleaning and coagulation for fouling mitigation[17]. Among the vast array of fouling mitigation methods, chemically enhanced backwashing (CEB) and cleaning in place (CIP) assisted by sodium hypochlorite (NaClO) seem to be the most effective method and are increasingly prevalent in practice[18]. While chemical cleaning is useful in recovering membrane permeability, backwashing membranes with chemical solutions have drawbacks that should be overcome. Some studies have reviewed the state of membrane cleaning in MBR and stated that chemical reagents could cause foaming problems when they contact the sludge in MBRs. Microbial activity can also be decreased by about 50% using 0.5% NaClO for two hours during CIP. They

also pointed out that nitrification rates can be restrained, and some chemicals increase the Chemical Oxygen Demand (COD) in the effluent[19]. Other studies showed a deterioration of sludge filterability with the increase in the concentration of NaClO in contact with the sludge. The concentration of the polysaccharide fraction of extracellular polymeric substances (EPS), a major foulant, increased significantly with the increase in the concentration of NaClO. Also, the use of chemicals presents a negative impact on the environment. Hence, energy-efficient and chemical-free solutions to the membrane fouling problem are desirable and would accelerate the widespread use of MBRs.

2.4 Ceramic membranes

Ceramic membranes, which are characterized by their physical and chemical robustness, have drawn significant attention in various fields of water and wastewater treatment, and many full-scale facilities have been constructed [20]. Ceramic membranes are

Figure 2.4-1: Flat-sheet ceramic membrane used in the experiments.

compact, can withstand heat and high pressures, have a long life and are resistant to chemical/physical damage. Therefore, ceramic membranes can be used with intensive cleaning without collapsing [21,22]. Kimura et al. (2019) [23] showed that granular scouring was effective for controlling membrane fouling. Intensive physical cleaning with granular materials was possible due to the high resistance of ceramic membranes. Another study applied intensive membrane cleaning enabling high flux operation. Such intensive cleaning and high flux operation was only possible due to the robustness of ceramic membrane. An illustration of ceramic membranes used in this study is shown in Figure 2.4-1.

2.5 Nanobubble backwashing

Nanobubbles (NBs) are small gas entities in water with a diameter smaller than one μm[24]. Since their first observance, they have been surrounded by mystery, and a lot has been said about their existence, stability, applications, and properties. Their existence was even dismissed in 1997 based on their expected lifetime[25]. CEB is a convenient method for fouling mitigation, as the membranes can be cleaned without being removed from the reactor. However, while backwashing is an efficient method for the mitigation of membrane fouling, the use of chemicals in MBRs has several drawbacks, as stated previously. NBs, on the other hand, have been used to clean contaminated surfaces, mitigate biofouling [26] and are environmentally friendly. Thus, NB cleaning is a potential alternative to chemical cleaning. In addition, NBs can pass through the pores of microfiltration membranes used for MBRs and can be used for membrane backwashing. .Figure 2.5-1 shows representative size distributions of NBs measured before and after passage through 0.1 μm pore size ceramic membrane used in this study. A ceramic membrane was backwashed with NB water, and samples were taken for size distribution analysis. The backwashing flux was 8 LMH. A new membrane was used for this test. As shown in Figure 2.5-1 a significant portion of NBs could penetrate the ceramic membrane. In the sample for which data are shown in Figure 2.5-1, the total NB concentration before filtration was 1.96×108 NB/mL, which is

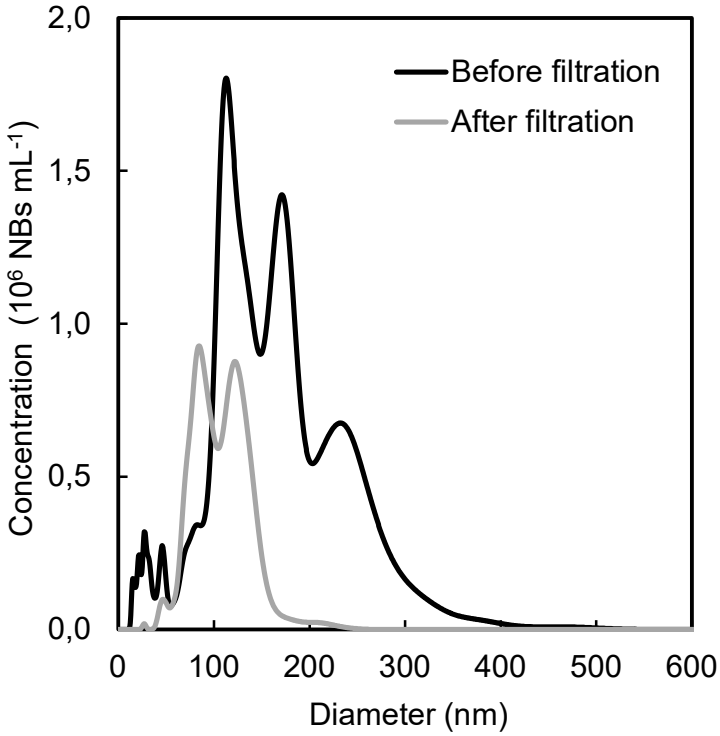

Figure 2.5-1: Representative size distributions of NBs before and after passing through a 0.1 μm membrane.

comparable to the reported values in related papers [27,28]. The average sizes of NBs before and after passage through the membranes were 168 nm and 108 nm, respectively. It was clearly demonstrated that, by the sieving effect, small NBs selectively penetrated the membrane, and large NBs could not penetrate it. It was therefore assumed that NBs could be transported to the fouling layer from the permeate side during NBB. There has not been a single study using nanobubbles water as a backwash solution, so it is an unexplored field that deserves attention.

REFERENCES

[1] WHO | Water for health enshrined as a human right, (2020) 1. https://www.who.int/mediacentre/news/releases/pr91/en/ (accessed December 1, 2020).

[2] IAEA Bulletin 53-1, 2011.

[3] A. Haddad, Coping with water scarcity, Water and Wastewater International 22 (2007) 10. https://doi.org/10.1007/978-1-4020-9579-5.

[4] UN, Resolution adopted by the General Assembly on 6 July 2017, 2017.

[5] Metcalf, Eddy, Wastewater engineering : treatment, disposal, and reuse, 5th ed., McGraw Hil Educationl, 2014.

[6] K. Yamamoto, M. Hiasa, T. Mahmood, T. Matsuo, Direct solid-liquid separation using hollow fiber membrane in an activated sludge aeration tank, 1989. https://doi.org/10.1016/B978-1-4832-8439-2.50009-2.

[7] C.V.J. Smith, D.D. Gregorio, R.M. Talcott, The use of ultrafiltration membrane for activated sludge separation, 24th Annual Purdue Industrial Conference (1969).

[8] P. Côté, H. Buisson, M. Praderie, Immersed membranes activated sludge process applied to the treatment of municipal wastewater, in: Water Science and Technology,

No longer published by Elsevier, 1998: pp. 437–442. https://doi.org/10.1016/S0273-1223(98)00543-5.

[9] S. Rosenberger, U. Krüger, R. Witzig, W. Manz, U. Szewzyk, M. Kraume, Performance of a bioreactor with submerged membranes for aerobic treatment of municipal waste water, Water Res 36 (2002) 413–420. https://doi.org/10.1016/S0043-1354(01)00223-8.

[10] W.J. Davies, M.S. Le, C.R. Heath, Intensified activated sludge process with submerged membrane microfiltration, Water Science and Technology 38 (1998) 421–428.

[11] A. Drews, Membrane fouling in membrane bioreactors-Characterisation, contradictions, cause and cures, J Memb Sci 363 (2010) 1–28. https://doi.org/10.1016/j.memsci.2010.06.046.

[12] M. Kraume, A. Drews, Membrane Bioreactors in Waste Water Treatment – Status and Trends, Chem Eng Technol 33 (2010) 1251–1259. https://doi.org/10.1002/CEAT.201000104.

[13] A. Fenu, J. Roels, T. Wambecq, K. de Gussem, C. Thoeye, G. de Gueldre, B. van de Steene, Energy audit of a full scale MBR system, Desalination 262 (2010) 121–128. https://doi.org/10.1016/J.DESAL.2010.05.057.

[14] X. Yang, D. Li, Z. Yu, Y. Meng, X. Zheng, S. Zhao, F. Meng, Biochemical characteristics and membrane fouling behaviors of soluble microbial products during the lifecycle of Escherichia coli, Water Res 192 (2021) 116835. https://doi.org/10.1016/j.watres.2021.116835.

[15] M. Bagheri, S.A. Mirbagheri, Critical review of fouling mitigation strategies in membrane bioreactors treating water and wastewater, Bioresour Technol 258 (2018) 318–334. https://doi.org/10.1016/J.BIORTECH.2018.03.026.

[16] W. Fu, X. Wang, J. Zheng, M. Liu, Z. Wang, Antifouling performance and mechanisms in an electrochemical ceramic membrane reactor for wastewater treatment, J Memb Sci 570–571 (2019) 355–361. https://doi.org/10.1016/j.memsci.2018.10.077.

[17] S. Wang, J.W. Chew, Y. Liu, An environmentally sustainable approach for online chemical cleaning of MBR with activated peroxymonosulfate, J Memb Sci 600 (2020) 117872. https://doi.org/10.1016/j.memsci.2020.117872.

[18] F. Meng, S. Zhang, Y. Oh, Z. Zhou, H.-S. Shin, S.-R. Chae, Fouling in membrane bioreactors: An updated review, Water Res 114 (2017) 151–180. https://doi.org/10.1016/J.WATRES.2017.02.006.

[19] Z. Wang, J. Ma, C.Y. Tang, K. Kimura, Q. Wang, X. Han, Membrane cleaning in membrane bioreactors: A review, J Memb Sci 468 (2014) 276–307. https://doi.org/10.1016/J.MEMSCI.2014.05.060.

[20] H. Sakamoto, A. Hafuka, T. Tsuchiya, K. Kimura, Intensive routine cleaning for mitigation of fouling in flat-sheet ceramic membranes used for drinking water production: Unique characteristics of resulting foulants, Sep Purif Technol 301 (2022). https://doi.org/10.1016/j.seppur.2022.121950.

[21] K. Hashimoto, A. Onzuka, W. Nishijima, M. Yamazaki, M. Aoki, T. Sao, Effect of fine bubbles for washing of monolith type porous ceramic membranes treating oil-in-water emulsions, Chemosphere 305 (2022) 135487. https://doi.org/10.1016/J.CHEMOSPHERE.2022.135487.

[22] Y. Ninomiya, K. Kimura, T. Sato, T. Kakuda, M. Kaneda, A. Hafuka, T. Tsuchiya, High-flux operation of MBRs with ceramic flat-sheet membranes made possible by intensive membrane cleaning: Tests with real domestic wastewater under low-temperature conditions, Water Res 181 (2020) 115881. https://doi.org/10.1016/j.watres.2020.115881.

[23] K. Kimura, H. Uchida, Intensive membrane cleaning for MBRs equipped with flat-sheet ceramic membranes: Controlling negative effects of chemical reagents used for membrane cleaning, Water Res 150 (2019) 21–28. https://doi.org/10.1016/j.watres.2018.11.030.

[24] A. Azevedo, H. Oliveira, J. Rubio, Historical perspective Bulk nanobubbles in the mineral and environmental areas: Updating research and applications, (2019). https://doi.org/10.1016/j.cis.2019.101992.

[25] M. Alheshibri, J. Qian, M. Jehannin, V.S.J. Craig, A History of Nanobubbles, (2016). https://doi.org/10.1021/acs.langmuir.6b02489.

[26] Y. Xiao, S.C. Jiang, X. Wang, T. Muhammad, P. Song, B. Zhou, Y. Zhou, Y. Li, Mitigation of biofouling in agricultural water distribution systems with nanobubbles, (2020). https://doi.org/10.1016/j.envint.2020.105787.

[27] T. Sugimoto, S. Hamamoto, T. Nishimura, Inhibited nanobubble transport in a saturated porous medium: Effects of deposited colloidal particles, J Contam Hydrol 242 (2021) 103854. https://doi.org/10.1016/J.JCONHYD.2021.103854.

[28] Y. Fan, X. Yang, Z. Lei, Y. Adachi, M. Kobayashi, Z. Zhang, K. Shimizu, Novel insight into enhanced recoverability of acidic inhibition to anaerobic digestion with nano-bubble water supplementation, Bioresour Technol 326 (2021) 124782. https://doi.org/10.1016/j.biortech.2021.124782.

CHAPTER 3: BASIC CONCEPTS

3.1 Membrane bioreactors

3.1.1 MBR configurations

The initial concept of an MBR was based on crossflow filtration (Figure 3.1-1 (a)), a configuration in which the membranes are installed outside of the sludge tank, and the sludge is pumped parallel to the membrane surface. The sludge is returned to the tank, while water is filtrated perpendicularly to the membrane, thus the name crossflow filtration. On the other hand, in a dead-end filtration system, since the membranes are submerged in the sludge tank, all the water and particles come in contact with the membrane. Submerged membrane bioreactor (SMBR), as shown in

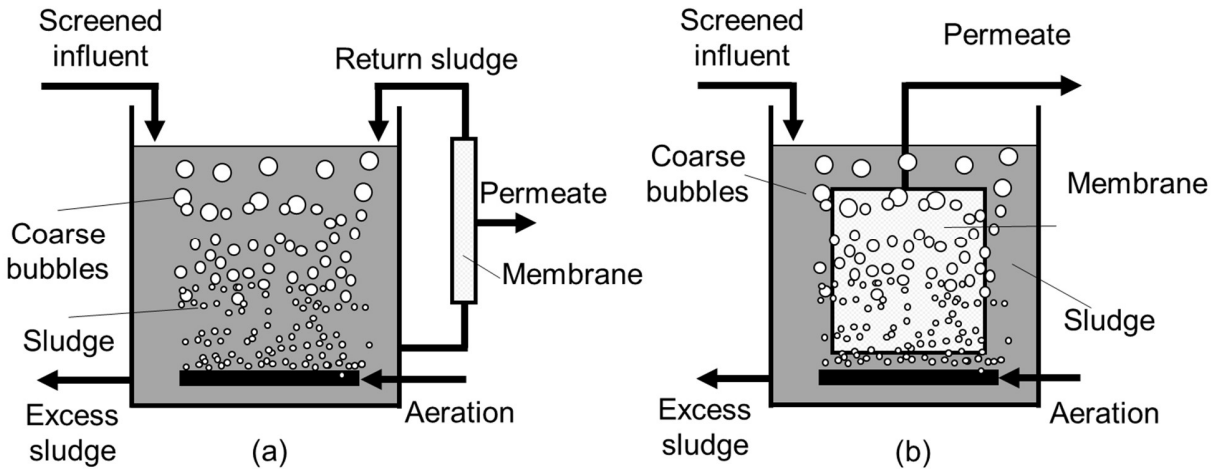

Figure 3.1-1: Configurations of MBR: (a) crossflow MBR, (b) submerged MBR.

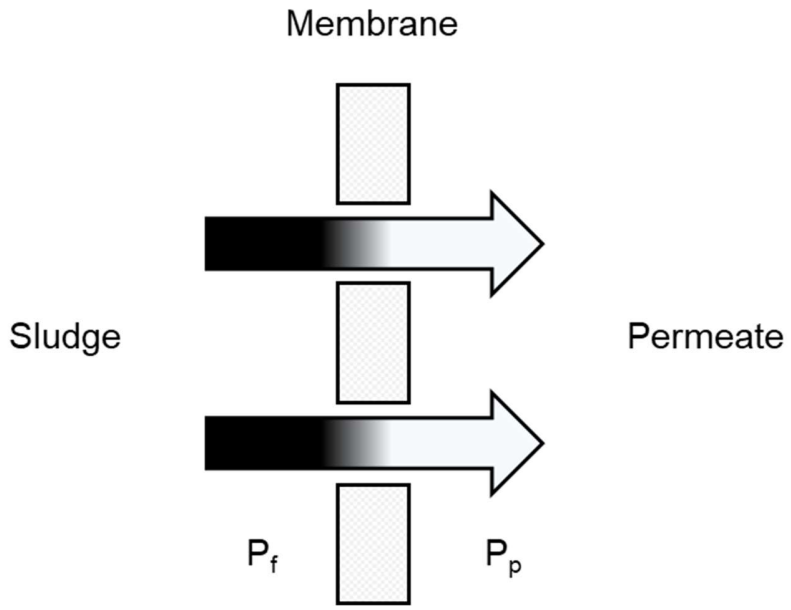

Figure 3.1-2: Pressure difference between the feed side (Pf) and the permeate side (Pp) of a membrane filtration system.

Figure 3.1-1 (b), is a modification of a crossflow MBR's initial concept. It operates in a dead-end condition. The membranes are submerged in the sludge within the biological reactor, allowing the membrane filtration and biodegradation to occur in the same compartment. Air diffusers supply the oxygen demand within the reactor. Coarse bubble (CB) aeration is necessary to scour the membrane surface, removing attached particles, and transfer the oxygen needed by the aerobic bacteria.

3.1.2 Transmembrane pressure

Membrane filtration technologies can be classified as driven by high-pressure or low-pressure membranes. The membranes used in this study were low-pressure microfiltration (MF) membranes with a pore size of 0.1 micrometers. The permeation pressure is necessary to force the water to flow from inside the reactor through the membrane pores to the membrane's permeate side. The pressure difference between the two sides of the membrane, shown in Equation 1 and illustrated in Figure 3.1-2, is denominated transmembrane pressure (TMP). TMP is a standard measure of

membrane fouling. A low TMP is desirable, as it indicates that the membrane is clean. Contrarily, a high TMP is an indication of the occurrence of membrane fouling. Thus, plotting the TMP against time is a common way to assess membrane fouling.

$$\Delta P = P_f - P_p \quad (1)$$

Where:

ΔP is the pressure difference between the feed and the permeate side of the membrane (kPa)

P_f is the pressure in the feed side of the membrane (kPa)

P_p is the pressure in the permeate side of the membrane, all measured in kilopascal (kPa)

3.1.3 Membrane flux and permeability

Wastewater reclamation systems consist of treating a low-quality influent into an effluent with better quality. The effluent of an MBR system is commonly denoted as permeate. On the other hand, membrane flux is the permeate flow rate per unit area of the membrane surface or the volume of filtered water per unit membrane area per unit time. Flux is an essential parameter in the operation of MBRs, and is usually expressed in liters per square meter per hour (L m^{-2} h) or simply LMH. Specific flux or permeability is also commonly measured in MBRs. Permeability is the flux rate divided by the TMP. MBR operation is generally set at a constant flux leading to a temporal increase of TMP or at a constant TMP leading to a decrease in flux over time, as shown in Figure 3.1-3, respectively. Flux and permeability, in MBR systems is calculated as follows:

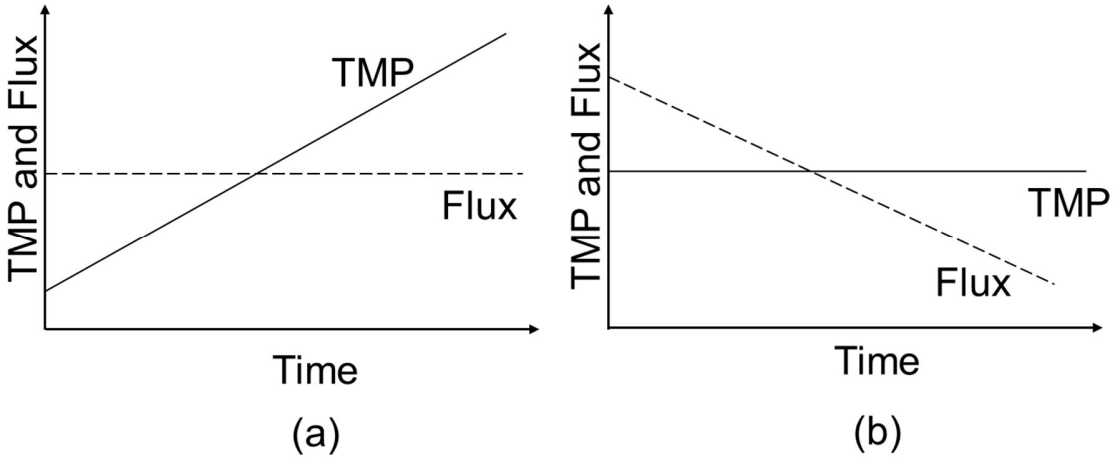

Figure 3.1-3: Modes of membrane operation: (a) constant flux, (b) constant TMP.

$$J = \frac{Q_p}{A} \tag{2}$$

$$J_{sp} = \frac{J}{TMP} \tag{3}$$

Where:

J is the membrane permeating flux (LMH)

Q_p is the membrane permeating flow rate ($m^3\ h^{-1}$ 1000 L)

A is the membrane area (m^2),

J_{sp} is the membrane specific flux or permeability (LMH kpa^{-1})

In MBRs systems physical or chemical cleanings in place (CIP) are applied to mitigate membrane fouling. Physical cleanings include relaxation and backflushing. Relaxation is the ceasing of permeation to allow membrane scouring by air bubbles and remove fouling. Backflushing is the hydraulic reverse flow during relaxation, using tap water or MBR permeate. Chemical cleaning is the periodical reverse flow after a certain number of relaxation cycles or after a definite time, in the case of

absence of relaxation. Chemical cleaning is usually performed by backwashing with chemical agents (e.g. NaClO). The net flux for MBRs using relaxation, backflushing or backwashing is defined as follows:

$$J_{net} = \frac{n(Jt_p - J_p\tau_p) - J_c\tau_c}{n(t_p + \tau_p) + \tau_c} \quad (4)$$

Where:

J_{net} is the net flux (LMH)

t_p is the period between physical cleaning (relaxation or backflushing) (min)

τ_p is the duration of physical cleaning (min)

J_p is the flux during physical cleaning (LMH)

τ_c is the duration of chemical cleaning (min)

J_c is the flux during chemical cleaning (LMH)

n is the number of physical cleaning cycles per chemical cleaning, as defined below:

$$n = \frac{t_c}{t_p + \tau_c} \quad (5)$$

3.1.4 Mixed liquor suspended solids

Mixed liquor suspended solids (MLSS) is the mixture of solids and microorganisms kept in suspension by coarse bubble aeration within the membrane tank. Using membrane filtration to separate solids from liquids, MBR provides the conditions to maintain a high MLSS concentration compared with CAS. Typical MLSS concentrations in MBR range from 5,000 to 12,000 milligrams per liter (mg L^{-1}). Concentrations as high as 20,000 mg/L can be observed, although at the expense of a

rapid increase in membrane fouling [1]. Mixed liquor volatile suspended solids (MLVSS) are the organic or volatile solid fraction of the MLSS, which is a measure of the quantity of microorganisms. MLSS and MLVSS can be calculated based on the standard methods [2]. The sludge samples are centrifuged twice for 10 minutes at a 5-rpm speed. A dried dish is weighed, the wet sludge is placed in the dried dish and weighed. After being dried for 24 hours within an oven at 105 ºC, the dish and the dried sludge are weighted again. The dried residue and the dish are measured again after being inserted in an oven at 550 ºC for 1 hour. The equations used to calculate MLSS and MLVSS are shown below.

$$MLSS = \frac{(B - A)}{V} \tag{6}$$

$$MLVSS = \frac{(A - C)}{V} \tag{7}$$

Where:

A is the weight of a dried dish (g)

B is the weight of the dish and sludge residue after being dried for 24 hours in an oven at 105 ºC (g)

C is the weight of the dish and the sludge residue after being dried for one hour in an oven at 550 ºC (g)

3.1.5 Sludge filterability

Sludge filterability is an important factor in the operation of MBRs. Low sludge filterability leads to an excessive accumulation of solids on the membrane surface, while higher sludge filterability is desirable. Capillary suction time (CST) is a

Figure 3.1-4: Capillary suction timer.

common method applied as a measure of sludge filterability. A device (CST-304B) from Triton Electronics Ltd. consistent of a paper filter, sludge chamber, sensors, and a timer are used to measure the suction time. An image of a capillary suction timer can be seen in Figure 3.1-4. The sludge is introduced in the chamber in contact with a membrane. By capillary forces, the sludge spreads on the membrane and touches two sensors at a certain distance from each other. The time difference between each sensor's activation is the capillary suction time and measures the sludge's filtration properties.

3.1.6 Solids and hydraulic retention times

Solid retention time (SRT) and hydraulic retention time (HRT) are essential parameters in MBR operation. SRT expresses the amount of time in days that a single sludge particle remains in the reactor until it is washed away. SRT is calculated by dividing the total volume of sludge in the reactor by the daily sludge withdrawal amount.

$$SRT = \frac{V}{Q_w} \tag{8}$$

Where:

SRT is the sludge retention time (days)

V is the total volume of sludge in the reactor (L)

Q_w the daily sludge wastage volume (L d^{-1})

HRT expresses the amount of time hours (h) that a single liquid drop remains in the reactor until it is washed away. HRT is expressed by dividing the total volume of sludge in the reactor by the permeate flow rate.

$$HRT = \frac{V}{Q_p} \tag{9}$$

Where:

HRT is the hydraulic retention time (h)

V is the total volume of sludge in the reactor (L)

Q_p is the membrane permeating flow rate (L h^{-1})

3.1.7 Membrane fouling

Membrane fouling is the accumulation of particles inside the pores or in the membrane surface. The occurrence of fouling is related to increasing TMP values and decreasing membrane flux. Controlling membrane fouling is an important step in MBR maintenance and operation. Thus, understanding its mechanisms is crucial. Three mechanisms by which membrane fouling can occur are pore narrowing, pore plugging, and gel/cake layer formation [3]. Figure 3.1-5 (a) illustrates a clean

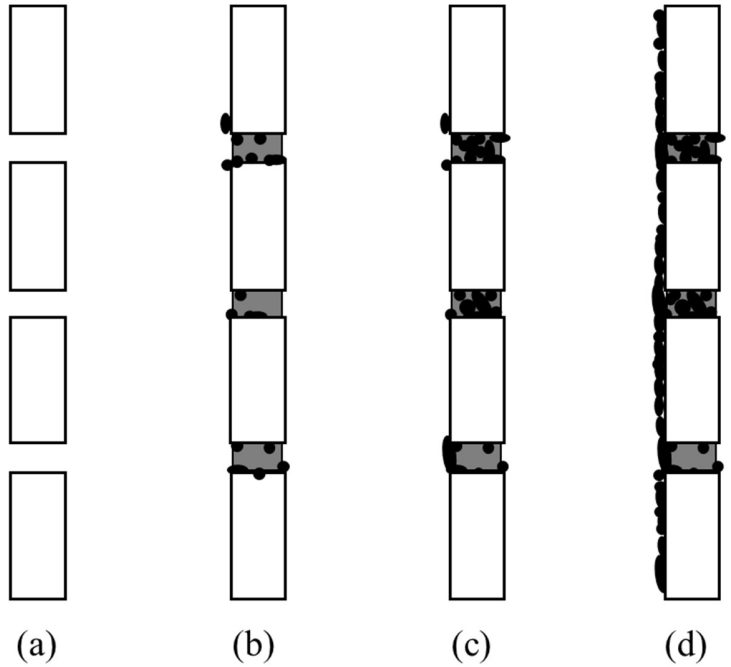

Figure 3.1-5: Membrane fouling mechanisms: (a) clean membrane, (b) pore narrowing, (c) pore plugging, and (d) cake layer formation.

membrane. As shown in Figure 3.1-5 (b), pore narrowing is the deposition of particles in the inner pore resulting in reduced pore diameter. Pore plugging occurs when a particle as big or bigger than the membrane pore size completely blocks it. Figure 3.1-5 (c). Gel/cake layer formation occurs due to large particle deposition on the membrane surface Figure 3.1-5(d).

3.1.8 Membrane filtration resistance

Friction forces between the solvent-solute and the membrane pore wall and the feed viscosity leads to a resistance to the flow through a membrane. The occurrence of fouling increases the hydraulic resistance, leading to an increase in TMP when operating at constant flux. Virgin membranes have an inherent filtration resistance due to friction forces between the filtrate and the membrane pore wall. When a pure solvent is filtered, the filtration resistance is the membrane's inherent resistance. If solutes are present in the feed and deposit on the membrane pores and surface, physically reversible and irreversible fouling can occur. Physically reversible fouling,

hereafter reversible fouling, accounts for that which can be removed by physical methods like sponge cleaning or relaxation. On the other hand, physically irreversible fouling, or just irreversible fouling, cannot be removed by physical processes [4]. One standard method to mitigate this kind of persistent fouling is chemical cleaning, such as soaking in a 50ppm NaClO solution for twenty-four hours. Equation 10 below describes the membrane filtration resistance mathematically.

$$R_T = \frac{\Delta P}{\mu \times J} \tag{10}$$

Where:

R_T is the total membrane resistance (m^{-1})

μ is the viscosity of the filtered water (Pa s)

J is the membrane flux (LMH)

The total resistance is calculated as follows:

$$R_T = R_m + R_{rev} + R_{irr} \tag{11}$$

Where:

R_m is the virgin membrane inherent resistance

R_{rev} is the reversible membrane resistance

R_{irr} is the irreversible membrane resistance

All three resistances can be determined empirically by filtrating a pure solvent. R_m is measured just before the filtration experiments. R_{rev} is the membrane resistance after sponge cleaning subtracted from the fouled membrane resistance right after the

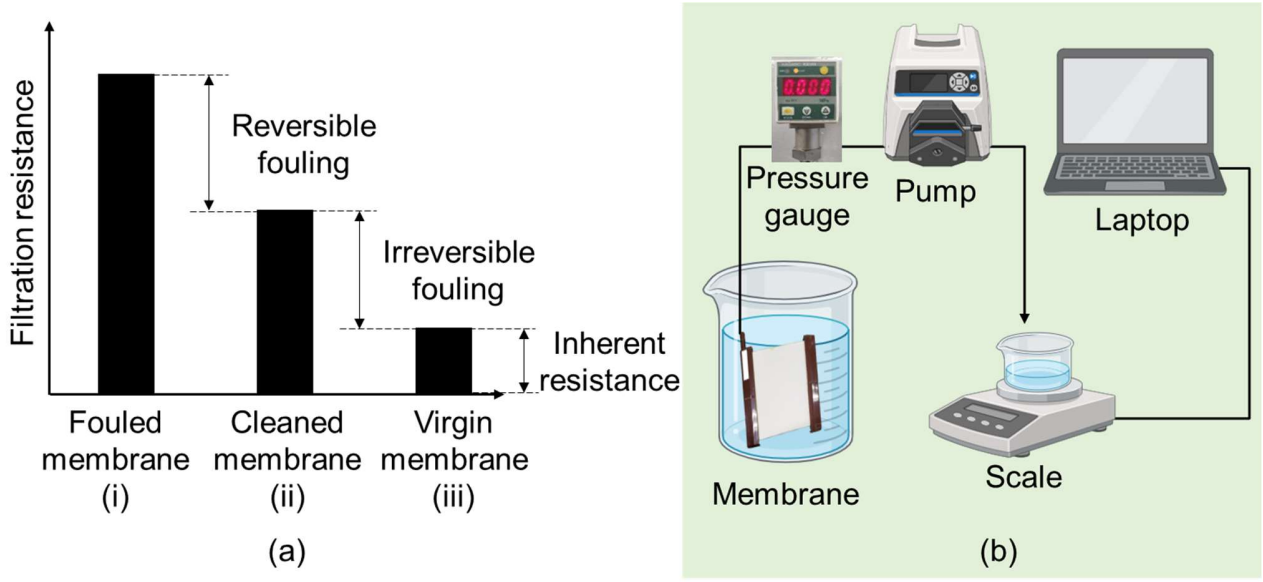

Figure 3.1-6: (a) Distribution of membrane filtration resistance: (i) fouled membrane after the filtration experiment, (ii) fouled membrane after sponge cleaning (iii) clean membrane before the filtration experiment. (b) Measurement of filtration resistance (made by biorender).

termination of the experiment. R_{irr} can be determined by subtracting R_m and R_{rev} from the fouled membrane resistance (Figure 3.1-6).

3.1.9 Membrane Cleaning

The occurrence of membrane fouling requires that the membranes are cleaned periodically. Membrane cleaning procedures are divided into physical and chemical methods. Physical methods include coarse bubble aeration, granules scouring, relaxation, sponge cleaning, and backflushing. Chemical cleanings include backwashing and recovery cleaning.

3.1.9.1 Coarse Bubble aeration

Coarse bubble aeration consists of the introduction of air bubbles in the MBR tank by an air compressor. Air diffusers are placed beneath the membrane units so that the rising bubbles generate shear and scour the membrane surface, reducing fouling propensity. Although aeration is also demanded to produce mixing inside the

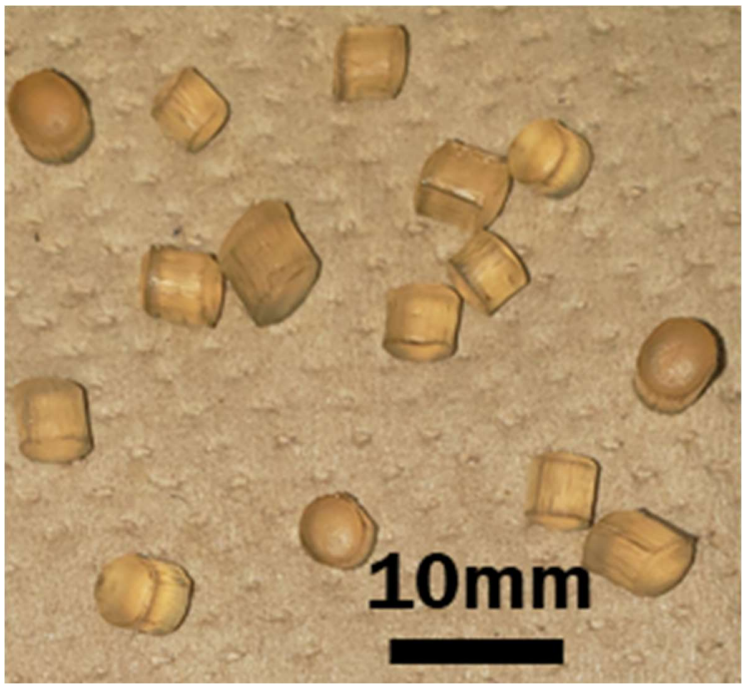

Figure 3.1-7: Polyethylene glycol (PEG) granules used in the experiments.

bioreactor and provide oxygen for biological degradation, the most significant share of energy consumption is membrane cleaning demands.

3.1.9.2 Granules scouring

Granules (Figure 3.1-7) are small particles of approximately 4 mm in diameter and height kept in suspension by the coarse bubble aeration conducted in the membrane unit tank. Adding granules generates more shear force, which removes the gel/cake layer formed in the membrane surface. In previous experiments, introducing granules increased the critical flux, reduced the aeration rate and reversible fouling was completely controlled [5].

3.1.9.3 Relaxation

Relaxation consists of an intermittent filtration operation. Permeation is periodically stopped while keeping the coarse bubble aeration and granules scouring to clean the membrane. This method ceases concentration polarization (CP) to the membrane,

allowing the coarse bubble aeration and granules to remove the cake/gel layer more efficiently.

3.1.9.4 Backflushing

Backflushing consists of reversing the membrane permeation to detach cake/gel layer formation from the membrane surface. Typically, treated permeate water or tap water is used in this kind of hydraulic backwashing.

3.1.9.5 Sponge cleaning

Ex-situ physical cleaning can be applied if membrane fouling has developed to a certain extent. A standard ex-situ physical cleaning method is Sponge cleaning, which consists of physically removing the gel/cake layer formation from the membrane surface. Sponge cleaning is used to remove the residual reversible fouling that could not be removed by air and granules scouring.

3.1.9.6 Backwashing

When membrane backwashing is applied, permeation is reversed to the membrane. The backwashing solution removes the deposited particles in the membrane pores and surface. Backwashing differs from backflushing in that the former consists of applying the reverse permeation of a chemical agent. Previous studies show that a 50 ppm NaClO solution is useful for membrane fouling mitigation [6].

3.1.9.7 Recovery cleaning

Recovery cleaning is conducted less frequently to remove persistent fouling from the membrane surface. The membrane is soaked in a high concentration cleaning agent and left for a few hours or a day. Recovery cleaning can be conducted (in-site or ex-situ) after a long-term operation in order to restore the membrane permeability closer to its initial value.

3.2 Nanobubbles

3.2.1 What are nanobubbles?

Nanobubbles, as the name suggests, are nanometer scale-gas entities present in water. In general, it is understood that NBs are smaller than 1 μm in diameter [7], but there are reports that consider them to be those with a diameter smaller than 200 nm [8]. In the latter definition, bubbles smaller than 1 μm but larger than 200 nm are defined as ultra-fine bubbles. However, some reports interchangeably use the terms nanobubbles and ultra-fine bubbles [9].

3.2.2 Generation of nanobubbles

Several nanobubble generation methods have been reported, including pressurized dissolution, rotational flow, turbulent static mixer, ejector nozzle, ultrasonic (Supersonic vibration), oscillator, venturi and mixed vapor direct contact condensation. This section will focus on two methods of generating NBs: pressurized dissolution method and pressurized shearing method.

Figure 3.2-1 (a) shows an overview of the pressurized dissolution method. In this method, pressurized liquid is pumped into the unit. As the pipe is narrowed, the pressure becomes negative and air is suctioned until the liquid is saturated with bubbles. The size of the pipe is enlarged, which increases the static pressure and pressurized dissolution (Pressure: 290 – 310 kPa) of gas takes place. Lastly, the saturated liquid is released by atmospheric pressure, causing it to become over-saturated, generating nanobubbles. Figure 3.2-2 (c) shows typical results of particle size distribution of nanobubble water measured by nanoparticle tracking analysis (NTA) Nanosight (NS500, Malvern Panalytical). In this study, nanobubbles were produced by pressurized dissolution using a generator from IDEC corporation (UltrafineGaLF, FZIN-07H) (Figure 3.2-1 (b)). The company's guidelines were followed to generate the NB water. Circulation of tap water between a water tank and the NB generator was applied for 30 minutes. A minimum volume of 100 L should be

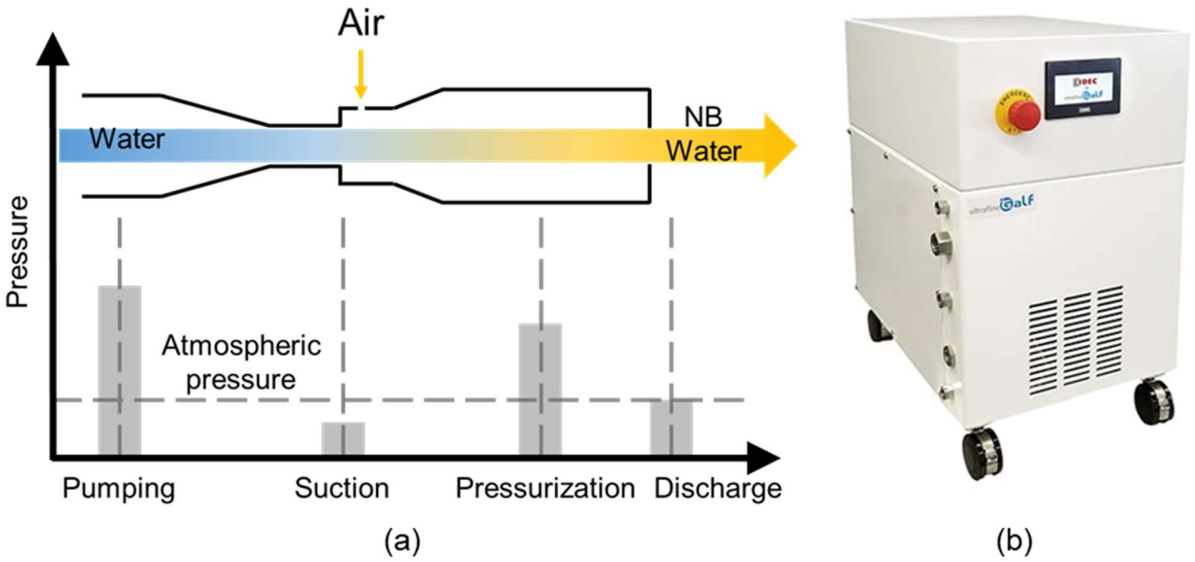

Figure 3.2-1: (a) Principle of generation of NBs by the pressurized dissolution method (source: essential-wes.com) and (b) UltrafineGaLF NB generator (source: jp.idec.com).

circulated to generate the NBs efficiently. The water tank had a volume of 10 L, and the NB generator circulates the water at a 12 L min^{-1}. Thus, the generation time was 3.6 times longer than the minimum requirement. The NB water was generated within the University facility, was stored in the tank, and carried to the wastewater treatment plant when needed, or used in the University. After transporting the NB water samples were taken and brought back to the University to confirm the presence of NBs. The presence, size, and concentration of the NBs used in this experiment were measured using nano-particle tracking analysis (NTA) software. The NTA Nanosight NS500 was used to measure a size distribution of the NB used in this experiment. The nanobubble water produced by this device are simply called nanobubble water (NBW).

An illustration of the pressurized shearing method is shown in Figure 3.2-2 (a). In the pressurized shearing method, water is forced under high pressure through a complex flow path inside a mixer with a honeycomb structure. This structure is displaced,

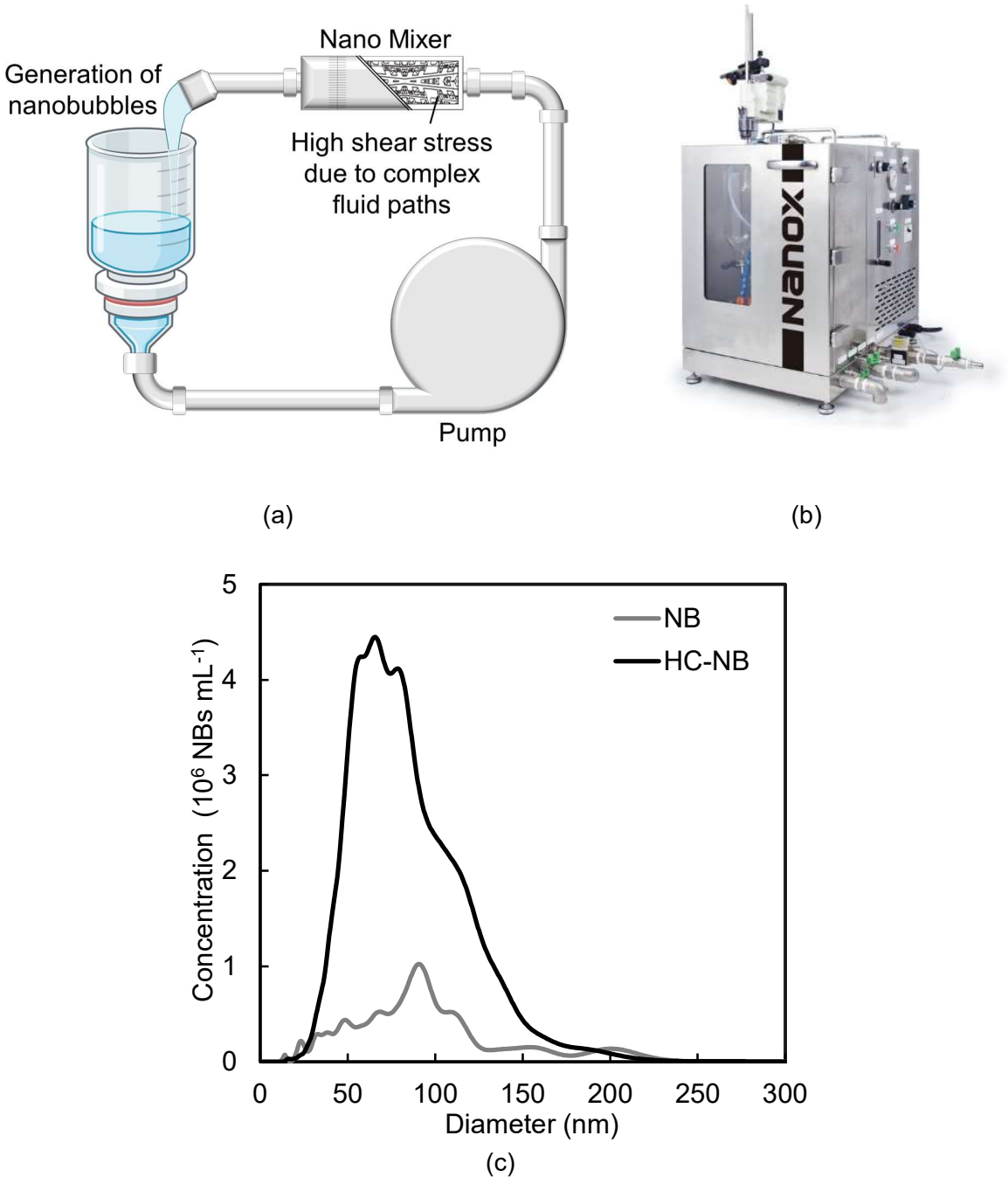

Figure 3.2-2: (a) Principle of generation of NBs by the pressurized shearing method (source: nano-x.co.jp), (b) Nanox HC-NB generator (source: nano-x.co.jp), and (c) size distributions of NBs.

causing pressure changes in the flow path, shearing due to turbulence, and pressurized dissolution (Pressure: 1000 kPa) at the same time, resulting in the

generation of highly concentrated nanobubbles. Figure 3.2-2 (b) and (b) show the nanobubble generator used in this study (Nanox corporation, NQ-KP-M1.5CD-200/60-R3S) and the typical particle size distribution of nanobubbles generated by this method, respectively. The average diameter was not significantly different from that of nanobubbles generated by pressurized dissolution, but the concentration was confirmed to be more than five times higher than that of ordinary nanobubble water. Therefore, the nanobubbles water generated by this method were named high concentration nanobubbles water (HC-NBW).

3.2.3 Properties of nanobubbles

NBs have several distinguishing features, as indicated in Figure 3.2-3 [10]. These tiny gas structures are so small that they follow Brownian motion, thus do not rise from buoyancy. Their small size also provides a higher surface area per unit volume, an essential feature in several applications. NBs are also very stable, being found in solution even after months. This feature also allows them to stably keep different types of gases, including nitrogen gas (N_2), Ozone (O_3), Hydrogen gas (H_2), and Carbon Dioxide (CO_2)) in their composition. Surface charge is another essential property of NBs which is important for industrial applications. Moreover, depending on the conditions, NBs can have an oxidative potential by generating reactive oxygen species (ROS).

3.2.4 Stability of nanobubbles

Nanobubbles stay in bulk for several weeks. Although there have been reports of NBs surviving for months, the reason for the unusual stability of NBs is not fully understood. Due to their nanometer size, the pressure inside a NB is too high to maintain the gas within it in equilibrium with the dissolved gas in solution. Therefore, it is expected that NBs wouldn't last for more than a second, according to the Laplace pressure. The pressure inside a bubble is inversely proportional to its diameter, as given by the by the Young-Laplace equation:

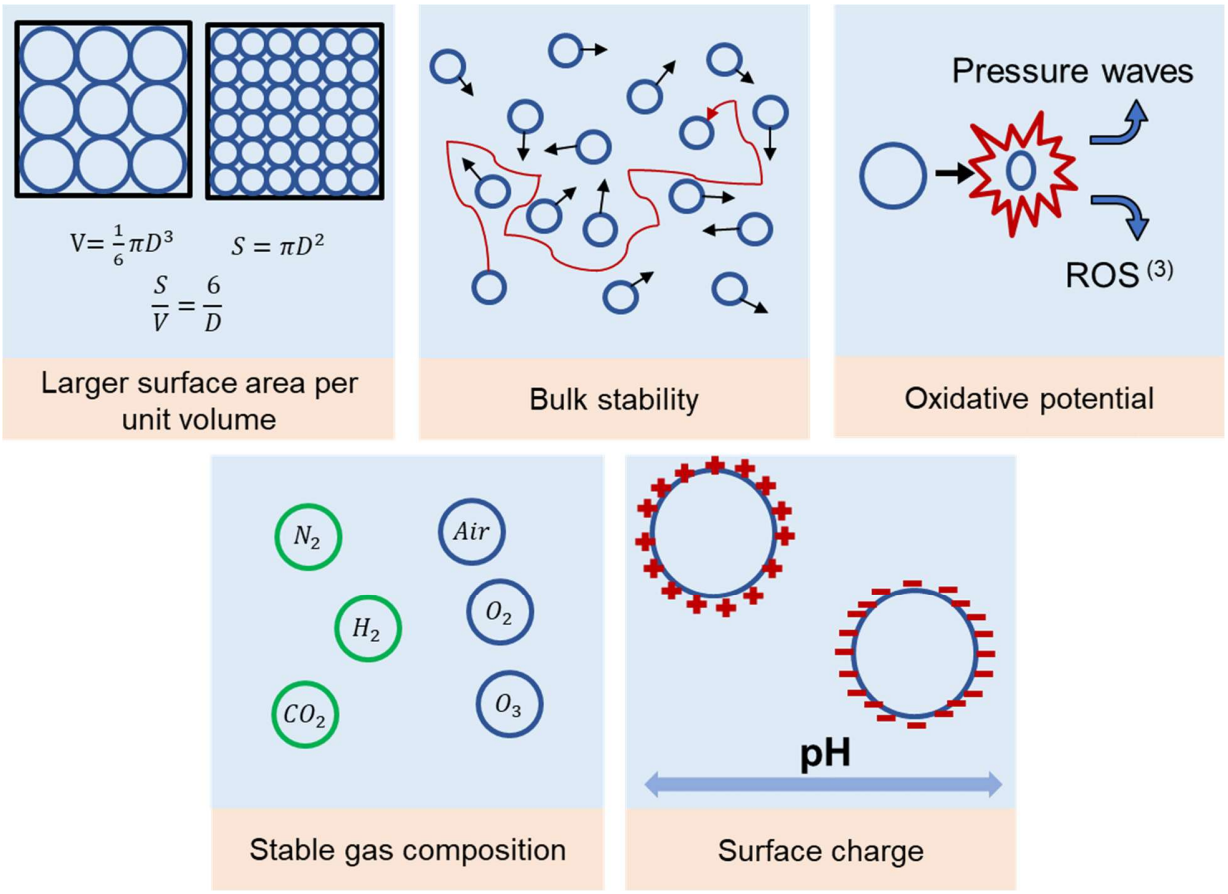

Figure 3.2-3: Characteristics of NBs.

$$\Delta P = P_{inside} - P_{outside} = \frac{4\sigma}{D} \tag{12}$$

Where:

ΔP is the difference in the pressure inside and outside a bubble

σ is the surface tension

D is the diameter of the bubbles

Several models to account for the unusual stability of NBs have been presented. The skin model predicts that an organic skin covers the surface of a NB. As the NB shrinks by diffusion, more of its surface is covered by the organic skin, which mechanically

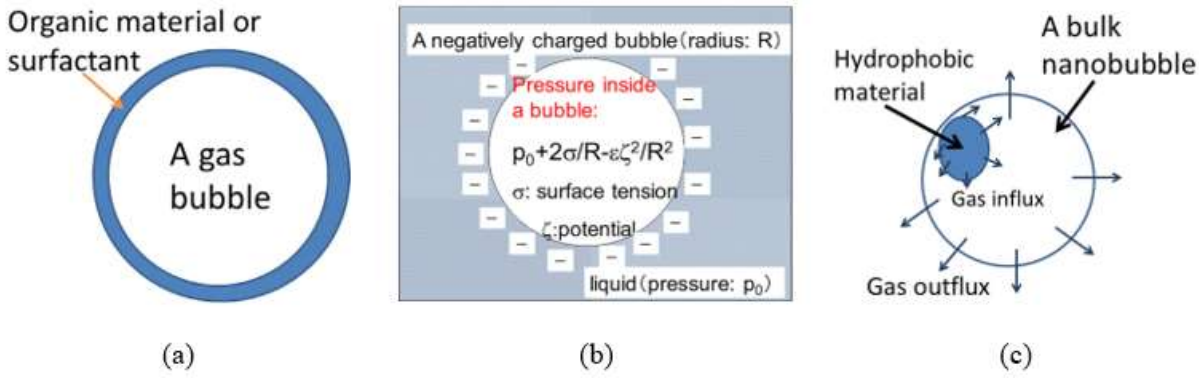

Figure 3.2-4: Models of the stability of NBs: (a) skin model, (b) electrostatic repulsion model and (c) dynamic equilibrium model (source: Yasui et al., (2018).

prevents it from losing gas by diffusion (Figure 3.2-4 (a)). The electrostatic repulsion model considers if the electrostatic repulsion of the negative charge on the surfaces of NBs could balance with the Laplace pressure. In this way, gas diffusion could be prevented and bubble stability achieved (Figure 3.2-4 (b)). The dynamic equilibrium model of a bulk nanobubble is based in a balance of influx and outflux gas in a bubble. Hydrophobic material partially covering the surface of a NB increases the concentration of gases near its surroundings. These gases diffuse into the bubbles cancelling the gas outflux and stabilizing the bubble (Figure 3.2-4 (c)).

3.2.5 Applications of nanobubbles

Although some things about NBs are still not well understood, research on their application has been increasing, and their existence has been established [11]. Due to their various properties, NBs have several industrial applications and have been applied in several different study fields. Their oxidative potential provides a door for use in disinfection, biology and water treatment. Researchers have identified strains of the bacteria *Vibrio parahaemolyticus* that causes early mortality syndrome/acute hepatopancreatic necrosis disease (EMS/AHPND) in shrimps. This has damaged shrimp farming is several areas in Asia and North America. Ozone is often used to prevent the spread of these bacteria, but it is unstable and decomposes rapidly. In this study NBs were used to stabilize ozone and applied to sterilize a stain of *Vibrio*

parahaemolyticus causing EMS/AHPND. White leg shrimp were placed in 10 L seawater containing ozone NBs (ONB) and a strain of *Vibrio parahaemolyticus* EMS/AHPND. After 1 minute incubation, all tested bacteria were killed [12]. The identification of reactive oxygen species (ROS) produced by NBs and their effect on vegetable seed germination was investigated. Fluorescent reagent Aminophenyl fluorescein (APF), a Fenton reaction, was used to identify which types of ROS, from among superoxide anion radical ($O_2^{\cdot -}$), hydrogen peroxide (H_2O_2), hydroxyl radical (·OH), and singlet oxygen ($^1O_2$), are produced by NBs. It was found that the ROS produced by NBs is the ·OH, and that its role in physiological processes depends on its concentration. Finally, the germination rate of spinach seed in distilled water, low-number density NB water, and high-number density NB water were investigated. The germination rates were 69%, 65%, and 54% for high-number density NB water, low-number density NB water, and distilled water, respectively [13,14]. The mass transfer of NB and its effect on biofilms growth were also investigated. NB aeration and coarse bubble (CB) aeration were applied in two separated biofilms systems, and their effect on biofilm growth was assessed. The NB aerated biofilm had a higher concentration of dissolved oxygen (DO), which increased microbial activity and enhanced its growth [15]. NBs have also been used in cleaning experiments. Defouling was performed by feeding air NBs into the surface of ceramic membranes clogged with humic acids. It was possible to restore the membrane flux to its initial state. The mechanism behind the cleaning potential of NBs was considered the generation of free radicals that bond with organic foulants and break them down. It was considered that NBs could provide an economic benefit by minimizing the usage of chemicals[16]. NBs have also been used to clean Protein-coated surfaces. Bovine serum albumin (BSA) was used as a surface contaminant in a solid-liquid interface. Electrochemically generated NBs cleaned both hydrophobic and hydrophilic surfaces. When this approach was compared with Sodium dodecyl sulfate (SDS) cleaning, different results were obtained in hydrophobic and hydrophilic surfaces. Nanobubble cleaning was more efficient than SDS cleaning in the hydrophobic surface and equally efficient in hydrophilic surfaces [17,18]. Other researchers obtained different conclusions about the efficiency

when hydrophobic surfaces were cleaned was not as apparent as when hydrophilic surfaces were cleaned. NBs generated by electrolysis could remove contaminants such as BSA and lysozyme from hydrophilic surfaces. It was also confirmed that, in addition to cleaning surfaces, NBs could prevent surface contamination. This effect was observed in both hydrophilic and hydrophobic substances [19]. Nanobubble's cleaning efficiency was also confirmed by other research groups that used similar foulants such as BSA and similar methods to generate NBs such as electrolysis. It was confirmed by atomic force microscopy that NBs could be produced in stainless steel (SS) surfaces either with or without absorbed BSA. This approach could remove more than 10% of the contaminants per cycle, totalizing 73% removal. On the other hand, only 3% removal per cycle was accomplished when washing with water and electrolyte. This study concludes that NBs are convenient, cheap, and promising for industrial application[20]. Other methods of generating NBs have also been used. Alcohol-water exchange processes generate NBs due to the difference in solubility in the solutions. Nanoparticles were removed from plain and patterned surfaces using alcohol-water exchange generated NBs. This method was compared with other methods that do not generate NBs, including water washing, alcohol wash, and water-alcohol exchange wash. These methods could not remove contaminants from the surfaces, while NBs could remove from 80-90 % of the particles in a single cleaning cycle [21].

REFERENCES

[1] T. Asano, L.F. Burton, L.H. Leverenz, R. Tsuchihashi, G. Tchobanoglous, Water Reuse. Issues, technologies, and applications, 1st ed., The McGraw-Hill Companies, 2007.

[2] L. Bridgewater L., Standard methods for the examination of water and wastewater, 23rt editi, American Public Health Association, 2017.

[3] Metcalf, Eddy, Wastewater engineering : treatment, disposal, and reuse, 5th ed., McGraw Hil Educationl, 2014.

[4] Z. Wang, J. Ma, C.Y. Tang, K. Kimura, Q. Wang, X. Han, Membrane cleaning in membrane bioreactors: A review, J Memb Sci 468 (2014) 276–307. https://doi.org/10.1016/J.MEMSCI.2014.05.060.

[5] T. Kurita, K. Kimura, Y. Watanabe, The influence of granular materials on the operation and membrane fouling characteristics of submerged MBRs, J Memb Sci 469 (2014) 292–299. https://doi.org/10.1016/j.memsci.2014.05.057.

[6] Y. Ninomiya, K. Kimura, T. Sato, T. Kakuda, M. Kaneda, A. Hafuka, T. Tsuchiya, High-flux operation of MBRs with ceramic flat-sheet membranes made possible by intensive membrane cleaning: Tests with real domestic wastewater under low-temperature conditions, Water Res 181 (2020) 115881. https://doi.org/https://doi.org/10.1016/j.watres.2020.115881.

[7] S.H. Chae, M.S. Kim, J.-H. Kim, J.D. Fortner, Nanobubble Reactivity: Evaluating Hydroxyl Radical Generation (or Lack Thereof) under Ambient Conditions, 10 (n.d.) 2023. https://doi.org/10.1021/acsestengg.3c00124.

[8] M.U. Farid, P.J. Choi, J.A. Kharraz, J.Y. Lao, S. St-Hilaire, Y. Ruan, P.K.S. Lam, A.K. An, Hybrid nanobubble-forward osmosis system for aquaculture wastewater treatment and reuse, Chemical Engineering Journal 435 (2022) 135164. https://doi.org/10.1016/J.CEJ.2022.135164.

[9] S. Tanaka, H. Kobayashi, S. Ohuchi, K. Terasaka, S. Fujioka, Destabilization of ultrafine bubbles in water using indirect ultrasonic irradiation, Ultrason Sonochem 71 (2021) 105366. https://doi.org/10.1016/j.ultsonch.2020.105366.

[10] A.J. Atkinson, O.G. Apul, O. Schneider, S. Garcia-Segura, P. Westerhoff, Nanobubble Technologies Offer Opportunities to Improve Water Treatment, Acc Chem Res 52 (2019) 1196–1205. https://doi.org/10.1021/acs.accounts.8b00606.

[11] A.J. Jadhav, M. Barigou, Bulk Nanobubbles or Not Nanobubbles: That is the Question, (2020). https://doi.org/10.1021/acs.langmuir.9b03532.

[12] K. Imaizumi, S. Tinwongger, H. Kondo, I. Hirono, Disinfection of an EMS/AHPND strain of Vibrio parahaemolyticus using ozone nanobubbles, J Fish Dis 41 (2018) 725–727. https://doi.org/10.1111/jfd.12783.

[13] S. Liu, S. Oshita, Y. Makino, Q. Wang, Y. Kawagoe, T. Uchida, Oxidative Capacity of Nanobubbles and Its Effect on Seed Germination, (2015). https://doi.org/10.1021/acssuschemeng.5b01368.

[14] S. Liu, S. Oshita, S. Kawabata, Y. Makino, T. Yoshimoto, Identification of ROS Produced by Nanobubbles and Their Positive and Negative Effects on Vegetable Seed Germination, Langmuir 32 (2016) 11295–11302. https://doi.org/10.1021/acs.langmuir.6b01621.

[15] W. Xiao, G. Xu, Mass transfer of nanobubble aeration and its effect on biofilm growth: Microbial activity and structural properties, Science of the Total Environment 703 (2020). https://doi.org/10.1016/j.scitotenv.2019.134976.

[16] A. Ghadimkhani, W. Zhang, T. Marhaba, Ceramic membrane defouling (cleaning) by air Nano Bubbles, Chemosphere 146 (2016) 379–384. https://doi.org/10.1016/J.CHEMOSPHERE.2015.12.023.

[17] G. Liu, V.S.J. Craig, Improved Cleaning of Hydrophilic Protein-Coated Surfaces using the Combination of Nanobubbles and SDS, (2009). https://doi.org/10.1021/am800150p.

[18] G. Liu, Z. Wu, V.S.J. Craig, Cleaning of Protein-Coated Surfaces Using Nanobubbles: An Investigation Using a Quartz Crystal Microbalance, (2008). https://doi.org/10.1021/jp805143c.

[19] J. Zhu, H. An, M. Alheshibri, L. Liu, P.M.J. Terpstra, G. Liu, V.S.J. Craig, Cleaning with Bulk Nanobubbles, (2016). https://doi.org/10.1021/acs.langmuir.6b01004.

[20] H. Chen, H. Mao, L. Wu, J. Zhang, Y. Dong, Z. Wu, J. Hu, Defouling and cleaning using nanobubbles on stainless steel., Biofouling 25 (2009) 353–357. https://doi.org/10.1080/08927010902807645.

[21] S. Yang, A. Duisterwinkel, Removal of Nanoparticles from Plain and Patterned Surfaces Using Nanobubbles, (2011). https://doi.org/10.1021/la2010776.

CHAPTER 4: NANOBUBBLE-ASSISTED BACKWASHING

In this chapter NBB is investigated for the first time. A comparative study between NBB, TWB and CEB was made. An assessment of the effect of the concentration of NBs and their impact on the mixed-liquor suspension was made. It was shown that NBB is more effective than TWB. The concentration of NBs influences the cleaning efficiency.

4.1 Methods

4.1.1 Parallel operation of bench-scale MBRs

Flat-sheet ceramic membranes (material: Alumina-Al_2O_3) with a nominal pore size of 0.1 µm and an available area of 0.04 m^2 (Meidensha, Tokyo, Japan) were inserted in each of the three identical bench-scale MBRs. Pure water permeability and porosity of the membrane used in this study were 7.7±0.4 L m^{-2} h^{-1} kPa^{-1} and 44.1±1.0 [1], respectively. The three MBRs were repeatedly operated side by side at an existing municipal wastewater treatment plant in Sapporo, Japan. Average values of the pH and electrical conductivity of the influent wastewater were 7.3 and 400 µS cm^{-1}, respectively. In Japan, any industrial wastewater that may have harmful effects on treatment needs to be adequately treated before it is discharged to the public sewer

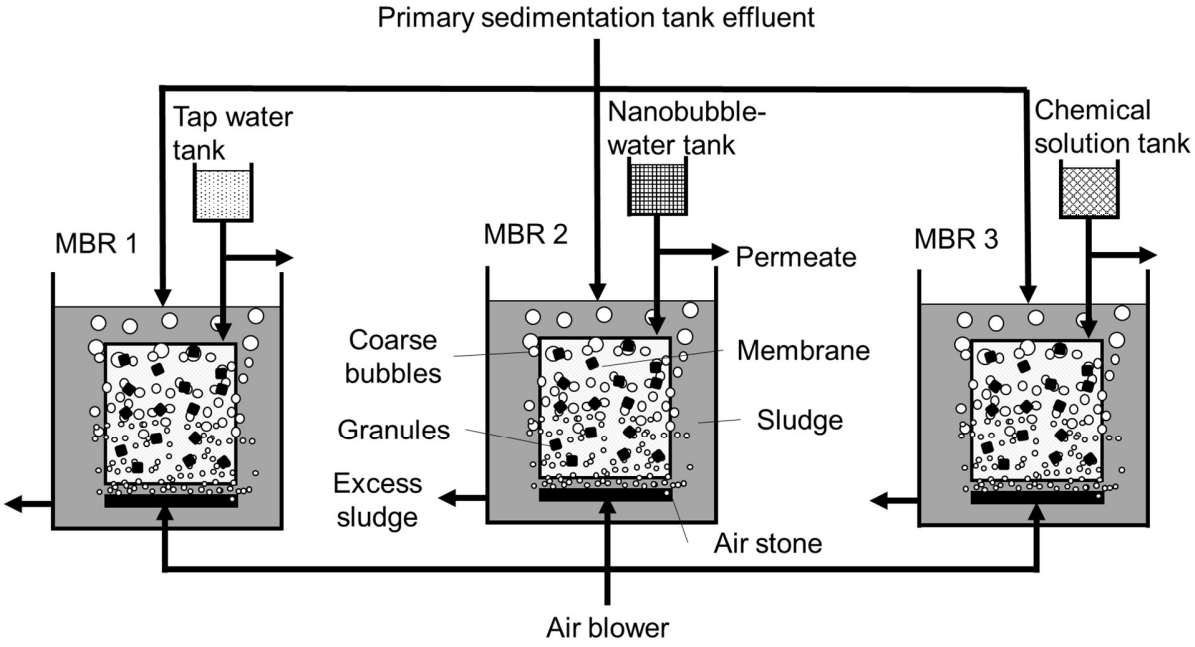

Figure 4.1-1: Schematic figure of the experimental setup in the NBB experiment.

system. Therefore, it is thought that the impact of industrial wastewater was minor in this study. A schematic figure of each MBR system is presented in Figure 4.1-1. The seed biomass used in all experiments was sourced from a pilot-scale MBR installed at the same facility. A volume of 7.5 liters of aerated sludge was manually transferred from the pilot-scale MBR to each bench-scale MBR before starting the operation. All three bench-scale MBRs shared the same influent wastewater (effluents from the primary sedimentation tank) and were operated under the same conditions except for the backwash solutions as described in the next section.

The operation of the bench-scale MBRs was conducted at a SRT of 30 days, which was the same as that for the pilot-scale MBR. It was therefore assumed that acclimatization for the bench-scale MBRs was not necessary, and the operation of the reactors was initiated immediately after the seeding of the biomass. Aeration was continuously conducted in the tanks during the operation at a fixed rate of 0.012 Nm3 min^{-1}. Four runs of the experiments (Runs 1-4) were conducted in different seasons and at different permeate fluxes to investigate the efficiency of NBB. The operational

Table 4.1-1: Experimental conditions in Runs 1-5.

	MBR	Temperature (ºC)	MLSS (g L^{-1})	pH	Permeate flux (LMH)	Influent (mg L^{-1})			
						TOC*	SS	T-N	T-P
Run 1 (Summer)	TWB	22.0±0.7	8.3±0.2	6.0±0.3	60	59.0	104.5±35.5	29.0±5.0	5.2±0.7
	NBB	22.0±0.7	8.1±0.1	5.9±0.5					
	CEB	22.2±0.6	8.4±0.3	6.1±0.5					
Run 2 (Autumn)	TWB	19.8±0.5	8.3*	6.9±0.2	50	28.5	66.0±6.0	27.0±2.0	2.7±0.2
	NBB	19.9±0.5	7.6*	6.7±0.3					
	CEB	19.9±0.4	7.1*	6.7±0.2					
Run 3 (Winter)	TWB	19.0±0.5	5.6±0.1	5.4±0.4	50	25.1	47.0±5.0	26.5±1.5	2.6±0.2
	NBB	19.4±0.4	5.1±0.1	5.4±0.5					
	CEB	19.4±0.4	4.7±0.2	5.1±0.4					
Run 4 (Winter)	TWB	19.9±0.5	3.2±0.4	6.8±0.6	50	35.9	63.0±10.0	24.0±0.0	2.3±0.0
	NBB	20.4±0.5	3.0±0.7	6.1±0.8					
	CEB	20.4±0.5	2.7±0.8	6.0±0.5					
Run 5 (Summer)	TWB	25.3±0.3	7.1±0.9	6.6±0.3	80	47.9	52.0±5.0	29.0±1.0	2.9±0.1
	NBB	25.2±0.3	7.2±0.7	6.8±0.3					
	CEB	25.3±0.3	6.4±0.8	6.6±0.3					

*: Average values cannot be shown because only one data was available

conditions in Runs 1-4 are shown in Table 4.1-1. The permeate fluxes of the bench-scale MBRs in Runs 1-4 were set at high values of 50 and 60 and L m^{-2} h^{-1} (LMH), which is considerably high compared to the standard practice in a full-scale MBR operation in which the flux is generally set in the range of 15–25 LMH [2]. Such high fluxes were applied in this study to accelerate membrane fouling and facilitate distinguishing the differences in fouling in the three MBRs backwashed with different solutions. The cleaning intensity applied in this study was high and it was expected that it would take a long time to observe fouling when the flux was set at a normal

value such as 20 LMH. The MLSS concentration in the bench-scale MBRs were different in each run of experiments, reflecting fluctuations in the quality of wastewater entering the wastewater treatment plant (WWTP) and the conditions in the pilot-scale MBR from which the seeding biomass was obtained.

To investigate the mechanisms by which NBB can mitigate fouling, another experiment (Run 5) was carried out to perform various analyses for the fouled membranes and the characteristics of sludge. The operational conditions in Run 5 are also shown in Table 4.1-1. In Run 5, a further higher flux of 80 LMH was set in order to accelerate fouling and clarify the differences caused by different backwashing solutions.

4.1.2 Membrane cleaning measures

Intermittent filtration was carried out in all runs. A 1-min pause was provided for every 11 min of filtration time. Cylindrical PEG granular materials (size: 4 mm, specific density: 1.01 g cm^{-3}) were placed in each membrane tank (5% volume of the membrane tank) to scour the membrane surface. The granules were kept suspended by coarse bubble aeration provided from the bottom of the reactor. High efficiency of granular scouring for cleaning membranes in MBRs, particularly when combined with CEB [3], has already been confirmed [4]. The use of robust membranes enables the application of such intensive cleanings, and that is why ceramic membranes were used in this study.

Periodical backwashing cleaning was automatically carried out in this study. Different solutions were used for backwashing in the three MBRs, whereas the frequency, duration, and backwashing flux were the same. MBR 1 was operated with hydraulic backwashing using tap water (TWB). Tap water was also used for the preparation of NB water and the 50 ppm NaClO solution used for NBB (MBR 2) and CEB (MBR 3), respectively. In this study, 50 ppm NaClO was chosen as a reagent for CEB because it could effectively control the fouling in MBRs operated at the same WWTP [3]. Backwashing was conducted periodically for every 5 hours of filtration, at

a constant flux of 8 LMH. Backwashing lasted for 60 min with aeration and granular scouring in each event. These backwashing conditions were chosen on the basis of our previous study [3], in which the combination of granular scouring and CEB using 50 ppm NaClO exhibited a high cleaning efficiency.

4.1.3 Generation of nanobubbles (NBs)

Nanobubbles (source: air) were generated using a commercially available NB generator manufactured by IDEC Corporation (FZ1N-7H, Osaka, Japan). NB water was generated in the laboratory with tap water and used for NBB at the experimental site within 15 hours after generation. It has been reported that NBs stably exist in water over a long period (e.g., several weeks) [5,6]. The long-term stability of NBs was also verified in our previous study (APPENDIX Fig. A1). Particle numbers before and after generating NBs were measured (APPENDIX Fig. A2). As shown in appendix Fig. A2, the particle number significantly increased after the generation of NBs, and it was confirmed that NBs quantified in this study were not other particles. It was therefore assumed that NBs were present in bulk and mostly maintained when they were used for NBB at the experimental site. NTA NanoSight 500 was used to measure the size distribution and concentration of NBs.

4.1.4 Measurement of filtration resistances of membranes

The distribution of filtration resistances of the membranes was assessed prior to and at the termination of each run. The fouled membranes were taken out of the tanks, immersed in tap water and subjected to the measurement of water filterability. The filtration resistances were measured according to the method described in section 3.1.8.

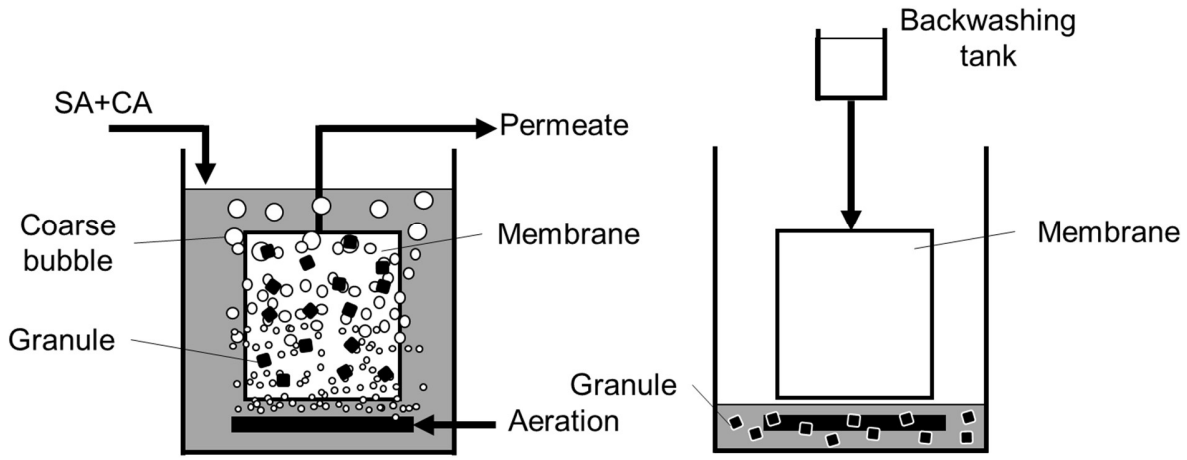

Figure 4.1-2: Experimental apparatus of the experiment on model foulants and HC-NB.

4.1.5 Effect of the concentration of nanobubbles on fouling mitigation

4.1.5.1 Membrane backwashing using model foulants

Figure 4.1-2 summarizes the experimental apparatus. Additional information about the experimental conditions is shown in Table 4.1-2.Three types of backwashing agents were used: tap water (TW), NBW, and HC-NBW. The experimental procedures can be summarized in two steps: fouling test and cleaning test. To obtain the fouled membranes, filtration a sodium alginate solution (20 mg-TOC L^{-1} + Ca 20 mg L^{-1}) was

Table 4.1-2: Experimental conditions on model foulants and HC-NB.

Operational conditions	
Membrane type	Flat-sheet ceramic
Membrane area	0.02 m^{-2}
Membrane pore size	0.1 μm
Volume of tank	447.5 L
Influent foulant	Sodium alginate (20 mg-TOC L^{-1}) + CA (20 mg L^{-1})
Granules	PEG (5%)

performed for one hour at a constant flux of 50 LMH. This was followed by one hour of backwashing at 9.6 LMH with each type of backwashing solution. The backwashing was conducted after draining the membrane tank, and the backwash water was collected. The amount of foulant released by backwash in each cleaning experiment was compared by measuring the TOC concentration in the collected backwash water.

In a previous experiment (data not shown), the cleaning efficiency of TW, NBW, and HC-NBW was compared using a similar procedure. A significant difference at a 5% significance level was observed in the permeation performance recovery rates between TW and HC-NBW, indicating the superiority of HC-NBW. Although HC-NBW had a higher permeation performance recovery rate than NBW, the difference was not significant. In the previous study, backwashing was conducted for 10 minutes in a tank filled with influent water. Extending the backwashing time and conducting it in an empty tank was expected to increase the contact time between the nanobubble water and the fouling layer, making the impact of nanobubble concentration on cleaning efficiency more noticeable.

The cleaning efficiency was evaluated by measuring the membrane filtration resistance values of the new membrane, the fouled membrane after the fouling step, and the membrane after each cleaning. The recovery rate of permeation performance was calculated using the following formula:

$$RE = \frac{R_f - R_m}{R_f - R_c} \times 100\% \quad (13)$$

Where:

RE recovery rate of permeation performance (%)

R_f is the membrane filtration resistance of the fouled membrane (m^{-1})

R_m the membrane filtration resistance of the virgin membrane (measure before the fouling test) (m^{-1})

R_c the membrane filtration resistance of cleaned membrane (measured after the cleaning step) (m^{-1})

4.1.5.2 Investigation of High-Concentration Nanobubble Backwashing in MBR

Figure 4.1-3 shows the experimental apparatus used in this study. This experiment aimed to investigate the effect of nanobubble concentration on cleaning efficiency by operating a bench-scale MBR treating real municipal wastewater and using high-concentration nanobubbles for backwashing. The previous experiment with model foulants demonstrated the higher cleaning efficiency of high-concentration nanobubbles compared to regular nanobubbles. This experiment investigated the cleaning efficiency against membrane fouling in an MBR treating real municipal wastewater using high-concentration nanobubble water for backwashing.

The same experimental apparatus used in previous studies were used in this study. Three bench-scale MBRs were operated simultaneously under identical conditions using influent water from the primary sedimentation tank at Soseigawa WWTP. Intermittent filtration was performed with 11 minutes of filtration followed by a 1-

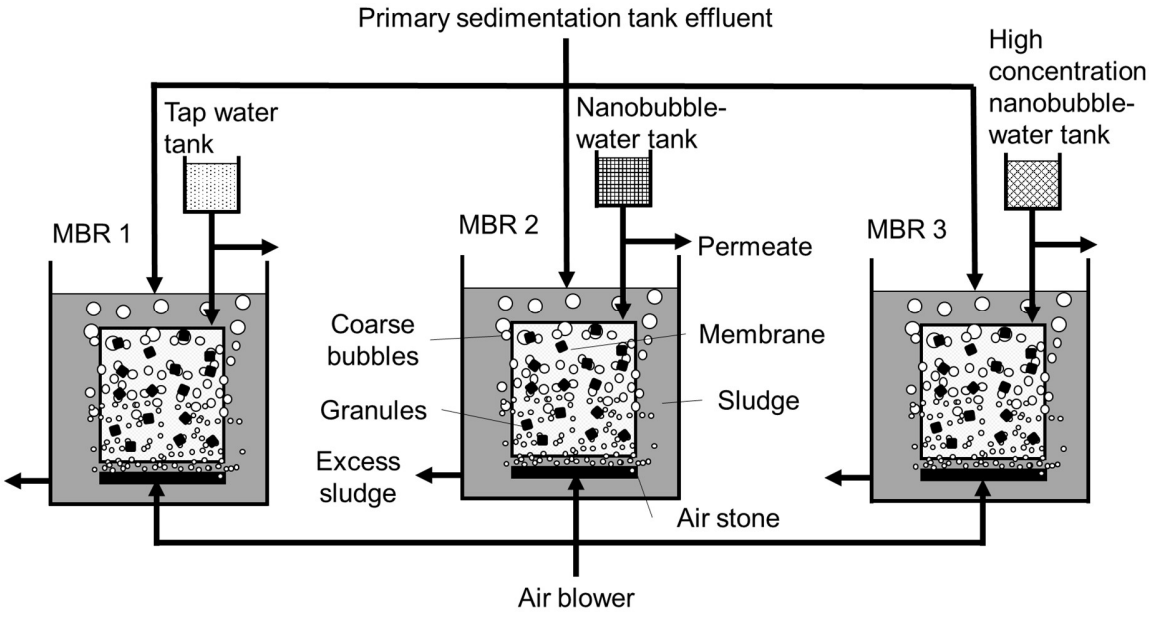

Figure 4.1-3: Schematic figure of the experimental setup of HC- NB experiment

minute rest. Backwashing was conducted for one hour after every 5 hours of intermittent filtration, following conditions from previous research where CEB with sodium hypochlorite showed high cleaning efficiency. Aeration was maintained at 12 L/min. The filtration flux was set at 50 LMH, higher than typical MBRs, to induce membrane fouling over a shorter period and evaluate the cleaning efficiency. The same ceramic flat membrane used in the previous model foulant experiment was employed, and PEG granules were used as carriers. Previous research indicated that these granules synergize with nanobubble cleaning. At the termination of the experiment, foulants attached to the surface of the membranes were collected with a brush. Measuring the TOC concentration of these foulants were conducted. HC-NBW used in this study was generated as described in section 3.2.2.

4.1.6 Generation of ROS by NBs

It was previously mentioned in section 3.2.3 that NBs could generate ROS, as reported by several studies. However, the generation of ROS by NBs might occur in very narrow conditions, and the measurement of NB-generated ROS is still a controversy. Therefore, the measurement of ROS generated by NBs was conducted. Two methods were applied: first, fluorescence Spectrophotometry using APF as a probe; and second, degradation of disodium terephthalate (TP) by NB-generated ROS.

4.1.6.1 ROS measurement APF fluorescein

APF generates fluorescein, a highly fluorescent compound, in the presence of ROS. Therefore, if NBs generate ROS, it is possible to detect them by measuring fluorescein in APF-added NB samples. NB water was generated as previously described (3.2.2). Three NB water samples were prepared with different dilution factors: No dilution, 10 times dilution and 100 times dilution. Hydrogen peroxide (H_2O_2) samples were prepared at three different concentrations (10mM, 1mM and 0,1 mM), serving as control samples. Two sets of samples were prepared: one that was submitted to ultrasonication and another that was not. APF was added to each sample and the

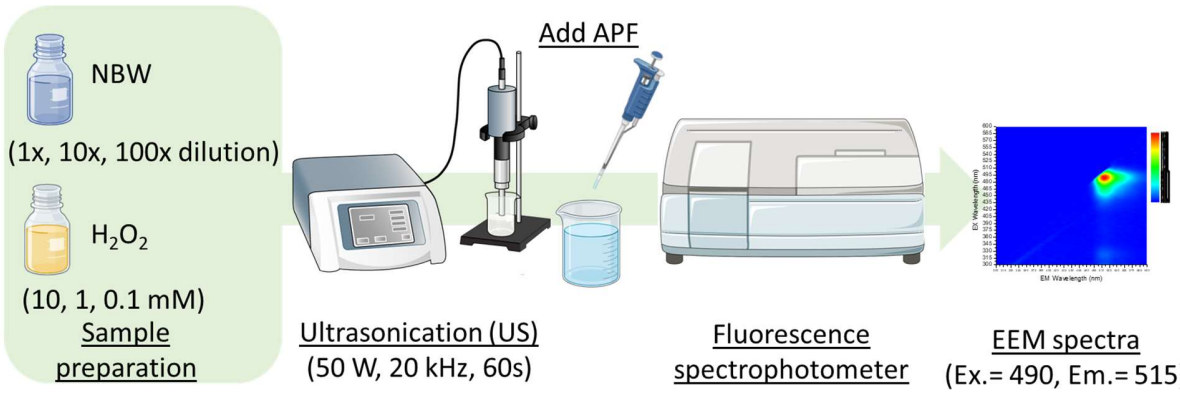

Figure 4.1-4: Schematic illustration of the ROS measurement by APF fluorescein (made with biorender)

fluorescence response at 515 nm with excitation at 490 nm was assessed by EEM. The experimental procedures are summarized in Figure 4.1-4.

4.1.6.2 ROS measurement by TPOH fluorescence

Disodium terephthalate (TP) generates 2-hydroxyterephthalate (TPOH) with a percent yield of 35% and other products in the presence of hydroxyl radicals (·OH), as shown in the reaction below. TPOH has a fluorescence intensity emitted at 425 nm when excited at 315 nm. NBs were generated in a TP water (30 mg-TOC L^{-1}) for 120 minutes. Samples were taken and fluorescence intensity was measured with EEM. As a control experiment, a commercially available TPOH was acquired and dissolved in water at a concentration of 3 mg-TOC L^{-1}. TPOH samples were also excited at 315 nm. The experimental procedures are summarized in Figure 4.1-5.

Disodium terephthalate + ·OH radical ➔ 2-hydroxyterephthalate + further products (14)

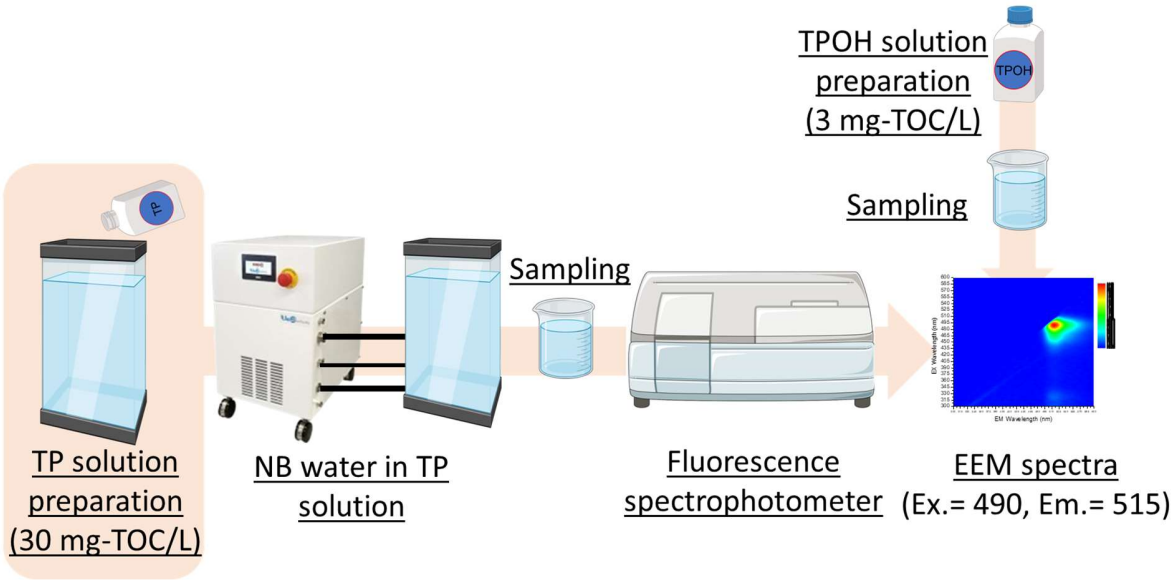

Figure 4.1-5: Schematic illustration of the ROS measurement by TPOH fluorescence (made with biorender)

4.1.6.3 Contact angle of nanobubble suspensions

Contact angles of tap water, nanobubble water and high concentration nanobubble water were measured on a Polyvinylidene fluoride (PVDF) ultrafiltration membrane sheet. Contact angles of fluids on a surface are an indirect measurement of their surface tension, which indicates the liquids' wetting properties. Lower contact angles and surface tension suggest higher wetting properties, and therefore, higher cleaning capabilities. On the other hand, if the contact angle is high, surface tension is also high and the wetting/cleaning properties of the fluid in question are reduced. That being said, the contact angles of backwashing solutions used for the cleaning of membranes used in MBRs can indirectly measure their cleaning properties. Therefore, in this section a description of the measurement of the contact angles of backwashing solutions used in this study (TW, NBW, HC-NBW) are presented. The contact angle measurements ware conducted by using a contact angle meter (DropMaster 300), as illustrated in Figure 4.1-6.

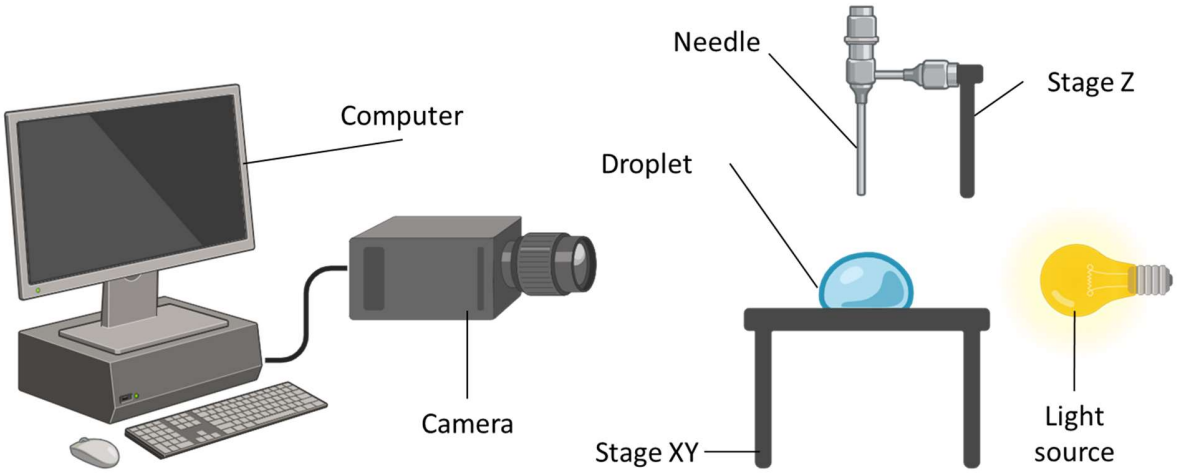

Figure 4.1-6: Schematic illustration of contact angle measurement (made with biorender)

4.1.7 Analytical methods

Sludge samples from each bench scale MBR were aerated until reaching saturation. They were placed inside an incubator (MIR-154-PJ, PHC Holdings Corporation, Tokyo-Japan). The oxygen consumption was measured and recorded every 10 minutes by a dissolved oxygen (DO) meter (DKK-TOA Corporation, MM-20P).

The concentrations of total organic carbon (TOC) and dissolved organic carbon (DOC) in the feed and permeate samples were measured by a TOC analyzer (TOC-VCSH, Shimadzu, Kyoto, Japan). Concentrations of inorganic nitrogen forms, including ammonium NH_4^+, nitrite NO_2^- and nitrate NO_3^- were measured using an ion chromatography device (Thermofisher Scientific, Waltham, United States of America). Concentrations of MLSS and MLVSS were determined according to the standard methods [7]. Filterability of sludge in each MBR was characterized by CST, which was measured by a specifically designed device (CST-304B, Triton Electronics Ltd–United Kingdom). A liquid chromatography device equipped with an organic carbon detector (LC-OCD-Model 8, DOC-LABOR Dr. Huber, Karlsruhe, Germany) was used to fractionate the dissolved organic matter. Excitation-emission matrixes (EEMs) were generated by using a fluorescence spectrophotometer (Aqualog-DRJR764F, Horiba, Kyoto, Japan). Before the analysis for DOC, LC-OCD and EEMs, samples were

filtered through a 0.45-μm polytetrafluoroethylene (PTFE) filter (Advantec, Tokyo, Japan).

Foulants deposited on the membrane surface were collected for analysis using Fourier-transform infrared spectroscopy (FT-IR). Freeze-dried samples were mixed with potassium bromide (KBr) at a 1:200 ratio and then analyzed using an infrared spectrophotometer (FT-IR-8400S, Shimadzu, Kyoto, Japan). Scanning electron microscopy (SEM) (S-4000, Hitachi, Tokyo, Japan) was used to observe the surfaces and cross-sections of the membranes fouled in Run 5. To observe the cross-section of the fouling layer, the fouled membranes were broken into small pieces (about 1 cm^2) by using a needle and a hammer, and they were immersed in 2% glutaraldehyde with 0.1 M phosphate buffer (pH 7.2) at 5°C for two hours to fix the structure of the fouling layer. The treated samples were then fixed with 1% osmium tetroxide with 0.1 M phosphate buffer at room temperature for 2 hours. The fixed samples were dehydrated at a series of different concentrations of ethanol. Before observing the membrane surfaces by SEM, the samples were dried using a critical point drying apparatus (EM-CPD300, Leica microsystems, Wetzlar, Germany). They were subsequently coated with an Auto Fine Coater (JFC-1200, JEOL, Tokyo, Japan) using a platinum sputter to prevent the accumulation of a static electric charge during observations. The morphology of the fouled membrane surface was also visualized by using atomic force microscopy (AFM) (SPA-400, Hitachi, Tokyo, Japan).

4.2 Results and discussion

4.2.1 NB size distribution

Representative size distributions of NBs measured before and after passage through the ceramic membrane used in this study were shown in section 2.5. It was assumed that NBs could be transported to the fouling layer from the permeate side during NBB.

4.2.2 Cleaning achieved by NBB

Figure 4.2-1 shows increases in TMP observed in Runs 1-4 in the three MBRs operated side by side with different backwashing solutions (MBR 1: TWB, MBR 2: NBB, MBR 3: CEB). The increase in TMP shown in Figure 4.2-1 was relatively rapid as a result of setting membrane fluxes at high values of 50-60 LMH. Runs 1-4 were

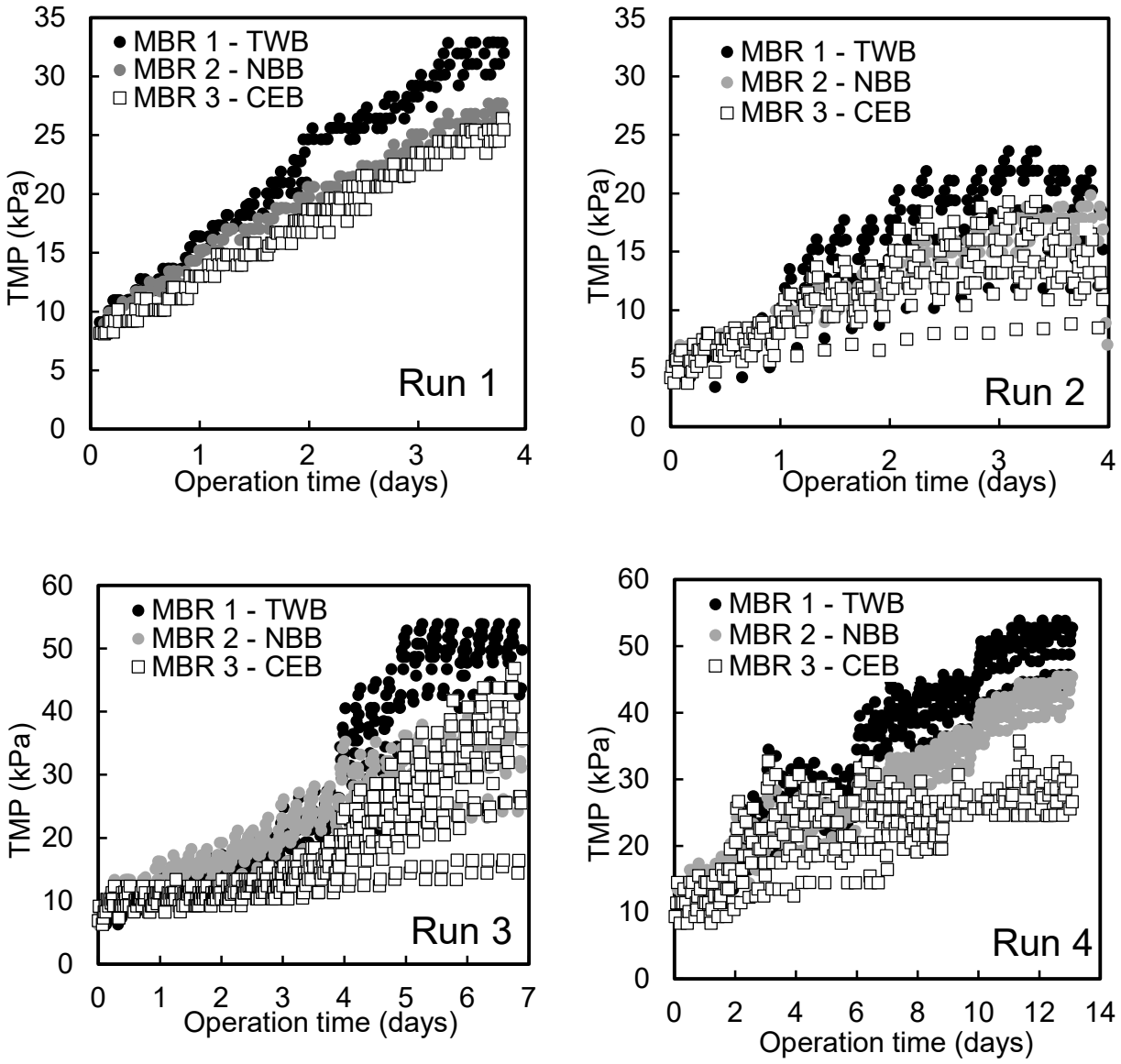

Figure 4.2-1: Increases in TMP observed in Runs 1-4. Permeate fluxes: Run 1 (60 LMH), Runs 2-4 (50 LMH).

carried out in different seasons. The quality of the feed water (i.e., the effluent from

the primary sedimentation basin) was therefore different in Runs 1-4: it should be noted that real domestic wastewater was used in this study. Differences in the rates of TMP increases and displayed in the four panels of Figure 4.2-1 partly reflect the differences in the feed water quality. Oscillations in TMP shown in Figure 4.2-1 represent quick reattachments of foulants that were dislodged and/or compaction of the fouling layer that was loosened in the previous backwash. Regardless of the season when the experiments were carried out (i.e., quality of the feed wastewater), as shown in Figure 4.2-1, NBB exhibited better cleaning performance than did TWB. Data on the filtration resistance assessed in Runs 1-4 are shown in appendix Fig. A3. The mitigation of reversible fouling was more significant in the case of NBB when compared to TWB. Irreversible fouling could be controlled relatively well by NBB and CEB, although protection by the fouling layer (reversible fouling) was limited. This indicates that NBs enhanced cleaning efficiency when introduced into the backwashing solution. As expected, CEB was much more efficient than TWB. It

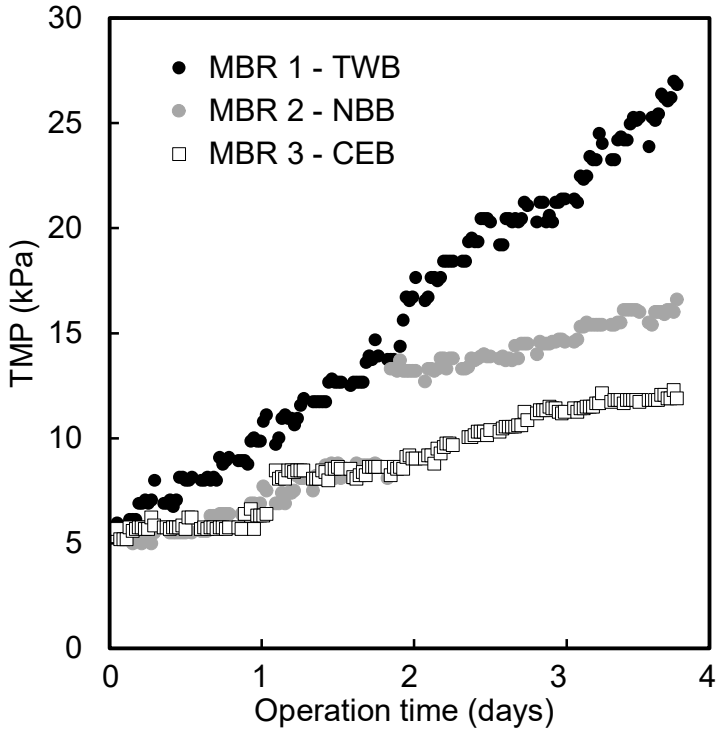

Figure 4.2-2: TMP increases in Run 5 (permeate flux: 80 LMH).

should be noted, though, that the performance of NBB was sometimes comparable to that of CEB (Runs 1 and 2). Inevitable changes in the quality of municipal wastewater and temperature in the MBR tanks might explain the different effectiveness of NBB in Runs 1-4 compared to CEB. TMP data were converted to temperature-corrected permeability data to remove the effect of temperature differences, as shown in appendix Fig. A4. Membranes cleaned with TWB showed more significant decreases in permeability than those cleaned with NBB and CEB. NBB was effective for fouling mitigation, and possible reasons for the high cleaning efficiency of NBB are discussed in the next section. The data shown in Figure 4.2-1 indicates an immense potential of NBB as an environmentally-friendly measure for cleaning fouled membranes.

4.2.3 Investigation of fouling mitigation caused by NBB in Run 5

4.2.3.1 Distribution of filtration resistances

Based on the results obtained in Runs 1-4, another experiment (Run 5) was conducted in order to try to reveal the mechanisms by which NBB improves cleaning efficiency. Figure 4.2-2 shows the increases in TMP observed in Run 5. Although a high permeate flux of 80 LMH was applied in Run 5, the rate of TMP increase was not much higher than that in Runs 1-4. This is due to the higher temperature in Run 5 (see Table 4.1-1) and a very good condition of the mixed liquor suspension in terms of filterability, as supported by low values of CST of the sludge samples collected from each bench-scale MBR (APPENDIX Fig. A5). In the cases of the reactors operated with CEB and NBB, the rates of TMP increase were low in Run 5, even at the high flux of 80 LMH. As shown in Figure 4.2-2, the performance of NBB was clearly higher than that of TWB and slightly less than that of CEB. On the second day of Run 5, a sudden increase in TMP was observed in MBR 2 (NBB). Although the reason for this increase in TMP could not be clearly identified, it is very likely that it was due to the daily adjustment of permeate flux. After that, however, increase in TMP in MBR 2 was hardly seen and the rate of TMP increase with NBB was comparable to that with CEB.

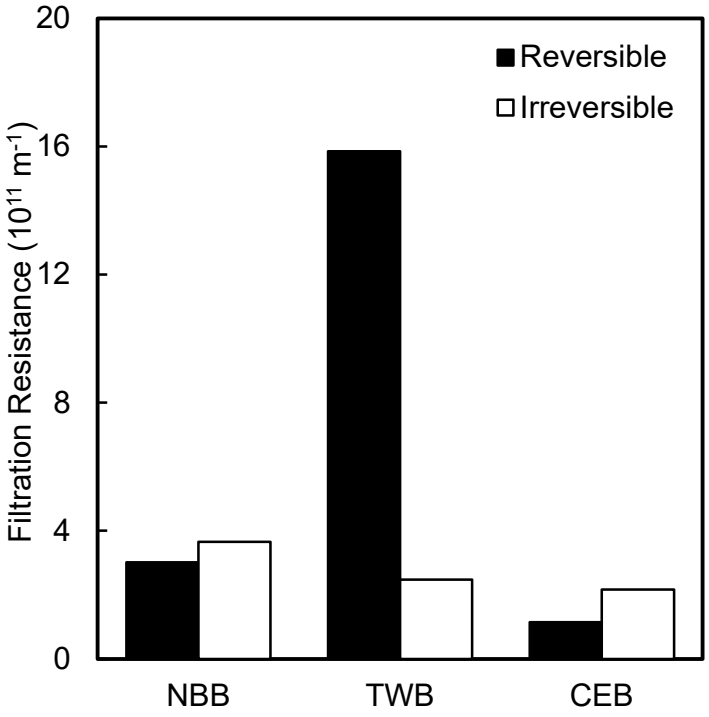

Figure 4.2-3: Distributions of membrane filtration resistances at the termination of Run 5.

The high cleaning efficiency of NBB observed in Runs 1-4 (Figure 4.2-1) could therefore be confirmed in Run 5. Temperature correction of membrane permeability was also performed for the data obtained in Run 5, as shown in appendix A4. Deterioration of permeability was less significant in the MBR cleaned with CEB. It was shown again that NBB was more effective for maintaining the permeability than was TWB. Temperature-corrected permeability data corroborates the TMP data shown previously. When Run 5 was terminated, the distribution of filtration resistances in the three MBRs was assessed. The intrinsic filtration resistances of the membranes used in Run 5 and operated with TWB, NBB and CEB were 2.17×10^{11} m^{-1}, 2.06×10^{11} m^{-1} and 2.15×10^{11} m^{-1}, respectively. The summation of the intrinsic and irreversible fouling resistances did not vary among the three MBRs, suggesting that differences in the degree of membrane fouling shown in Figure 4.2-2 were due not to pore fouling but to gel/cake layer formation. The distributions of filtration resistance assessed at the termination of Run 5 are shown in Figure 4.2-3, indicating

that surface fouling was dominant in the MBR operated with TWB. The severe degree of reversible fouling, which can be partly attributed to the high flux imposed in Run 5 (80 LMH), could not be mitigated with the combined effects of granular scouring and hydraulic backwashing. In contrast, MBR 2 (NBB) and MBR 3 (CEB) exhibited significantly lower degrees of reversible fouling, whereas the degrees of irreversible fouling were comparable among the three MBRs. It is expected that a thick fouling layer (as shown in section 4.2.3.5) on the surface of membranes operated with TWB would serve as a protective film helping to mitigate irreversible fouling. On the other hand, the low degree of irreversible fouling resistance in the cases of membranes cleaned by NBs and NaClO indicates that NBB and CEB were effective for mitigation of irreversible fouling even in the absence of such thick protective layers. The high cleaning efficiency of NBB observed was therefore attributed to the reduction of reversible (surface) fouling, which was also observed in Runs 1-4.

It could be argued that such a high permeate flux is uncommon in municipal applications of MBRs. Thus, the fouling developing in this study was more difficult to control/remove than that formed in MBR systems working at lower fluxes. As demonstrated in this work, NBB could work for control of the difficult fouling formed in this study. Therefore, it is safe to assume that NBB can also work for control of "easy" fouling observed in other MBRs operated at lower fluxes. As shown in the following sections, an attempt was made to determine why the introduction of NBs into the backwashing water can mitigate reversible fouling.

4.2.3.2 Influence of backwashing solution on sludge and treatment performance

The characteristics of the mixed liquor suspension and the permeate water quality in Run 5 are summarized in the appendix. Appendix Fig. A6 shows the concentration of nitrogen species in the permeate. Ammonium nitrogen was not detected in any permeate samples, indicating that sufficient nitrification occurred in the MBRs. Appendix Fig. A7 shows the concentration of TOC in the permeate obtained in Run 5. Rates of TOC removal was approximately 95% in all reactors. It can therefore be

concluded that differences in the backwashing solution did not affect the treatment performance in the three MBRs in Run 5. As shown in Appendix Fig. A8, MLSS/MLVSS concentrations in each MBR also did not vary significantly in Run 5. CSTs of sludge samples collected from each MBR (APPENDIX Fig. A5) were also similar in the three MBRs. Therefore, in Run 5, there was no significant difference among the three MBRs in terms of treatment performance and sludge properties. Although several studies suggested that exposures of microorganisms to NBs provided them with extra oxygen supply, leading to enhanced structures of microbial aggregates and evolution of bacterial communities [8–10], such benefits for microorganisms were not clearly seen in this study: NBs introduced to the MBR via backwashing did not alter the mixed liquor suspension significantly in Run 5. The high cleaning efficiency observed with NBB is therefore due to other factors.

4.2.3.3 Influence of backwashing solution on dissolved organic matter in the sludge supernatant

To further investigate the impacts of backwashing solutions on the mixed liquor suspension, dissolved organic matter in the sludge supernatant was analyzed. Several studies have shown that the dissolved organic matter (DOM) in the mixed liquor suspension of MBRs is a cause of the acceleration of membrane fouling [11,12]. Thus, sludge suspensions of the three bench-scale MBRs were taken at the termination of Run 5, and the respective supernatants were analyzed using LC-OCD and EEM apparatuses.

Figure 4.2-4 shows LC-OCD chromatograms of sludge supernatant samples collected from the three MBRs. Biopolymers, which have been shown to be related to membrane fouling in MBRs [13], were not observed in any samples. Very low CST values in Run 5, as shown in appendix Fig. A5, are a reflection of good filterability of the sludge and absence of large molecules such as biopolymers in the mixed liquor suspension. Instead, humic substances (HS, retention time of 100 minutes) and building blocks (BB, retention time of 110 minutes) were present in the sludge supernatant [13]. As

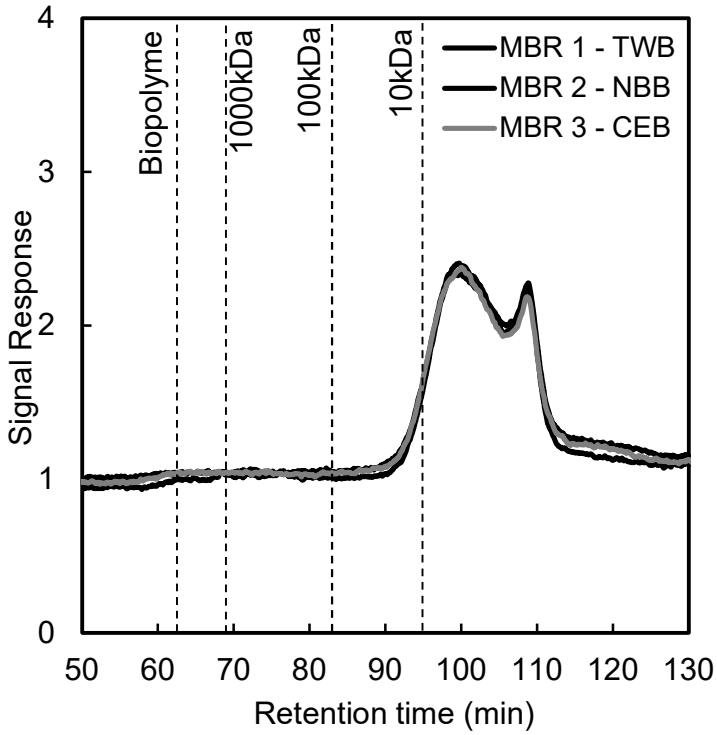

Figure 4.2-4: LC-OCD chromatograms of dissolved organic matter of sludge samples collected at the termination of the experiment.

indicated by the chromatograms, no significantly different peaks were observed among the three MBRs at the termination of Run 5. The same conclusion could be drawn from EEM analysis, as shown in Figure 4.2-5. All of the spectra showed distinctive peaks in the same regions. The fluorescence peaks observed in the samples collected from all of the bench-scale MBRs were very similar. Based on the data obtained by LC-OCD and EEM analysis, it can be concluded that DOM in the three MBRs was similar in Run 5 regardless of the backwashing solution used. DOM has been reported to influence membrane fouling with MBRs [14,15], and a favorable change in DOM might therefore explain the fouling mitigation observed in NBB. However, the results of LC-OCD and EEM analysis discounted this possibility.

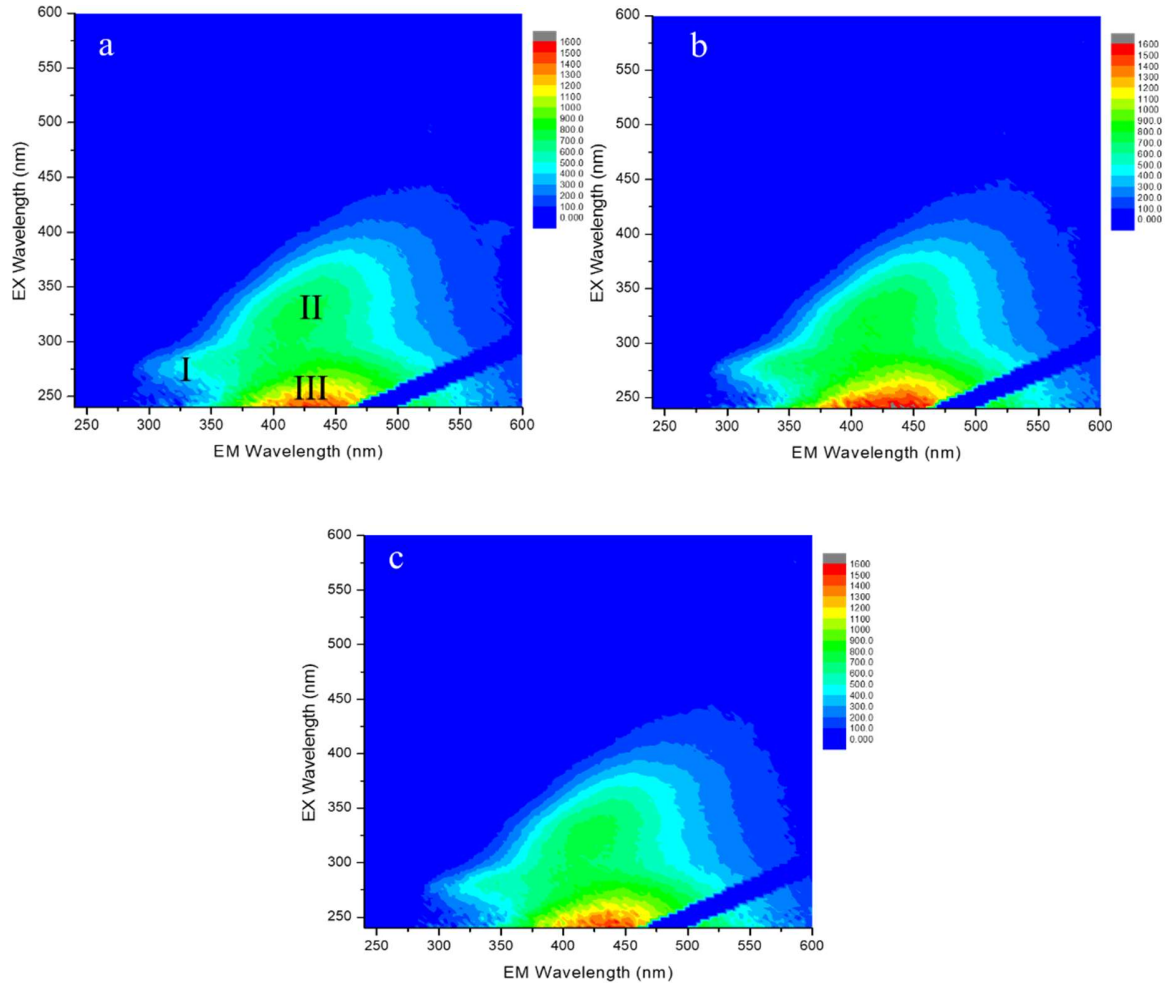

Figure 4.2-5: EEM spectra of dissolved organic matter of sludge samples collected at the termination of the experiment.

Figure 4.2-5 *(a): TWB.* Figure 4.2-55 *(b): NBB.* Figure 4.2-55 *(c): CEB. Region I (Ex. 275nm, Em. 325nm): Soluble Microbial Products-like (SMP), region II (Ex. 350nm, Em. 450nm): Fulvic Acid-like (FA), and region III (Ex. 275nm, Em. 450nm): Humic acid-like (HA).*

4.2.3.4 FT-IR of the fouling layer

FT-IR is a powerful analytical method for assessing the characteristics of diverse types of organic matter and has been used in fouling studies [16–18]. At the termination of Run 5, gel layers were collected from the membrane surfaces from the bench-scale MBRs operated with TWB and NBB and were analyzed by FT-IR. Figure 4.2-6 shows FT-IR spectra of samples collected at the termination of Run 5. FT-IR

spectra of the sample collected from MBR 3 (CEB) could not be obtained due to the limited amount of the sample. Peaks at 1040 cm^{-1} and 3400 cm^{-1} wavenumbers represent polysaccharides [19], while peaks at 1411 cm^{-1}, 1550 cm^{-1} and 1655cm^{-1} wavenumbers are attributed to amide-like substances, suggesting the presence of proteins [20]. On the other hand, absorption peaks around 2920 cm^{-1} represent lipids [21]. The relative signal intensity profiles were quite similar in the two samples, suggesting that the gel layers collected from the two MBRs operated with TWB and NBB had similar compositions. It can be concluded that introducing NBs into the backwashing solution did not alter the components of the fouling layer. Thus, in this study, it was not likely that the fouling layer composition explained the difference in TMP evolution observed with TWB and NBB. Instead, it was hypothesized that the fouling layer structure played a more critical role in the high performance of NBB.

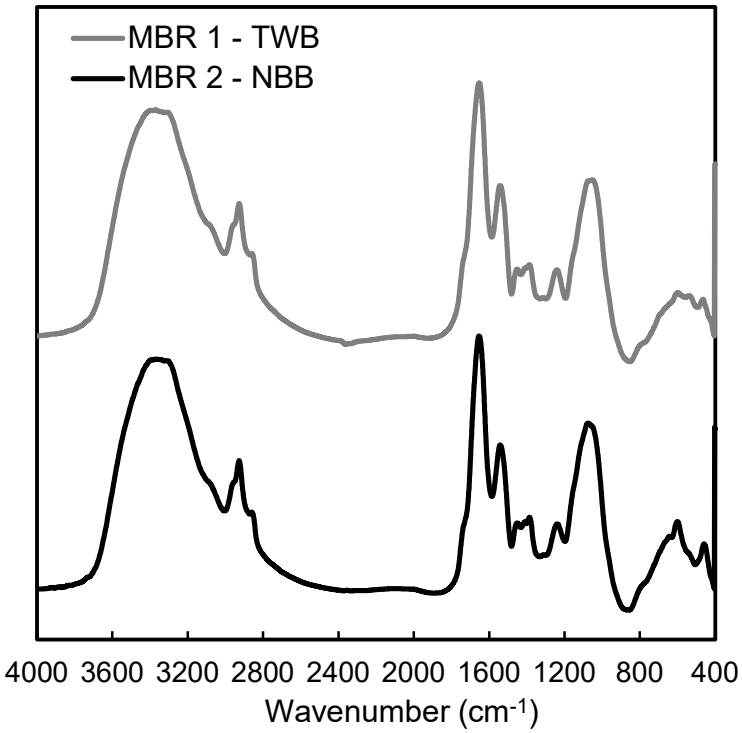

Figure 4.2-6: FT-IR spectra of gel layer samples on the membrane surface collected at the termination of Run 5.

4.2.3.5 Structures of the fouling layer observed by SEM and AFM

SEM and AFM were used to visualize the fouling layer developed on the membrane surface. Figure 4.2-7 (a) shows a cross-section of a membrane backwashed by TWB, whereas Figure 4.2-7 (b) shows a fouled membrane backwashed by NBB. In Figure 4.2-7, cross-section images corresponding to the ceramic membrane are hidden, as the supplier of the membrane did not permit it to be shown. We attempted to determine the thicknesses of the fouling layers by observing different pieces of the samples of the fouled membranes (APPENDIX Fig. A9). The thickness of the fouling layer on the TWB sample (1.93 µm ± 0.38 µm) was larger than that on the NBB sample (1.49 µm ± 0.38 µm), as shown in appendix Fig. A10. The significance of the difference between the mean thicknesses of the fouling layers was statistically assessed. The p-value obtained from Student's t-test was smaller than 0.05 (i.e., 0.001), meaning that the thickness of the fouling layer on the TWB sample was significantly greater than that on the NBB sample (Appendix Table A1 and 2). Formation of a thick fouling layer could be linked to the high degree of reversible fouling observed with TWB. However, the difference in the thicknesses of fouling layers observed with TWB and NBB in Run 5 (30%) was not proportional to the difference in reversible fouling (424%) (Figure 4.2-2). Additional factors such as differences in the structure of the fouling layer might

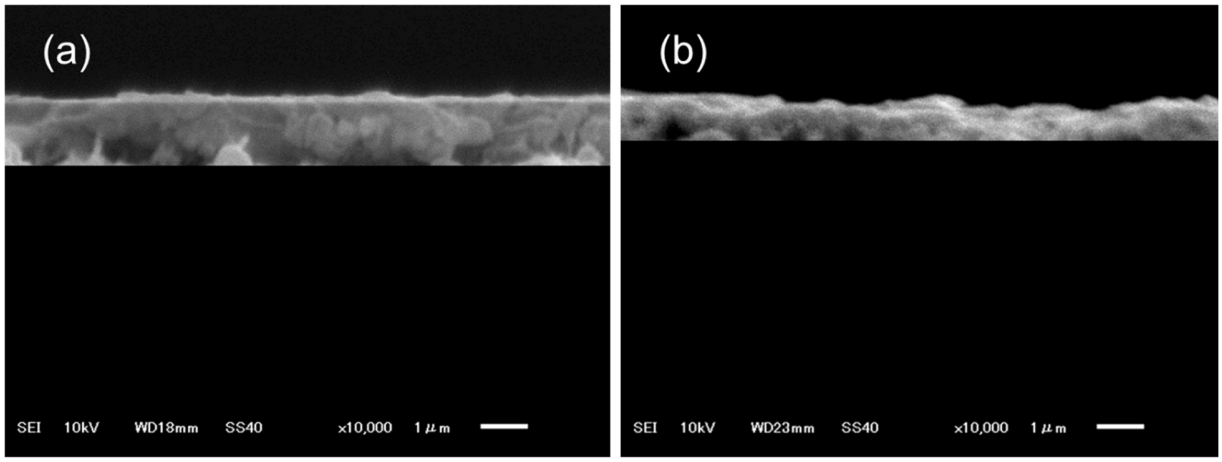

Figure 4.2-7: SEM images of cross-sections of membrane samples taken after the termination of the experiments: (a) Membrane cleaned by TWB; (b) Membrane cleaned by NBB.

play a role in enhancing the fouling mitigation effect of NBB. However, such differences could not be detected by SEM observation.

To assess the potential differences in the structures of fouling layers formed with TWB and NBB, the surfaces of the fouled membranes were observed after the termination of Run 5 using AFM. Figure 4.2-8 shows representative AFM images obtained. The surface roughness of each fouling layer was also determined from the AFM images. Six different areas were quantitively assessed. The mean surface roughness was calculated at ten different sites from a total of sixty observations. Appendix Fig. A11 shows the results of the measurements. The membrane operated with TWB showed a surface roughness of 382.9 nm ± 102.78 nm, while the membrane cleaned by NBB had a roughness of 414.8 nm ± 94.8 nm. In AFM images, the fouling layer on the surface of the membrane backwashed by NBB appears to be rougher, suggesting that the fouling layer in the MBR backwashed with NBB had a more porous structure than that with TWB. This might enhance the effectiveness of granular scouring. However, the rougher fouling layer could also entrap pollutants in its the valleys. It is thought though that the enhanced granular scouring could offset

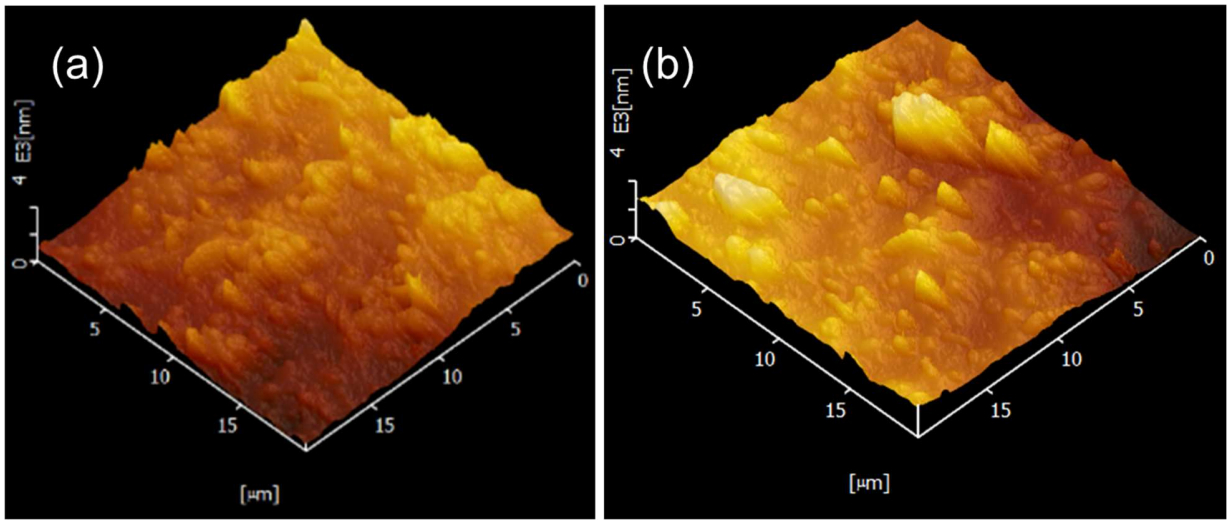

Figure 4.2-8: AFM images of membrane samples taken after the termination of the experiments: (a) Membrane cleaned by TWB; (b) Membrane cleaned by NBB.

the accumulation of pollutants. This is the current possible explanation for the low degree of reversible fouling with NBB (Figure 4.2-3). Although neither SEM nor AFM could demonstrate that the surface structure of the fouling layer was altered by NBB, it was postulated that NBs intruded into the gel layer and made its internal structure loose. The disproportion between the thickness of the fouling layer and the degree of reversible fouling mentioned above support this postulation. Also, we postulate that NBs might have lifted up the gel layer when they were introduced at the interface between the membrane and the gel layer. It has been reported that free radicals could be produced when NBs collapse [22–24], which might also contribute to the changing of the structure of the gel layer. However, it was shown in this study that the resolution of the SEM/AFM was not sufficient to detect the changes in the structure of the gel layer caused by NBB. Thus, further investigation is needed to determine the causes of the high cleaning efficiency of NBB.

4.2.4 Effect of the concentration of nanobubbles on fouling mitigation

In this section, an investigation of the effects of the concentration of NBs on fouling mitigation was made. The cleaning efficiencies of TW, NBW and HC-NBW were compared. In section 4.2.4.1 ceramic membranes fouled by model foulants were backwashed by TW, NBW and HC-NBW. In section 4.2.4.2 the same backwashing solutions were used in an intermittent filtration experiment with bench-scale MBRs backwashed periodically. NBW and HC-NBW were prepared as described in section 3.2.2.

4.2.4.1 Membrane backwashing using model foulants

Figure 4.2-9 (a) shows the results of the permeation performance recovery rates when using TW, NBW and HC-NBW as backwashing solutions. Each condition was tested three times. The results, similar to the previous study, showed that higher nanobubble concentrations led to higher cleaning efficiency. A significant difference ($p = 0.012$) at the 5% significance level was observed between the permeation

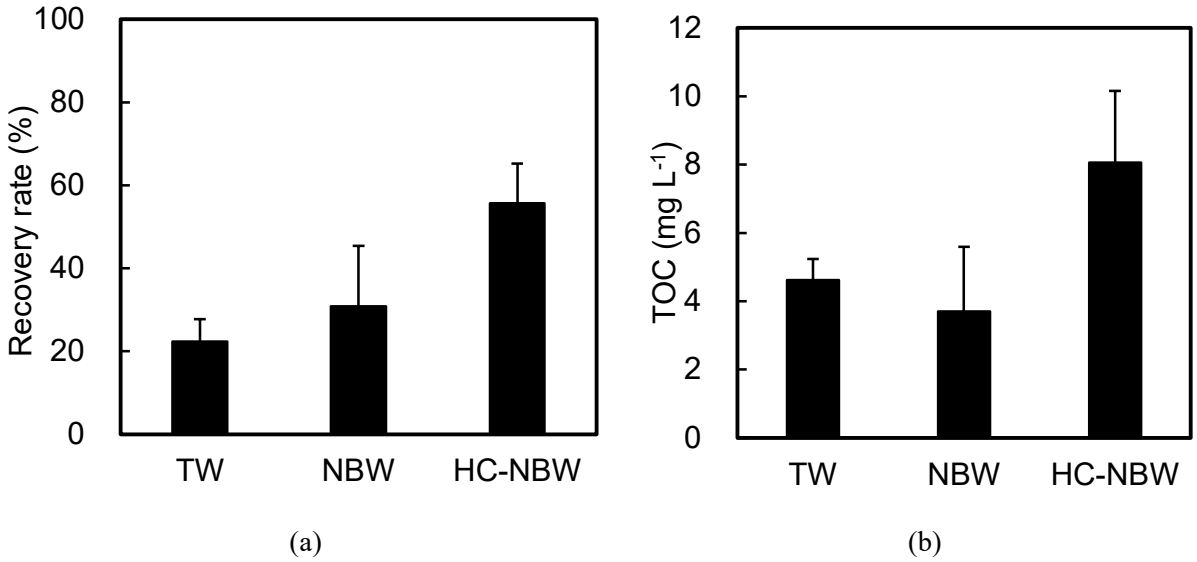

(a) (b)

Figure 4.2-9: (a) Permeation performance recovery rates of different backwashing solutions and (b) TOC concentration released in the backwashing tank according to the backwashing solutions.

performance recovery rates of HC-NBW and TW. However, no significant difference ($p = 0.11$) was found between the recovery rates of NBW and HC-NBW, consistent with the previous study. Even when extending the backwashing time and conducting it in an empty tank, the HC-NBW did not significantly outperform regular NBW. This can be an indicator that the nanobubble concentration in HC-NBW exceeded a threshold at which nanobubbles cease to have a major influence in the cleaning performance. The TOC concentration in the collected backwash water is shown in Figure 4.2-9 (b). However, the highest TOC concentration was observed when HC-NBW was used, indicating that it removed the most foulant, supporting its superior cleaning efficiency.

4.2.4.2 Investigation of High-Concentration Nanobubble Backwashing in MBR

Figure 4.2-10 shows the concentration of nanobubble in the backwashing water during the operation. HC-NBW maintained a concentration 2.5 to 5 times higher than regular NBW. Figure 4.2-11 shows the temperature, ORP, pH, and CST in the

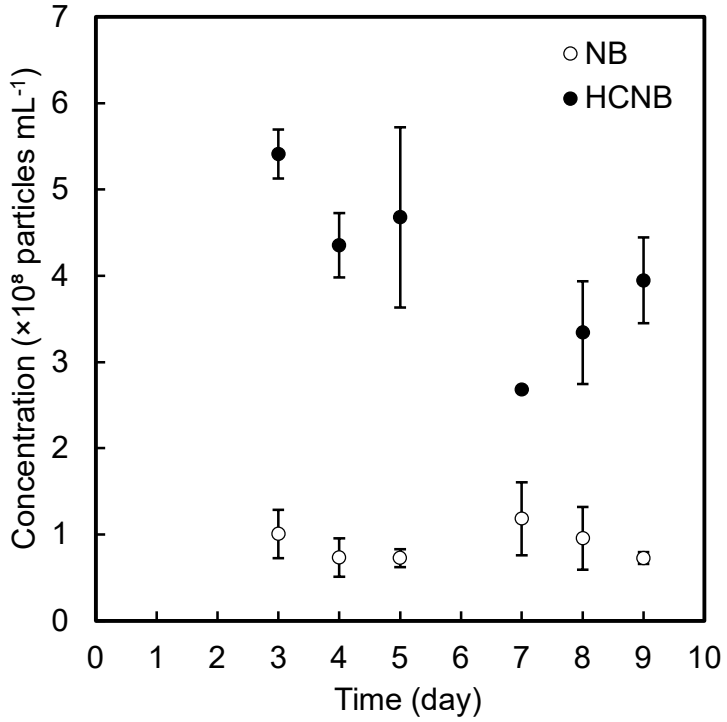

Figure 4.2-10: Concentration of NBs and HC-NB over time.

bioreactor during the operation, confirming that the three MBRs operated under the same initial conditions.

Figure 4.2-12 shows TMP changes over time for the three MBRs using TW, NBW, and HC-NBW as backwashing solution. Both NBW and HC-NBW mitigated the increases in TMP more than TW, which consistent with previous research indicating nanobubbles' cleaning effect on MBR fouling. High-concentration nanobubble water was more effective in suppressing fouling than regular nanobubble water. This result, similar to the model foulant experiment, showed that HC-NBW had the highest cleaning efficiency in the MBR. Further investigation is needed to determine whether the increased cleaning efficiency justifies the higher cost of using HC-NBW for practical applications. Figure 4.2-13 shows the reversible and irreversible membrane filtration resistance values measured before and after operation. As in the model foulant experiment, the increase in membrane filtration resistance was mainly due to reversible fouling. The total reversible and irreversible fouling values were highest for the systems backwashed with TW, followed by NBW and HC-NBW, which was

consistent with the TMP increasing trend. This indicates that nanobubbles primarily targets reversible fouling.

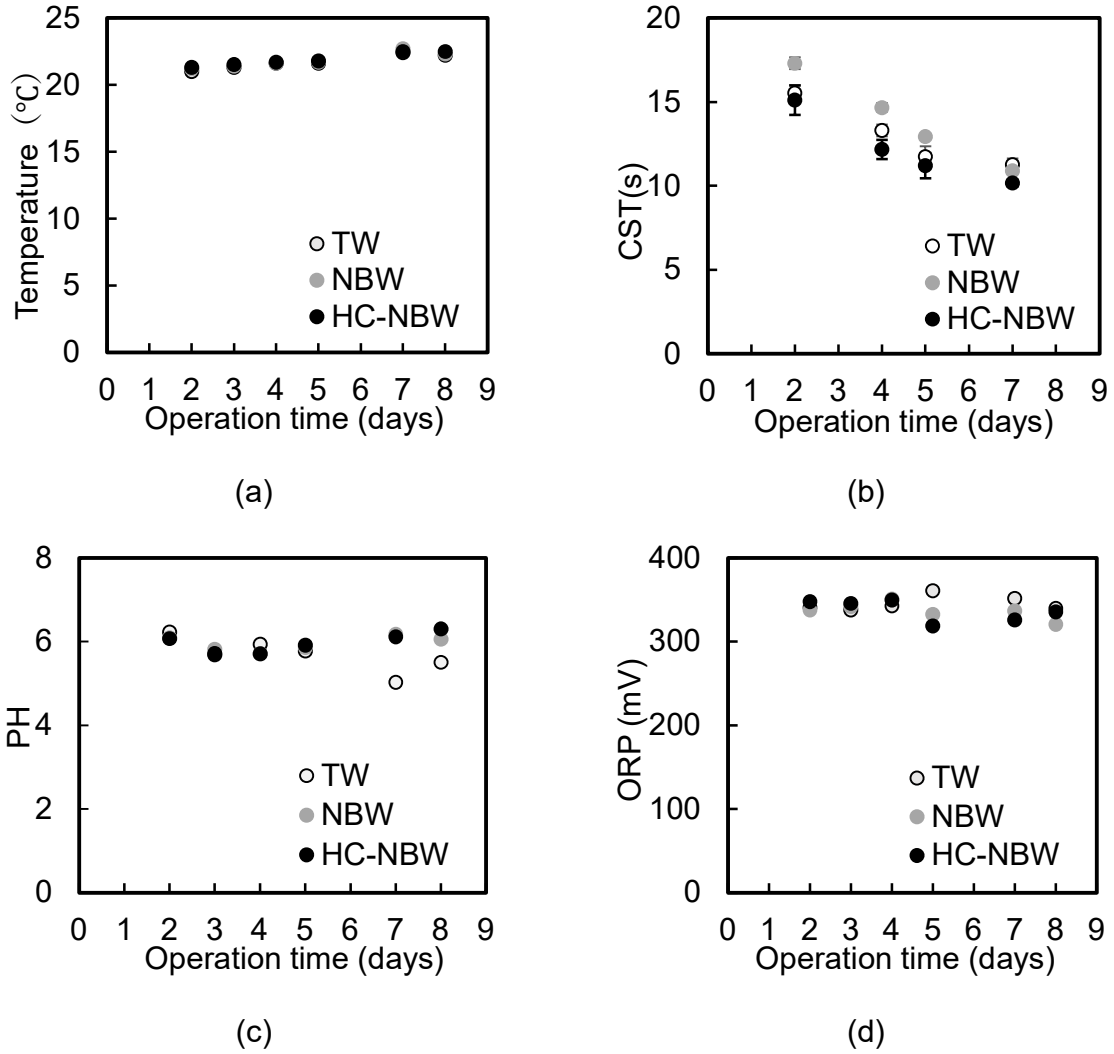

Figure 4.2-11: Condition of the mixed-liquor suspension in the reactors: (a) Temperature, (b) CST, (c) pH, and (d) ORP.

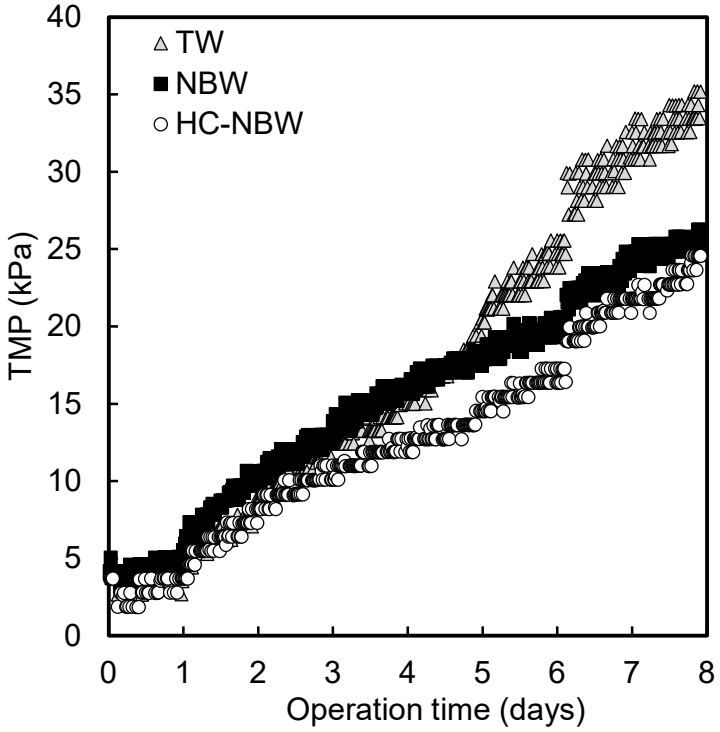

Figure 4.2-12: TMP increases in the HC-NB experiment.

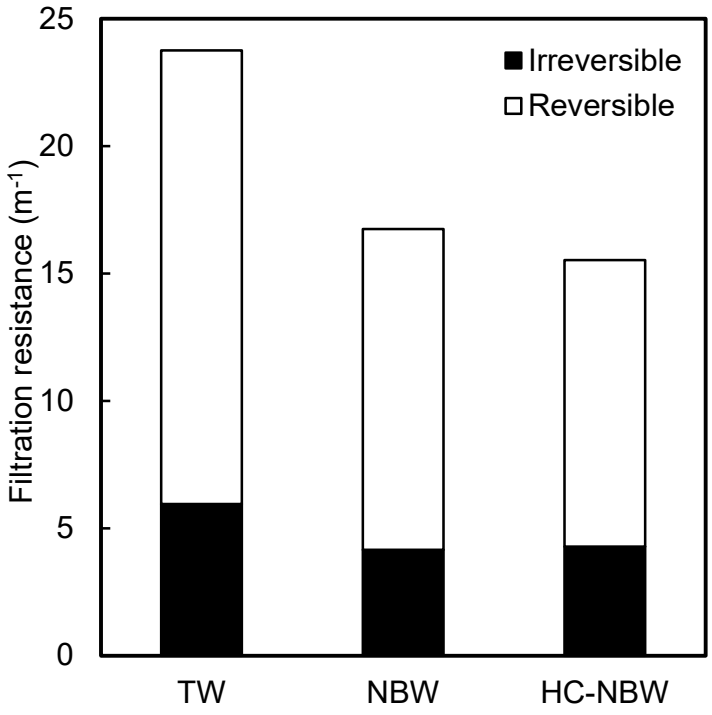

Figure 4.2-13: Distributions of membrane filtration resistances at the termination of the HC-NB experiment.

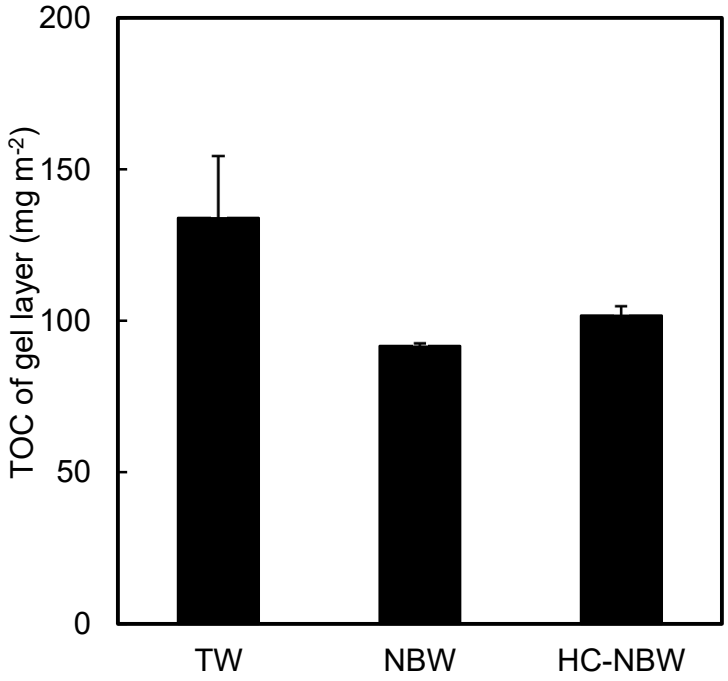

Figure 4.2-14: TOC of gel layer on the membranes at the termination of the HC-NB experiment.

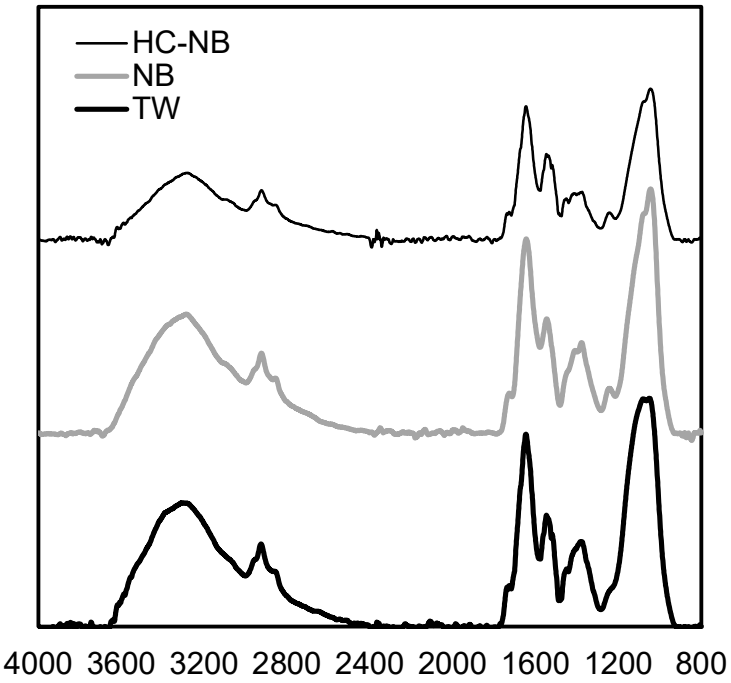

Figure 4.2-15: FT-IR spectra of gel layer samples on the membrane surface collected at the termination of the HC-NB experiment.

Figure 4.2-14 and Figure 4.2-15 show the TOC concentration in the membrane deposits and the FT-IR analysis results, respectively. The FT-IR results indicated no significant differences in the foulant composition between the membranes backwashed with TW, NBW and HC-NBW. However, the TOC concentration in the membrane deposits was lower in the systems using NBW and HC-NBW compared to TW, indicating that more foulant was removed with nanobubble backwashing.

4.2.5 Generation of ROS by nanobubbles

4.2.5.1 ROS measurement APF fluorescein

Figure 4.2-16 shows the fluorescence intensities of NBs and H_2O_2 samples measured by an EEM instrument. All samples submitted to US showed peaks varying in intensity. The NBW sample showed an intense peak, confirming the generation of

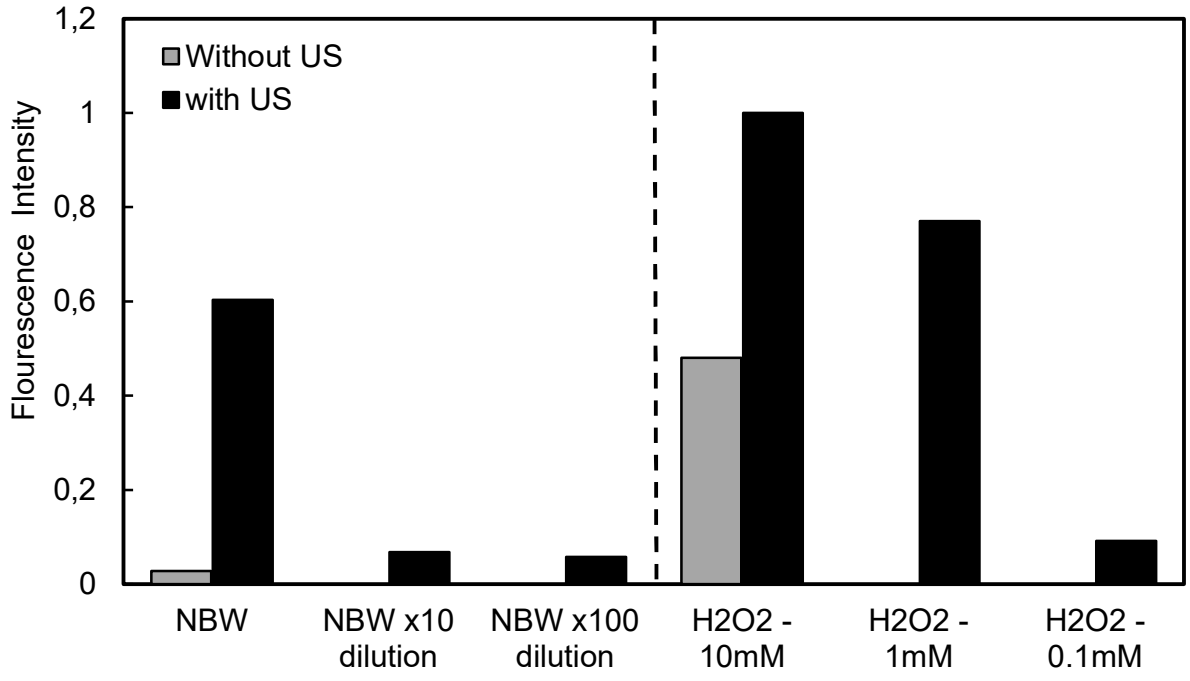

Figure 4.2-16: Fluorescence intensities of NB and H2O2 samples added with APF.

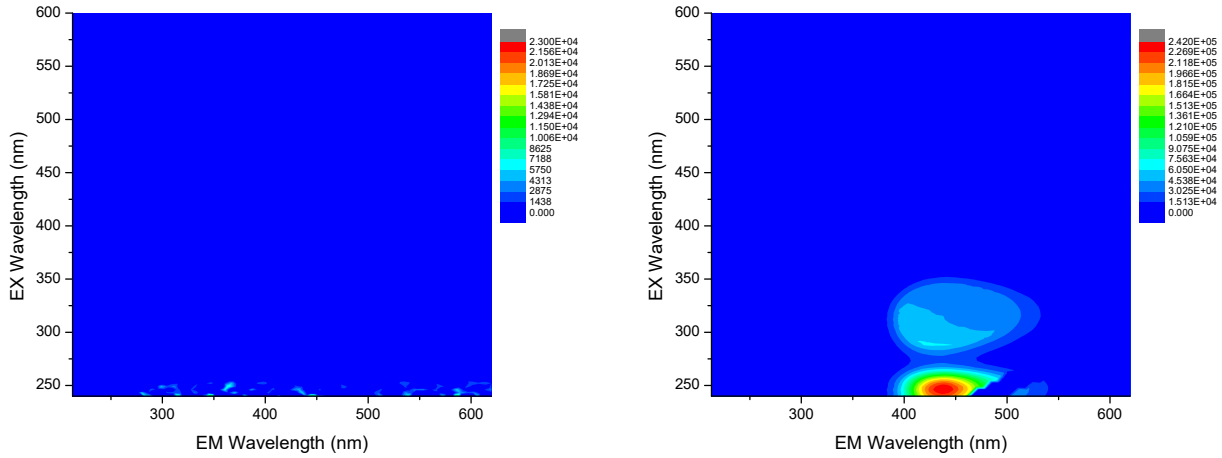

(a) (b)

Figure 4.2-17: EEM spectra of samples the TP degradation experiment and TPOH samples.

ROS by NBs, which reduced in intensity in the diluted samples. However, in the absence of US all the NBW samples had weak/inexistant peaks, indicating that the generation of ROS by NBs does not take place or is minimum in the absence of a stimulus. On the other hand, as expected, H_2O_2 samples had fluorescent peaks even in the absence of US. The peak intensities reduced at lower concentrations. Since it is very unlikely that backwashing of membranes in MBRs mimic the conditions of US, the results of the fluorescence intensities of NB samples added with APF show that, in our experiments, the generation of significant amount of ROS is unlikely.

4.2.5.2 ROS measurement by TPOH fluorescence

Figure 4.2-17 shows the spectra of samples analyzed with an EEM instrument. Figure 4.2-17(a) shows the spectra of samples from the TP degradation experiment, while Figure 4.2-17 (b) shows the spectra of TPOH samples. TPOH produced by the degradation of TP by ROS emits fluorescence at 425 nm when excited at 315 nm. However, no peaks were detected in the samples from TP degradation experiment, indicating that ROS were not produced by the NBs generated in TP solution. On the

other hand, when a TPOH solution was prepared and excited at 425 nm a peak at 315 nm could be observed.

4.2.6 Contact angle of NB-containing water

Contact angles of TW, NBW and HC-NBW measured on a PVDF ultrafiltration membrane filter are shown in Figure 4.2-18. The contact angle reduces with the concentration of NBs. The contact angle of NBW is lower than that of TW, and that of HC-NBW is the lowest among all. The data suggests that the number of NBs in the bulk of water reduces its contact angle, and by consequence its surface tension. Tuziuti et al., (2023) observed the same in their recent study [25] and predicted that, in accordance to the dynamic equilibrium model, the decrease in surface tension is due to the Janus-like structures of a bulk nanobubbles [26]. Janus-like structure have surfaces with two or more distinct physical properties. The dynamic equilibrium model considers that NBs are Janus-like structures because it predicts the stability of NBs is due to the presence of impurities on their surfaces. However, since these models are not yet proven, the causes for reductions in surface tension by NBs is still a not well understood. In any case, it seems that NBs do reduce the surface tension of water, and therefore, improving its wetting and cleaning properties. The fouling mitigation properties of NB water could be related to the improvement of the cleaning properties of water by NBs.

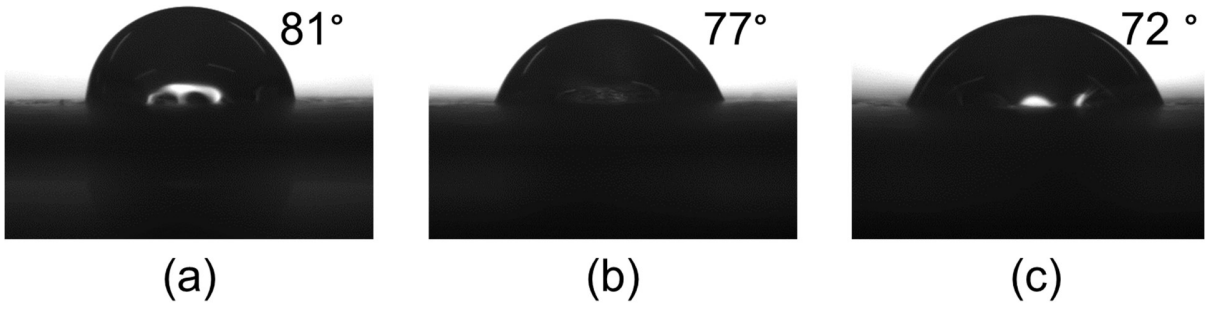

Figure 4.2-18: Contact angles of (a) TW, (b) NBW and (c) HC-NBW measured on a PVDF ultrafiltration membrane filter

4.3 Summary

A novel method for cleaning of membranes fouled in MBRs, backwashing with NB-containing water, was investigated. Experiments were carried out at an existing wastewater treatment plant with real municipal wastewater. Regardless of the season when the experiments were carried out (i.e., differences in the quality of the feed wastewater), the cleaning performance of NBB was always higher than that of TWB, clearly indicating the high potential of NBB for membrane cleaning. It was found that NBB could lower the degree of reversible fouling and was also effective for the control of irreversible fouling. The degree of reversible fouling observed with TWB was 424% higher than that with NBB. We attempted to identify the reasons why NBB lowered the reversible fouling. Comprehensive analysis of the mixed liquor suspension revealed that introduction of NBs did not alter the characteristics of the mixed liquor suspension. Also, the composition of the fouling layer did not change with NBB. On the other hand, significant reduction in the thickness of the fouling layer was observed by SEM observations when NBB was applied. The fouling layer on the surface of TWB samples was 30% thicker than that on NBB samples. It was therefore postulated that, rather than changes in the composition, the structure of the fouling layer might have been modified when NBB was carried out. NBs might have lifted up the gel layer when they were introduced at the interface between the membrane and the gel layer, as illustrated in Figure 4.3-1, although conventional SEM/AFM observation could not detect such changes. It was also shown that the concentration is NBs is an important factor that affects cleaning with NBs. However, the studies could not conclude which is the optimal concentration of NBs which maximizes the cleaning efficiency. Also, though batch experiments as well as bench-scale operation on an MBR, it could be concluded that NBs don't have an adverse effect on the microbial community in the mixed liquor suspension in MBRs.

Although the mechanisms of fouling mitigation by NBB could not be fully revealed, this study gives a major contribution to the research on fouling mitigation by NBs.

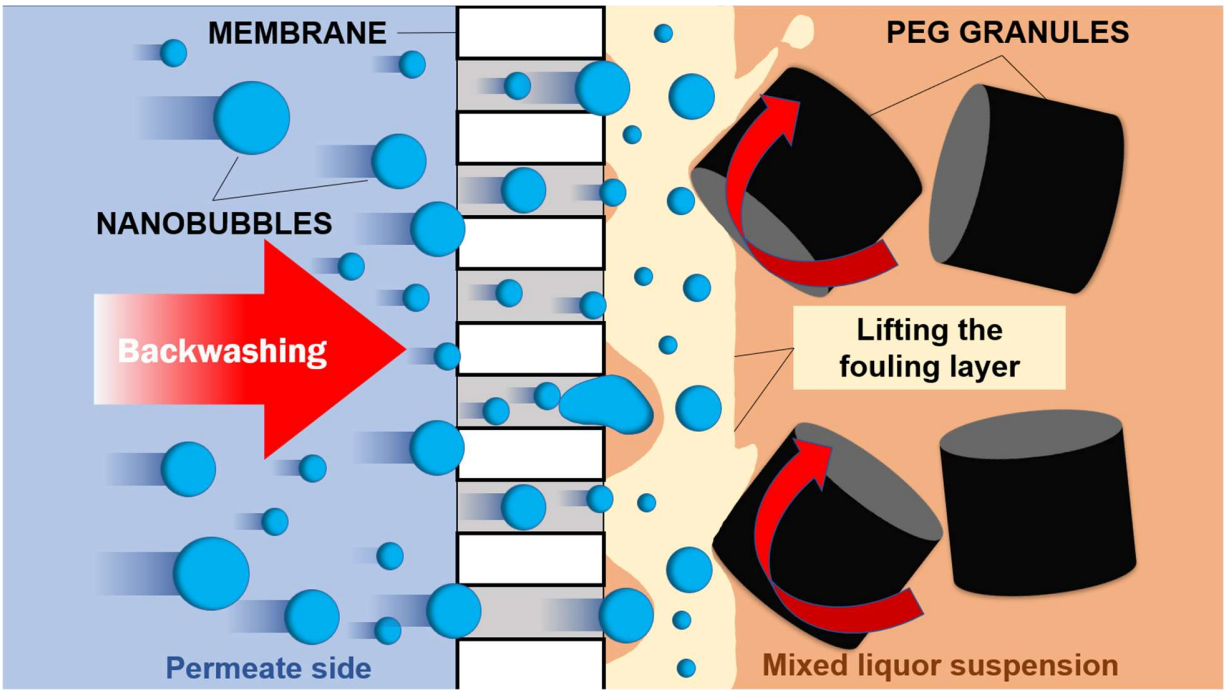

Figure 4.3-1: Proposed mechanism in place during NBB.

Since this study is the first study on the application of NBB, there is a lot of room for investigation. For instance, the backwashing conditions used in this study were based on previous research that confirmed the efficiency of CEB for mitigation of membrane fouling. However, the backwashing conditions for NBB were not optimized and further research on backwashing conditions should therefore be carried out. In addition, there is a need to investigate the effects of varying characteristics of NBs on the cleaning efficiency of NBB. We postulate that altering the, size or zeta potential of NBs would further enhance the cleaning efficiency of NBB.

Finally, by revealing the mechanisms by which NBB mitigates fouling, NBB could be established as an environmentally friendly measure for membrane cleaning. To do so, innovative methods of observation for the fouling layer might be necessary.

REFERENCES

[1] S. Dong, E.S. Kim, A. Alpatova, H. Noguchi, Y. Liu, M. Gamal El-Din, Treatment of oil sands process-affected water by submerged ceramic membrane microfiltration system, Sep Purif Technol 138 (2014) 198–209. https://doi.org/10.1016/J.SEPPUR.2014.10.017.

[2] S.J. Judd, The status of industrial and municipal effluent treatment with membrane bioreactor technology, Chemical Engineering Journal 305 (2016) 37–45. https://doi.org/10.1016/j.cej.2015.08.141.

[3] Y. Ninomiya, K. Kimura, T. Sato, T. Kakuda, M. Kaneda, A. Hafuka, T. Tsuchiya, High-flux operation of MBRs with ceramic flat-sheet membranes made possible by intensive membrane cleaning: Tests with real domestic wastewater under low-temperature conditions, Water Res 181 (2020) 115881. https://doi.org/10.1016/j.watres.2020.115881.

[4] T. Kurita, K. Kimura, Y. Watanabe, The influence of granular materials on the operation and membrane fouling characteristics of submerged MBRs, J Memb Sci 469 (2014) 292–299. https://doi.org/10.1016/j.memsci.2014.05.057.

[5] N. Nirmalkar, A.W. Pacek, M. Barigou, On the Existence and Stability of Bulk Nanobubbles, (2018). https://doi.org/10.1021/acs.langmuir.8b01163.

[6] W. Kanematsu, T. Tuziuti, K. Yasui, The influence of storage conditions and container materials on the long term stability of bulk nanobubbles —

Consideration from a perspective of interactions between bubbles and surroundings, Chem Eng Sci 219 (2020). https://doi.org/10.1016/j.ces.2020.115594.

[7] R.B. Baird, A.D. Eaton, E.W. Rice, Standard methods for the examination of water and wastewater, 2017.

[8] W. Xiao, G. Xu, Mass transfer of nanobubble aeration and its effect on biofilm growth: Microbial activity and structural properties, Science of the Total Environment 703 (2020). https://doi.org/10.1016/j.scitotenv.2019.134976.

[9] W. Xiao, G. Xu, G. Li, Effect of nanobubble application on performance and structural characteristics of microbial aggregates, Science of The Total Environment (2020) 142725. https://doi.org/10.1016/j.scitotenv.2020.142725.

[10] H. Zhuang, X. Hong, H. Han, S. Shan, Effect of pure oxygen fine bubbles on the organic matter removal and bacterial community evolution treating coal gasification wastewater by membrane bioreactor, Bioresour Technol 221 (2016) 262–269. https://doi.org/10.1016/J.BIORTECH.2016.09.029.

[11] S. Rosenberger, C. Laabs, B. Lesjean, R. Gnirss, G. Amy, M. Jekel, J.C. Schrotter, Impact of colloidal and soluble organic material on membrane performance in membrane bioreactors for municipal wastewater treatment, Water Res 40 (2006) 710–720. https://doi.org/10.1016/j.watres.2005.11.028.

[12] J. Teng, M. Zhang, K.T. Leung, J. Chen, H. Hong, H. Lin, B.Q. Liao, A unified thermodynamic mechanism underlying fouling behaviors of soluble microbial products (SMPs) in a membrane bioreactor, Water Res 149 (2019) 477–487. https://doi.org/10.1016/j.watres.2018.11.043.

[13] F.Y. Sun, X.M. Wang, X.Y. Li, Effect of biopolymer clusters on the fouling property of sludge from a membrane bioreactor (MBR) and its control by ozonation, Process Biochemistry 46 (2011) 162–167. https://doi.org/10.1016/J.PROCBIO.2010.08.003.

[14] Y. Ding, Y. Tian, Z. Li, H. Wang, L. Chen, Microfiltration (MF) membrane fouling potential evaluation of protein with different ion strengths and divalent cations

based on extended DLVO theory, Desalination 331 (2013) 62–68. https://doi.org/10.1016/j.desal.2013.10.017.

[15] T. Jiang, M.D. Kennedy, V. De Schepper, S.N. Nam, I. Nopens, P.A. Vanrolleghem, G. Amy, Characterization of soluble microbial products and their fouling impacts in membrane bioreactors, Environ Sci Technol 44 (2010) 6642–6648. https://doi.org/10.1021/ES100442G/SUPPL_FILE/ES100442G_SI_001.PDF.

[16] R. Zhang, S. Yu, W. Shi, J. Tian, L. Jin, B. Zhang, L. Li, Z. Zhang, Optimization of a membrane cleaning strategy for advanced treatment of polymer flooding produced water by nanofiltration, (2016). https://doi.org/10.1039/c6ra01832g.

[17] Z. Zhou, X. He, M. Zhou, F. Meng, Chemically induced alterations in the characteristics of fouling-causing bio-macromolecules – Implications for the chemical cleaning of fouled membranes, Water Res 108 (2017) 115–123. https://doi.org/10.1016/j.watres.2016.10.065.

[18] S. Habibi, M. Rabiller-Baudry, F. Lopes, F. Bellet, B. Goyeau, M. Rakib, E. Couallier, New insights into the structure of membrane fouling by biomolecules using comparison with isotherms and ATR-FTIR local quantification, Environmental Technology (United Kingdom) 0 (2020) 1–18. https://doi.org/10.1080/09593330.2020.1783370.

[19] S.R.P. Shariati, B. Bonakdarpour, N. Zare, F.Z. Ashtiani, The effect of hydraulic retention time on the performance and fouling characteristics of membrane sequencing batch reactors used for the treatment of synthetic petroleum refinery wastewater, Bioresour Technol 102 (2011) 7692–7699. https://doi.org/10.1016/J.BIORTECH.2011.05.065.

[20] H. Hazrati, A.H. Moghaddam, M. Rostamizadeh, The influence of hydraulic retention time on cake layer specifications in the membrane bioreactor: Experimental and artificial neural network modeling, J Environ Chem Eng 5 (2017) 3005–3013. https://doi.org/10.1016/j.jece.2017.05.050.

[21] R.R.E. Artz, S.J. Chapman, A.H. Jean Robertson, J.M. Potts, F. Laggoun-Défarge, S. Gogo, L. Comont, J.R. Disnar, A.J. Francez, FTIR spectroscopy can be used as a screening tool for organic matter quality in regenerating cutover peatlands, Soil Biol Biochem 40 (2008) 515–527. https://doi.org/10.1016/J.SOILBIO.2007.09.019.

[22] S. Liu, S. Oshita, S. Kawabata, Y. Makino, T. Yoshimoto, Identification of ROS Produced by Nanobubbles and Their Positive and Negative Effects on Vegetable Seed Germination, Langmuir 32 (2016) 11295–11302. https://doi.org/10.1021/acs.langmuir.6b01621.

[23] S. Liu, S. Oshita, Y. Makino, Q. Wang, Y. Kawagoe, T. Uchida, Oxidative Capacity of Nanobubbles and Its Effect on Seed Germination, (2015). https://doi.org/10.1021/acssuschemeng.5b01368.

[24] M. Takahashi, Y. Shirai, S. Sugawa, Free-Radical Generation from Bulk Nanobubbles in Aqueous Electrolyte Solutions: ESR Spin-Trap Observation of Microbubble-Treated Water, Langmuir 37 (2021) 5005–5011. https://doi.org/10.1021/acs.langmuir.1c00469.

[25] T. Tuziuti, K. Yasui, W. Kanematsu, Decrease in the Surface Tension of Nanobubble Dispersion in Water: Results of Surface Excess of Bulk Nanobubbles at Interfaces, Langmuir 39 (2023). https://doi.org/10.1021/acs.langmuir.3c00040.

[26] K. Yasui, T. Tuziuti, W. Kanematsu, Mechanism of the Decrease in Surface Tension by Bulk Nanobubbles (Ultrafine Bubbles), Langmuir 39 (2023). https://doi.org/10.1021/acs.langmuir.3c02545.

CHAPTER 5: ASSESSMENT OF THE IMPACT OF NANOBUBBLES ON THE MIXED-LIQUOR SUSPENSION

5.1 Methods

5.1.1 Batch experiment

The batch experiment was conducted using activated sludge acclimatized by synthetic wastewater. The synthetic wastewater (main carbon source: peptone and meat extract) used in this experiment was prepared by following the Organization for Economic Co-operation and Development (OECD) guidelines [1]. The solutions used in the backwash experiment (see CHAPTER 4) were added to the activated sludge, and their effect was investigated. The ratio of activated sludge to the amount of solution added was set to be equal to the ratio of the volume of the bench scale MBR used in the backwash experiment to the amount of backwash solution injected in once backwashing cycle. Three beakers were prepared for the experiments and filled up to the190 mL mark with activated sludge, while 8.1 ml of each solution was added to the respective beakers. TW, 50 ppm NaClO solution and NBW were added and their impact on activated sludge were compared. The mixture of sludge and the respective solutions were mixed with a magnetic stirrer for 1 h, after which they were

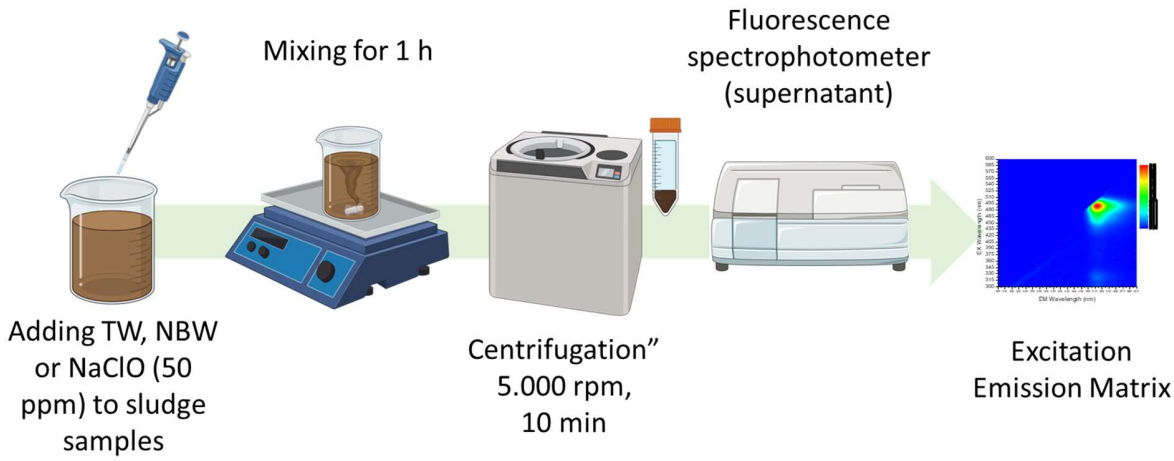

Figure 5.1-1: Schematic illustration of the experimental procedures of the batch experiment (made with biorender)

centrifuged. Sludge supernatant samples were taken and filtered through a 0.45 µm membrane before being analyzed. Chemicals in contact with activated sludge have been shown to degrade the organic matter present in them, increasing the concentration of dissolved organic matter causing membrane fouling [2]. On the other hand, NBs also have been reported to have oxidation properties themselves. However, there aren't many researches on the impacts of NBs on activated sludge. To consider the impacts of NBs on activated sludge, the concentration and property of dissolved organic matters were investigated. NBW was produced according to section3.2.2. The sludge supernatant samples were collected before and after the addition of solutions. The sludge supernatant was filtered by a 0.45 µm membrane. Fluorescence spectroscopy by EEM was applied to provide molecular fingerprint of the sludge supernatant samples. The samples were filtered by a 0.45 µm membrane and analyzed using a fluorescence spectroscopy device (Horiba, Aqualog-DRJR764E). A schematic illustration of the experimental procedure is shown in Figure 5.1-1.

5.1.2 Effect of NBB on microbial activity in Run 5

Several studies have related the presence of various organic substances in sludge to a decreasing microbial kinetic activity [3] due to their toxic effect. It has also been reported that chemicals, including NaClO, when in contact with activated sludge

triggered bacterial lysis [4]. In short, the release of dissolved organic matter in the sludge bulk is an indication that the microbial suspension could be facing stressful conditions. Sludge samples were taken and centrifuged at 5,000 rpm for 10 minutes to investigate the release of organic matter. The samples were then filtered using a 0.45 µm membrane and analyzed using LC-OCD and EEM.

Since bacteria conduct the degradation of organic matter in activated sludge processes, the permeate water quality is a good indicator of microbial health. MBRs provide further treatment by filtration, but membranes cannot reject small molecules and ions. Thus, it is crucial that the microbial suspension grows in stable conditions, allowing the proper degradation of contaminants. Two parameters were chosen to assess the permeate water quality: the carbon removal and the occurrence of Nitrification by measuring the TOC and nitrogen species concentrations, respectively.

OUR is a measurement of microbial activity in MBRs. The OUR by the aerobic bacteria was measured using the method previously presented (section 4.1.8).

5.2 Results and discussion

5.2.1 Batch experiment

In this section an assessment of the impact of NBs on the mixed liquor suspension is presented. The backwashing solutions used so far in the membrane cleaning experiments were made to contact the sludge. The impact of each solution was measured by the changes in DOC measured in the sludge supernatants. The concentration of dissolved organic matter in the sludge supernatant is shown in Figure 5.2-1. It has been reported that NaClO solution causes cell lysis and increases DOC concentration when NaClO solution contacts activated sludge [2] causing membrane fouling. In this experiment, the DOC concentration increased when NaClO solution was added to the activated sludge. It is possible that the DOC released by the

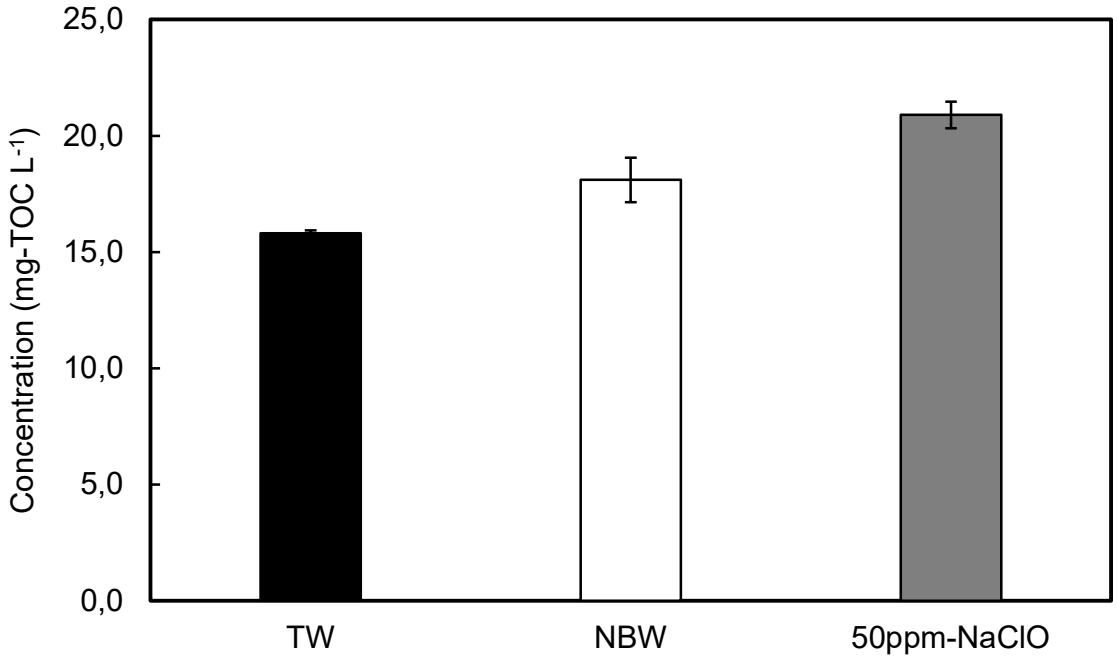

Figure 5.2-1: Dissolved organic carbon concentration in the sludge supernatant from each sample and measured by a TOC analyzer.

addition of NaClO could have deteriorated the sludge filterability and made it more propense to cause membrane fouling. On the other hand, the increase of DOC concentration was not observed when NBs were added to the activated sludge. The concentration of DOC when NBs were added was lower than that when tap water was added. It was possible that NBs did not cause negative impacts on the activated sludge and might not promote membrane fouling. However, further experiments are needed to better consider the relationship between the amount of DOC released and membrane fouling. The molecular fingerprint of the sludge supernatant samples was assessed by EEM. Figure 5.2-2Figure 5.2-2 shows the spectra generated from the sludge supernatant samples after adding the solutions. The location of peaks can identify the composition of organic matters [5], and were defined earlier in section 4.2.3.3. The intensity of the peak representing Soluble Microbial Products (SMP) was higher when NaClO was added to the activated sludge. It has been reported that SMP is a main reason of membrane fouling [6–8]. On the other hand, when NBs were added

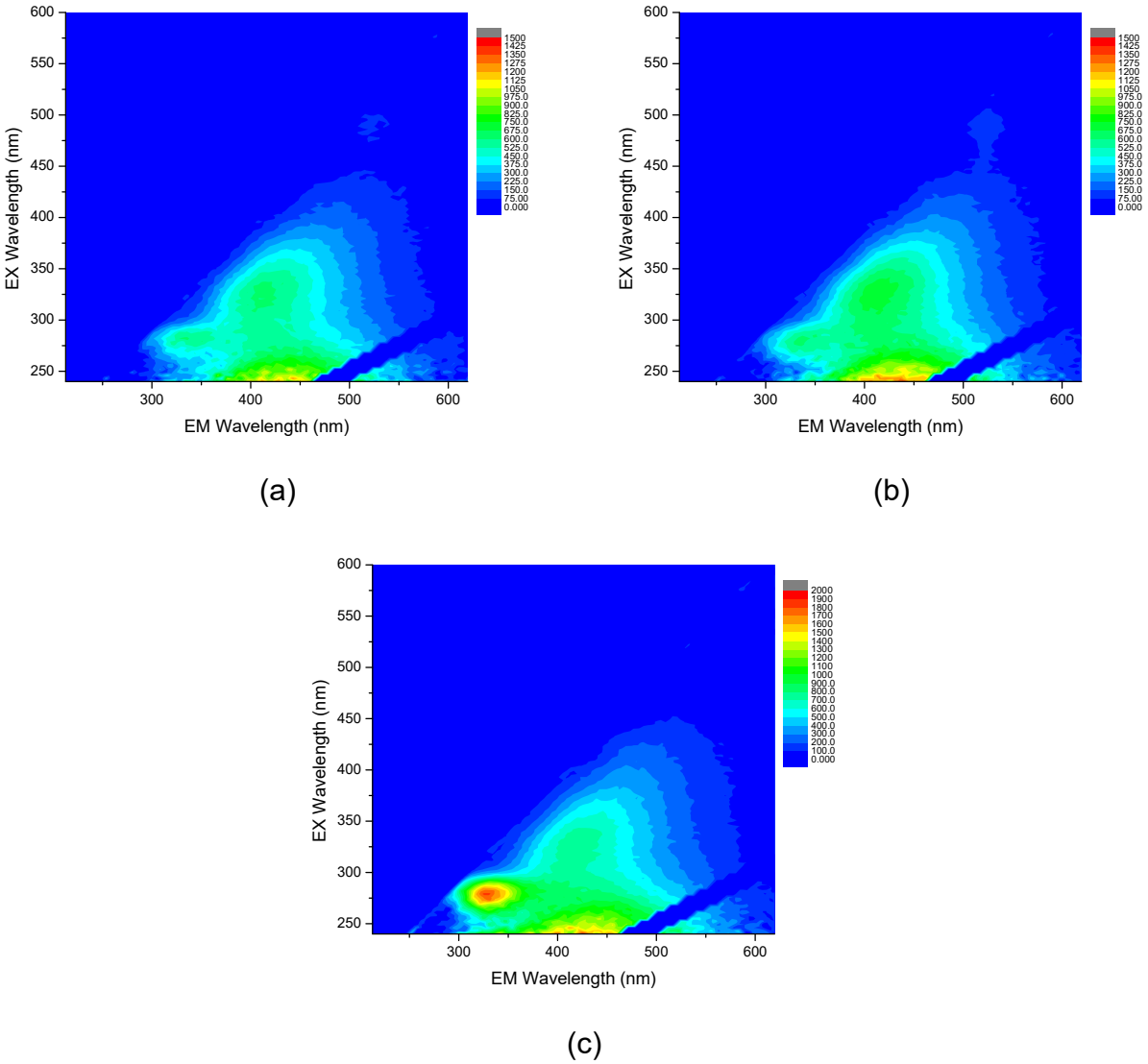

Figure 5.2-2: EEM spectra of dissolved organic matter of sludge samples collected at the termination of the HC-NB experiment.

(a): TWB. (b): NBB. (c): CEB. Region I (Ex. 275nm, Em. 325nm): Soluble Microbial Products-like (SMP), region II (Ex. 350nm, Em. 450nm): Fulvic Acid-like (FA), and region III (Ex. 275nm, Em. 450nm): Humic acid-like (HA).

to the activated sludge the intensity of peak which represents SMP did not increase. This result was consistent with the concentration of DOC in the sludge supernatant (Figure 5.2-1), and it could support the hypothesis that NBs do not have negative impacts on activated sludge.

5.2.2 Effect of NBB on microbial activity in Run 5

As stated previously, chemical cleaning in MBRs negatively affects the microorganisms in the mixed liquor suspension. The effects of NBs on microbial activity should be clarified before NBB can be considered. Membrane fouling is often related to the presence of microbial products in the mixed liquor suspension in MBRs. The release of these microbial products can be enhanced when chemicals contact the microorganisms [9]. In the next three subsections, the effect of NBB, as applied in Run 5, on microbial activity will be presented by direct and indirect methods. The organic matter concentration in the sludge supernatant of MBRs mixed liquor was analyzed using LC-OCD and EEM. More direct methods were also used. Oxygen uptake rate (OUR) and specific oxygen uptake rate (SOUR) directly measure the microbial activity by the oxygen consumption in a sludge sample, and the permeate water quality can indirectly measure the degradation process by bacteria in the reactor tank.

5.2.2.1 Release of organic matter into the mixed liquor suspension in Run 5

The results were shown in section 4.2.3.3, so the discussion is not repeated here. The results show that several dissolved organic matters were identified in the sludge supernatant in all experiments. However, there was no significant difference in the amount released. This suggests that, considering the release of organic matter by bacteria as evidence of stressful condition, none of the backwashing solutions negatively impacted the microbial suspension. At these short contact times and concentrations, both NB water and NaClO-50 ppm didn't have an adverse effect on the microorganisms.

5.2.2.2 Oxygen uptake rate

Figure 5.2-3 shows the dissolved oxygen concentration in the sludge samples over time, and the plot's slope represents the OUR. Equations y1 and y2 represent the TWB and NBB sample's trendline. As shown in the Figure below, equation y2 has a

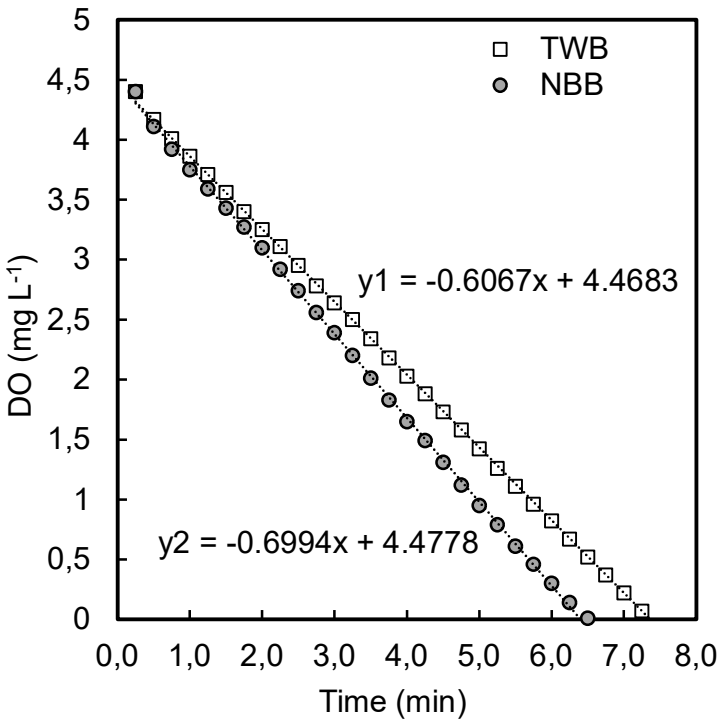

Figure 5.2-3: Dissolved oxygen consumption by bacteria in a sludge sample taken from the MBRs operated with TWB and NBB.

more negative slope coefficient, namely a more inclined slope. This suggests that the microorganisms in the NBB sludge samples consumed oxygen more rapidly than those in the TWB sample. However, the OUR doesn't consider the concentration of microorganisms in each sample. Thus, it is necessary to normalize these values to the microbial concentration. After normalizing the OUR by dividing it by the MLVSS concentration, the SOUR can be calculated. Figure 5.2-5 shows that the SOUR measured in the sludge taken from the MBR operated with NBB is higher than measured in the TWB sample. This might suggest that introducing NBs in the sludge bulk had a positive effect on bacterial activity. However, the difference between the two values is not that significant, and this experiment could only be conducted once. It is still necessary to repeat such kind of experiment in a long term to get more accurate data.

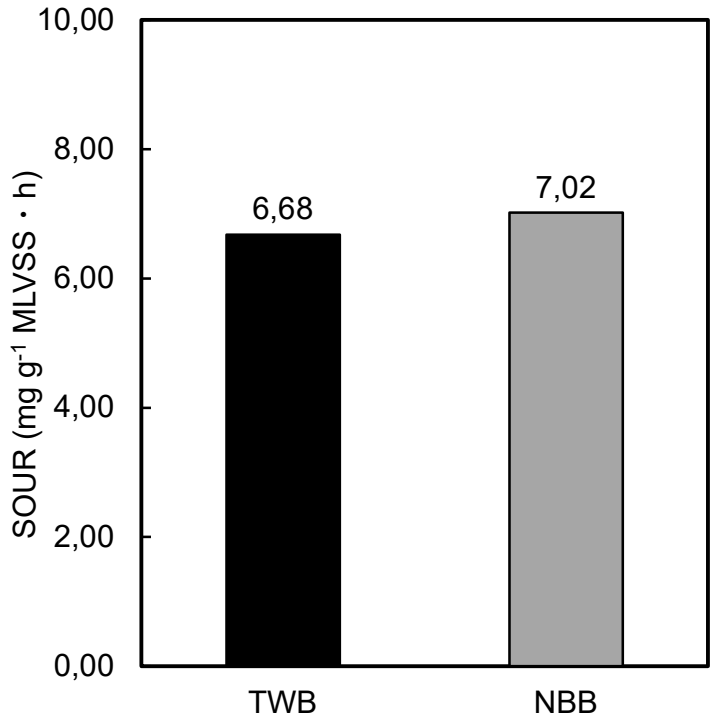

Figure 5.2-5: Specific oxygen uptake rate of the sludge samples taken from the MBRs operated with TWB and NBB.

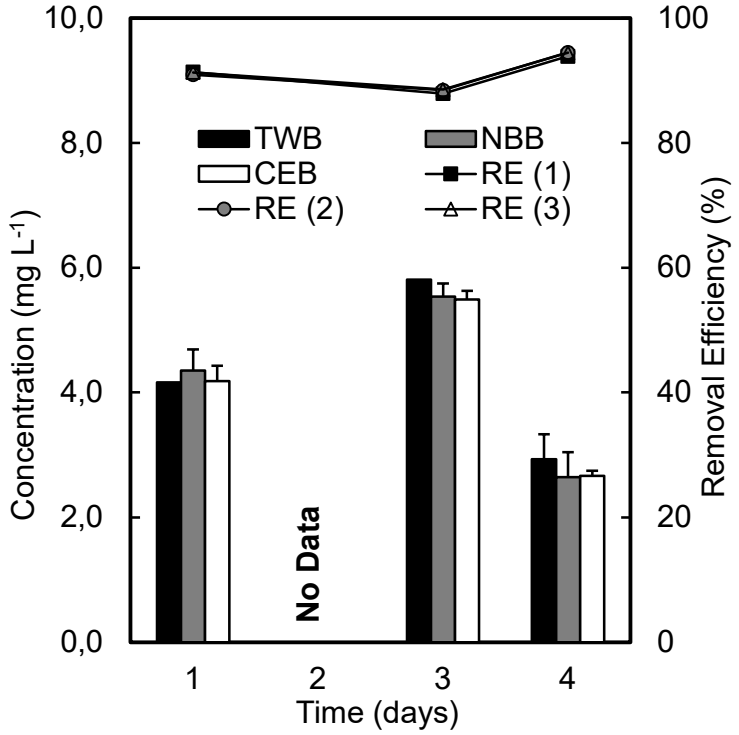

Figure 5.2-4: TOC concentration in the permeate water from each MBR.

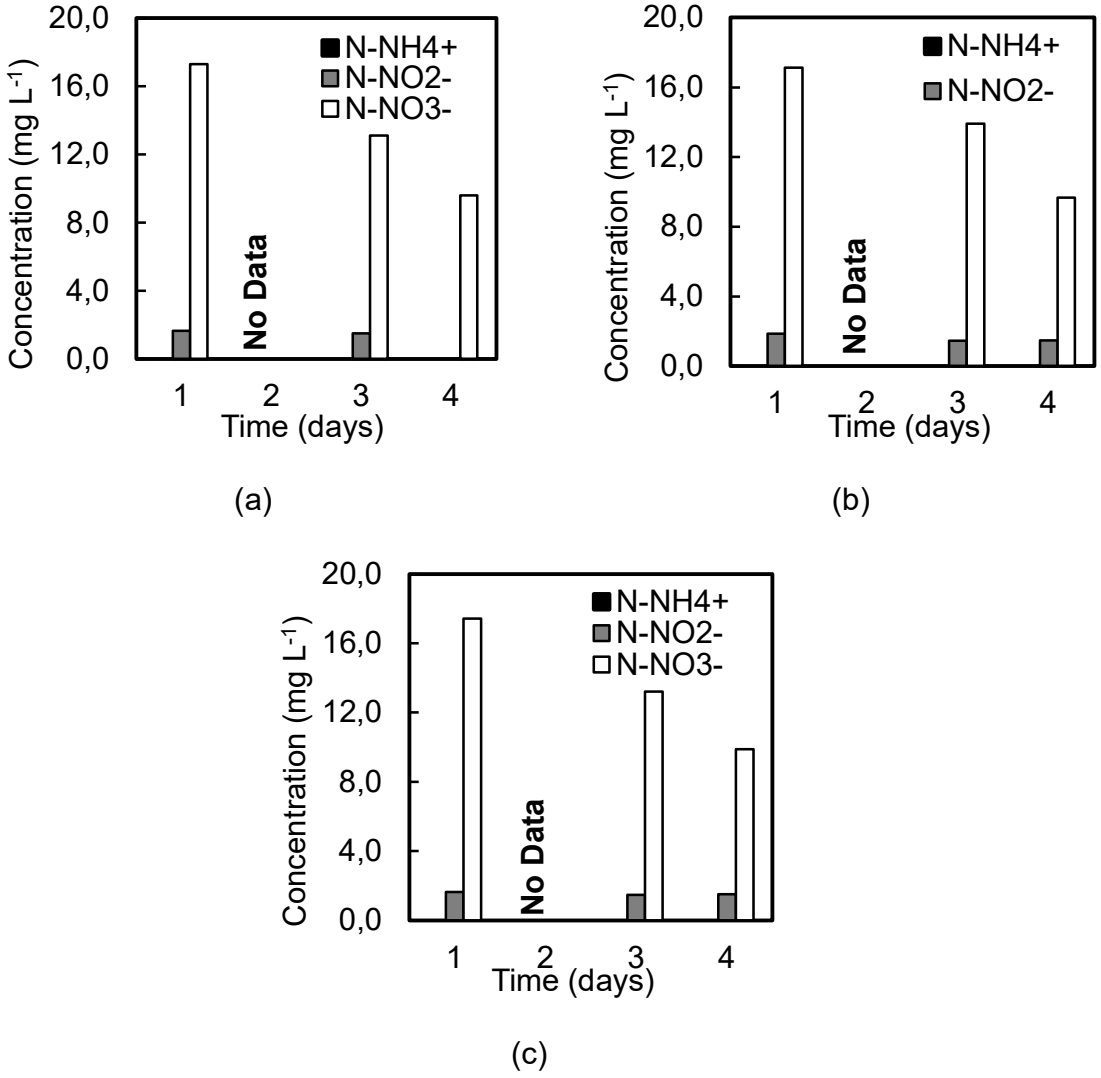

Figure 5.2-6: Concentrations of Nitrogen in the permeate water of the MBR backwashed with (a) TWB, (b) NBB and (c) CEB.

Figure 5.2-4 shows the TOC concentration in the permeate water on days one, three, and four. A common concentration of TOC in the MBR permeate water is 6 mg L^{-1} [10], which is almost three times the concentration observed in the experiments. The final TOC concentrations were 2.93 mg L^{-1} ± 0.4 mg L^{-1}, 2.64 mg L^{-1} ± 0.4 mg L^{-1} and 2.67 mg L^{-1} ± 0.08 mg L^{-1} for TWB, NBB and CEB, respectively. The removal efficiency was more than 90 % in all cases, so it is safe to conclude that the reactor had a high performance, and thus there was no adverse effect to the microbial activity.

Figure 5.2-6 sow the concentrations of Nitrogen as Ammonium ($N\text{-}NH_4^+$), Nitrite ($N\text{-}NO_2^-$), and Nitrate ($N\text{-}NO_3^-$) in the permeate water, analyzed by ion chromatography. Nitrification is the process that converts Ammonium to Nitrite and then to Nitrate. The conversion of Nitrite to Nitrate is very rapid, so it is expected the concentration of Nitrite is shallow and that Ammonium is totally consumed. Since denitrification does not occur, it is likely that the concentration of Nitrate is high when compared to other forms of Nitrogen. As shown in the Figures, $N\text{-}NH_4^+$ was totally consumed, while Nitrite was rapidly converted to Nitrate, keeping $N\text{-}NO_2^-$ concentration below 5 mg L^{-1} in all reactors at the end of the experiments. Since Nitrification was successfully conducted, $N\text{-}NO_3^-$ concentrations at the termination of the experiments were high and ranged between 9 mg L^{-1} and 10 mg L^{-1}. A stable Nitrification is an indicator that the microbial activity was not affected by the backwashing solutions.

5.3 Summary

Investigation of the impact of NBs on the mixed liquor suspension in MBRs was conducted. No evidence of a negative impact of NBs on microbial activity was found. NBs don't increase the releasing of dissolved organic matter into the mixed liquor suspensions, as shown by the batch experiment. On the other hand, CEB with 50 ppm NaClO significantly increase the DOC concentration in sludge supernatant samples. In addition, NBB improved the OUR by the microorganisms, when compared to TWB. Therefore, NBB is an environmentally friendly and low impact fouling mitigation methods.

REFERENCES

[1] Test No. 303: Simulation Test - Aerobic Sewage Treatment -- A: Activated Sludge Units; B: Biofilms, OECD Guideline for the Testing of Chemicals (2001). https://doi.org/10.1787/9789264070424-EN.

[2] E.J. Lee, J.S. Kwon, H.S. Park, W.H. Ji, H.S. Kim, A. Jang, Influence of sodium hypochlorite used for chemical enhanced backwashing on biophysical treatment in MBR, Desalination 316 (2013) 104–109. https://doi.org/10.1016/j.desal.2013.02.003.

[3] W. Cai, J. Liu, X. Zhang, W.J. Ng, Y. Liu, Generation of dissolved organic matter and byproducts from activated sludge during contact with sodium hypochlorite and its implications to on-line chemical cleaning in MBR, Water Res 104 (2016) 44–52. https://doi.org/10.1016/j.watres.2016.07.065.

[4] W. Cai, Y. Liu, Enhanced membrane biofouling potential by on-line chemical cleaning in membrane bioreactor, J Memb Sci 511 (2016) 84–91. https://doi.org/10.1016/j.memsci.2016.03.039.

[5] W. Chen, P. Westerhoff, J.A. Leenheer, K. Booksh, Fluorescence Excitation-Emission Matrix Regional Integration to Quantify Spectra for Dissolved Organic Matter, Environ Sci Technol 37 (2003) 5701–5710. https://doi.org/10.1021/ES034354C/ASSET/IMAGES/LARGE/ES034354CF00009.JPEG.

[6] Membrane Fouling in Pilot-Scale Membrane Bioreactors (MBRs) Treating Municipal Wastewater, (2005). https://doi.org/10.1021/es0502425.

[7] Y. Shi Jinhui Huang Guangming Zeng Yanling Gu Yi Hu Bi Tang Jianxin Zhou Ying Yang Lixiu Shi, Evaluation of soluble microbial products (SMP) on membrane fouling in membrane bioreactors (MBRs) at the fractional and overall level: a review, (2017). https://doi.org/10.1007/s11157-017-9455-9.

[8] C. Jarusutthirak, G. Amy, Role of soluble microbial products (SMP) in membrane fouling and flux decline, Environ Sci Technol 40 (2006) 969–974. https://doi.org/10.1021/ES050987A/ASSET/IMAGES/LARGE/ES050987AF00013.JPEG.

[9] Y. Ninomiya, K. Kimura, T. Sato, T. Kakuda, M. Kaneda, A. Hafuka, T. Tsuchiya, High-flux operation of MBRs with ceramic flat-sheet membranes made possible by intensive membrane cleaning: Tests with real domestic wastewater under low-temperature conditions, Water Res 181 (2020) 115881. https://doi.org/10.1016/j.watres.2020.115881.

[10] F.C. Kent, J. Citulski, K. Farahbakhsh, Water reclamation using membranes: Permeate water quality comparison of MBR and tertiary membrane filtration, Desalination 274 (2011) 237–245. https://doi.org/10.1016/j.desal.2011.02.019.

CHAPTER 6: SYNERGY OF NANOBUBBLES AND SODIUM HYPOCHLORITE

6.1 Background

In the previous chapter, NBW was used for the backwashing of membranes used for MBRs. The efficiency of NBB was found to be better than conventional hydraulic backwashing. In this chapter, we attempted to enhance the efficiency of NBB by a combination with NaClO: a small amount of NaClO was added to NB water and this mixture was used for backwashing to control fouling in MBRs. As shown later, this combination worked better than NBB or CEB using NaClO: a synergetic effect of NBB and NaClO was demonstrated. Chemical composition (i.e., pH) significantly altered NBs and subsequently affected the cleaning efficiency.

6.2 Materials and methods

6.2.1 Operation of bench-scale MBRs

Three identical bench-scale MBRs were operated side by side under the same conditions, except for the respective backwashing solutions. The bench-scale MBRs were installed at a municipal WWTP in Sapporo, Japan, and continuously treated

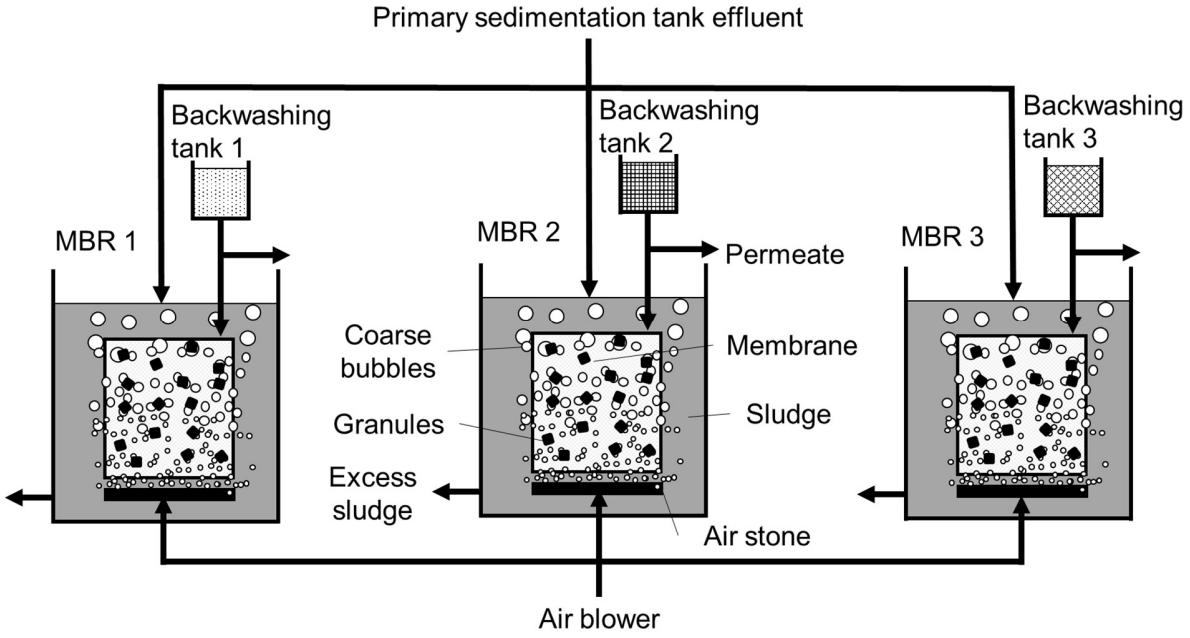

Figure 6.2-1: Schematic figure of the experimental setup.

real municipal wastewater. A schematic figure of the experimental apparatuses is shown in Figure 6.2-1. The effluent from the primary sedimentation tank at the WWTP was used as the feed wastewater to the bench-scale MBRs. At the beginning of the operation, seed biomass was transferred from a pilot-scale MBR installed at the same facility to each bench-scale MBR tank. The bench-scale MBRs were operated at a SRT of 30 days and HRT of 4.5 hours. Since the SRT set for each bench-scale MBR was the same as that of the pilot-scale MBR, it was assumed that acclimatization of the biomass was not necessary. Operation of the bench-scale MBRs was initiated readily after inoculation of the biomass. In this study, each bench-scale MBR was equipped with ceramic flat-sheet membranes (material: Alumina-Al2O3) with a nominal pore size of 0.1 μm (Meidensha, Tokyo, Japan). The available membrane surface area in each MBR was 0.04 m2. The permeability and porosity of the membranes used in this study were 7.7±0.4 L m–2 h–1 kPa^{-1} and 44.1±1.0, respectively [1]. Ceramic membranes, which are characterized by their physical and chemical robustness, have drawn significant attention in various fields of water and wastewater treatment, and many full-scale facilities have been constructed [2]. In all of the tests performed in this study, the permeate fluxes were set at 60 LMH, which

is 2 to 3-times higher than those set in the full-scale application of MBRs [3]. Such high permeate fluxes were applied to accelerate membrane fouling and clarify the differences in fouling observed with the respective backwashings. Intermittent filtration (1-min pause for every 11 min. of filtration) was carried out in all tests. Continuous aeration via air stones installed beneath the membranes was performed at a fixed flow rate of 0.012 Nm3 min^{-1}. Cylindrical granules (PEG, 4 mm) were placed in each MBR tank with a volume ratio of 5% to scour the membrane surface and control membrane fouling [4,5]. The backwashing conditions in this study, including the duration of backwash, which is longer than that applied in real-scale applications, were determined on the basis of the recommendation by the membrane manufacturer and our previous study [4], in which efficient fouling mitigation in bench-scale MBRs was observed with chemically enhanced backwashing (CEB). Flux, duration, and frequency of backwashing were set at 8 LMH, 1 hour, and every 6 hours, respectively. TMP was continuously monitored in each MBR to assess the degree of membrane fouling. To make the comparison among TMP profiles observed in the three MBRs reasonable in each run, the permeability of the membranes was carefully checked before being used. Also, each run was initiated after confirming that the three MBRs exhibited very similar increases in TMP under identical backwashing conditions using tap water.

6.2.2 Backwashing conditions and cleaning solutions

Table 6.2-1 summarizes the backwashing solutions used in each run. NB water was produced by using a commercially available NB generator (ultrafine Galf-FZ1N-7H, IDEC, Osaka, Japan) using tap water. In the generation of NBs, operational parameters recommended by the manufacturer were followed. In brief, circulation of TW between the water tank and the NB generator was carried out for 30 minutes at a flow rate of 12 L min^{-1}, and the pressure was kept between 290 and 310 kPa during the generation of NBs. In this study, to enhance the cleaning efficiency of NBB, NaClO

Table 6.2-1: Summary of backwashing solutions and respective purposes for Runs 1-4.

	MBR No.	Backwashing solution *	Purpose
Run 1	1	NaClO (pH=8.5)	Synergistic effects of NBs and NaClO
	2	NB+NaClO (pH=8.5)	
	3	NB (pH=7)	
Run 2	1	NaClO (pH=12)	Enhancement of cleaning efficiency under alkaline conditions
	2	NB+NaClO (pH=12)	
	3	NB+NaClO (pH=8.5)	
Run 3	1	NaClO (pH=4)	Investigation of cleaning efficiency of NBs and NaClO under acidic conditions
	2	NB (pH=4)	
	3	HCl (pH=4)	
Run 4	1	NaClO (pH=4)	Enhancement of cleaning efficiency under acidic conditions
	2	NB+NaClO (pH=4)	
	3	NB+NaClO (pH=8.5)	

*: Concentration of NaClO was 50 ppm.

(Wako Pure Chemical Industries, Ltd, Osaka, Japan), sodium hydroxide (Wako Pure Chemical Industries, Ltd, Osaka, Japan), and hydrochloric acid (Wako Pure Chemical Industries, Ltd, Osaka, Japan) were added to NB water. Mixed solutions of NBs and NaClO were prepared by dissolving NaClO into NB water so that the concentration of NaClO was 50 ppm. A simple NB-NaClO mixture exhibited a pH of 8.5. Afterwards, the pH of the solution was adjusted by adding hydrochloric acid (HCl) or sodium hydroxide (NaOH) depending on the purposes of the tests. Solutions aimed at an acidic condition were adjusted to pH of 4, whereas solutions intended to be alkaline were adjusted to pH of 12.

Run 1 was conducted to investigate the synergistic effects of the NB-NaClO mixture on backwashing efficiency in MBRs. Run 2 was performed to investigate the cleaning efficiency of backwashing using the mixture of NBs and NaClO under alkaline conditions. Run 3 was conducted to investigate the cleaning efficiency of backwashing using NBs or NaClO under acidic conditions. The purpose of Run 4 was to examine the synergistic effects of backwashing using the mixture of NBs and NaClO under acidic conditions. All backwash solutions were prepared in the university laboratory, stored in containers, and transferred to the wastewater treatment plant, where the experiments were carried out. During each run, a portion of the backwash solutions was brought back to the laboratory every day to analyze the bubble size distribution and zeta potential of NBs. The size distribution of NBs slightly fluctuated in each production batch. To show representative size distributions of NBs in the backwash solution in each run, averaged data are displayed later. Size distributions and zeta potentials of the NBs in the backwashing solutions used in this experiment were measured using an NTA instrument (Nanosight NS500, Malvern, UK).

6.2.3 Analytical methods

MLSS and MLVSS were measured by following the standard methods [6]. The TOC concentrations of influent wastewater were measured by using a TOC meter (TOC-VCSH, Shimazu, Kyoto, Japan). Concentrations of inorganic nitrogen forms, including ammonium (NH_4^+), nitrite (NO_2^-) and nitrate (NO_3^-), were measured using an ion chromatography device (Thermofisher Scientific, Waltham, USA). Foulants deposited on the membrane surface were analyzed by FT-IR spectroscopy. The samples were subject to sublimation using a freeze-drying device (FDU-2100, EYELA, Tokyo, Japan). The freeze-dried samples were analyzed using an infrared spectrophotometer (FT-IR-8400S, Shimadzu, Kyoto, Japan). A scanning electron microscope (S-4000, Hitachi, Tokyo, Japan) was used to visually observe the membrane surface. Before the SEM observations, the fouling layer was chemically fixed and dried using a critical point drying instrument, followed by coating with an Auto Fine Coater (JFC-1200, JEOL, Tokyo, Japan) using a platinum sputter.

6.3 Results and discussion

6.3.1 Synergistic effects of NBs and NaClO (Run 1)

Appendix Fig. B1 summarizes the treatment performances and sludge properties in each run. Four runs were conducted in different seasons with different influent qualities. It should be noted that real municipal wastewater was used in this study. As shown in Appendix Fig. B1, no significant differences in the treatment performances and sludge properties could be recognized among the three MBRs in all runs. Therefore, differences in membrane fouling observed among the three MBRs in each run should be attributed to efficiencies of different backwash conditions.

Figure 6.3-1 (a) and (b) show the average size distribution of NBs in the backwash solutions and increases in TMP observed in Run 1, respectively. One of the MBRs was

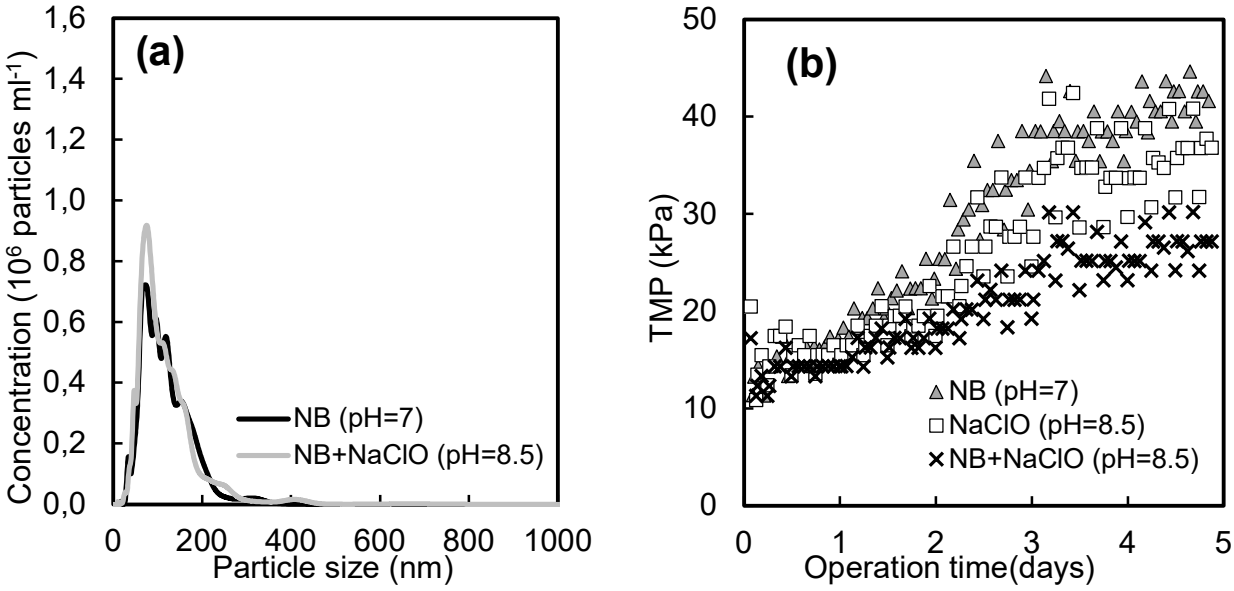

Figure 6.3-1: Average size distributions of NBs used for backwashing in Run 1 (a) and increases in TMP observed in Run 1 (b).

not operated with NBs: it was backwashed by NaClO solution (pH=8.5). The sizes of

NBs in the backwash solution similarly ranged from 20 to 300 nm, regardless of the presence of NaClO in Run 1. In the backwash solution, the mean sizes of NBs and NBs mixed with NaClO in the backwash solution were 119 nm and 96 nm, respectively. It was assumed that a significant portion of NBs could enter the micropores (100 nm) of the membrane [7]. In Run 1, the average concentration of NBs in the backwash solution (pH=7) was 0.73×10^{8} particles m L^{-1}, whereas that of NBs mixed with NaClO (pH=8.5) was 0.61×108 particles mL^{-1}.

The filtration resistances of the MBRs backwashed with NBs (pH=7), NaClO (pH=8.5) and NBs+NaClO (pH=8.5), assessed at the termination of Run 1, were 24.9×10^{11} m^{-1}, 21.8×10^{11} m^{-1} and 14.9×10^{11} m^{-1}, respectively. Increases in TMP observed in the MBR backwashed with NaClO were slightly slower than those observed in the MBR operated with NB backwash. When an MBR was operated with backwashing using the mixture of NBs and NaClO, increases in TMP were slower than those observed with the other two MBRs. This indicates synergistic effects of NBs and NaClO in backwashing. An additional test was carried out with the same backwashing conditions as those set in Run 1 in a different period and the TMP data are shown in the supporting information (Appendix Fig. B1). Although the feed wastewater characteristics were different (It should be noted that real wastewater was used in this study.), the combination of NBs and NaClO exhibited better performance than that of NB backwashing or NaClO backwashing. Thus, the effectiveness of the combination of NBs and NaClO for backwashing of MBRs was confirmed. Appendix Fig. B2 shows FT-IR spectra of the fouling layers at the termination of Run 1. FT-IR measurement was conducted to investigate the characteristics of organic compounds in the fouling layers deposited on the membrane surface. The presence of polysaccharides in the fouling layer was suggested by peaks at wavelengths of 1040 cm^{-1} and 3400 cm^{-1} [8], while peaks at wavelengths of 1411 cm^{-1}, 1550 cm^{-1} and 1655 cm^{-1} suggested the presence of amide-like substances and proteins [9]. Peaks around 2920 cm^{-1} were assigned to lipids [10]. FT-IR spectra measured for the three MBRs

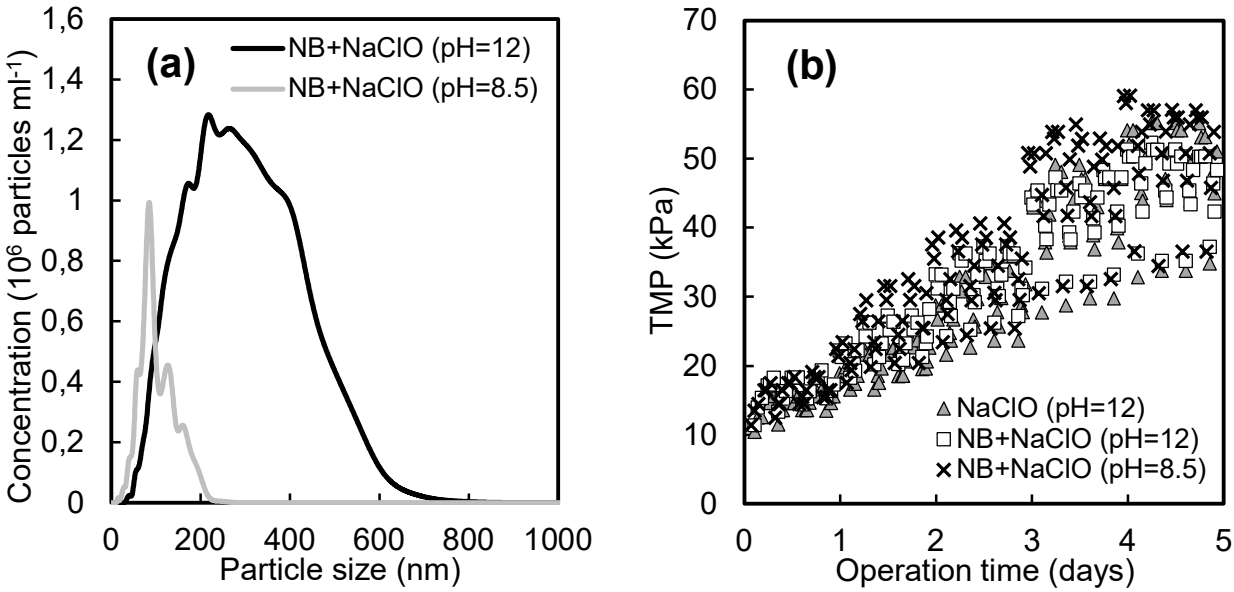

Figure 6.3-2: Average size distributions of NBs used for backwashing in Run 2 (a) and increases in TMP observed in Run 2 (b).

backwashed with different solutions were quite similar, implying that the fouling layers formed in the three MBRs in Run 1 had similar compositions. In the previous chapter, it was also suggested that backwashing with NB water did not significantly alter the compositions of fouling layers on the surface of membranes used for MBRs.

6.3.2 Mixture of NBs and NaClO under alkaline conditions (Run 2)

Figure 6.3-2 shows the average size distributions of NBs in the backwash solutions used in Run 2 (NBs mixed with NaClO (pH=8.5) and NBs mixed with NaClO (pH=12)) and increases in TMP observed in Run 2. The filtration resistances of the MBRs backwashed with NaClO (pH=12), NBs+NaClO (pH=12) and NBs+NaClO (pH=8.5), assessed at the termination of Run 2, were 20.4×10^{11} m^{-1}, 21.6×10^{11} m^{-1} and 21.3×10^{11} m^{-1}, respectively. It should be noted that one MBR was not operated with NB backwash in Run 2 but was operated with NaClO backwash (pH=12). Both the size and concentration of NBs significantly increased when pH was set at 12. Although no clear explanation for this observation is available at present, the reproducibility of this change in the average size and concentration of NBs caused by the elevation of

pH was carefully confirmed. A possible reason for this change in the NBs will be discussed later. Jadhav et al. (2021) also reported that the size (and concentration) of NBs increased when the pH of the solution was increased [11].

The strong oxidation capacity of NaClO is generally attributed to its protonated form hypochlorous acid (HOCl) rather than to hypochlorite (OCl^-). However, Wang et al. (2018) reported that the effectiveness of membrane cleaning using NaClO could be enhanced under an alkaline condition as diffusivities of NaClO could be increased via relaxation of the matrix structure of the fouling layer [12]. Therefore, this implies that the mixture of NBs and NaClO under alkaline conditions could exhibit a high cleaning efficiency. Backwashing with the mixture of NBs and NaClO at pH of 8.5 exhibited a high cleaning efficiency, which was comparable to that observed with backwashing using NaClO at pH of 12. This is a reflection of the synergetic effect of NBs and NaClO, as observed in Run 1. However, as shown in Figure 6.3-2 (b), the presence of NBs did not exhibit synergetic effects when pH was set at 12. When NBs were mixed with NaClO at pH of 12, their average size (303 nm) was much larger than the membrane's pore size (100 nm). It was assumed that NBs in backwash solution could not enter the micropores of the membranes when pH was set at 12. Increases in TMP observed in the MBR operated with NBs+NaClO (pH=12) backwash were comparable to those in the MBR operated with NaClO (pH=12) backwash.

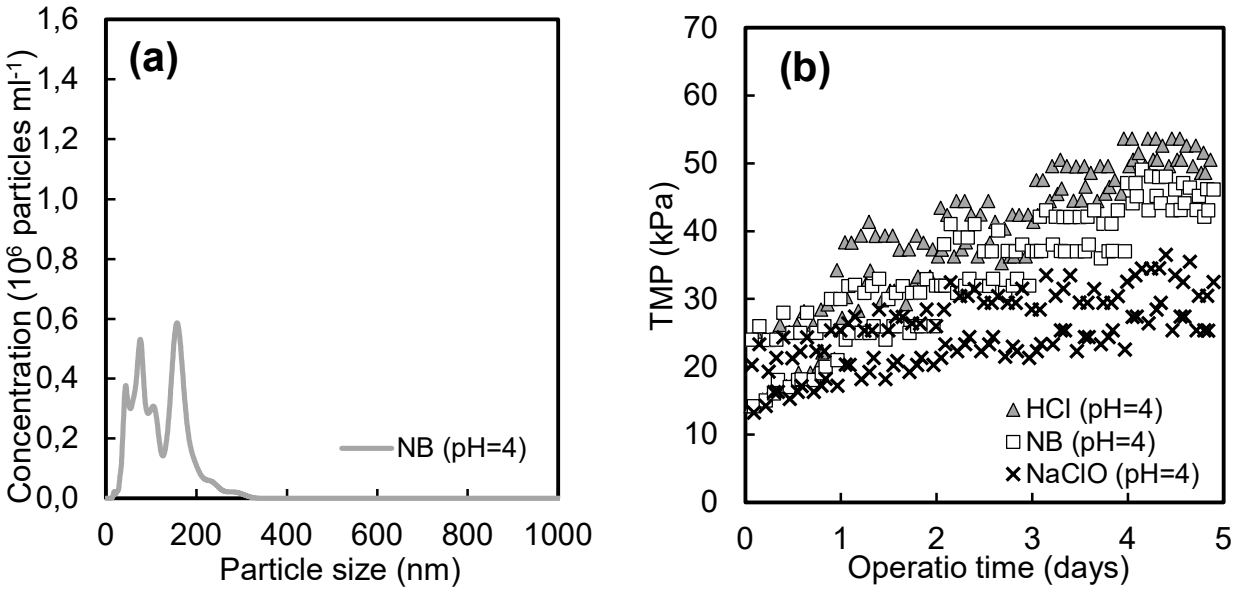

Figure 6.3-3: Average size distribution of NBs used for backwashing in Run 3 (a), and increase in TMP observed in Run 3 (b).

6.3.3 Backwashing with NBs and NaClO under acidic conditions (Run 3)

The average size distribution of NBs used for backwash in Run 3 and increases in TMP observed in Run 3 are shown in Figure 6.3-3. The filtration resistances of the MBRs backwashed with HCl (pH=4), NBs (pH=4) and NaClO (pH=4), assessed at the termination of Run 3, were 30.8×10^{11} m^{-1}, 28.7×10^{11} m^{-1} and 17.4×10^{11} m^{-1}, respectively. Two MBRs were operated without NBB in Run 3: water or NaClO solution acidified by HCl (pH=4) was used for backwash in the two MBRs. When pH was set at 4, the size distribution of NBs shifted towards smaller sizes compared with those at pH of 7 (Fig. 2). Reductions in the size of NBs when pH was lowered were also reported previously [11]. In Run 3, backwashing the membranes with NaClO (pH=4) was more effective than backwashing with NBs (pH=4) and HCl (pH=4). It is known that NaClO exhibits a high efficiency for disinfection under acidic conditions due to an increased concentration of HOCl [13]. Therefore, it was assumed that the degradation power of NaClO at pH of 4 was enhanced and that this contributed to the

efficient backwashing with NaClO at pH of 4 in Run 3. Increases in TMP in the MBR operated with NB backwashing (pH=4) were slower than those in the MBR backwashed with acidified water (pH=4), indicating that the presence of NBs in the backwash solution enhanced the cleaning efficiency under acidic conditions as well as neutral conditions. Shifts in the size distribution of NBs towards smaller sizes (Figure 6.3-3 (a)), which could facilitate intrusion of NBs into micropores during backwash under acidic conditions, contributed to the enhancement of cleaning efficiency.

6.3.4 Enhancement of cleaning efficiency by synergistic effects under an acidic condition (Run 4)

Considering that efficiencies of backwashing both with NBs and NaClO seemed to be enhanced under acidic conditions, it was hypothesized that backwashing with an acidic mixture of NBs and NaClO would exhibit a much higher cleaning efficiency. This hypothesis was investigated in Run 4. The average size distributions of NBs in backwash solutions used in Run 4 and increases in TMP observed in Run 4 are shown in Figure 6.3-4. The filtration resistances of the MBRs backwashed with NaClO (pH=4), NBs+NaClO (pH=8.5) and NBs+NaClO (pH=4), assessed at the termination of Run 4, were 24.2×10^{11} m^{-1}, 26.2×10^{11} m^{-1} and 17.5×10^{11} m^{-1}, respectively. One MBR was not operated with NBs in Run 4 but was operated with NaClO (pH=4). When pH was set at 8.5 in Run 4, the size distribution of NBs in the backwash solution with NaClO was similar to that observed in Run 1 (Fig. 2). When pH was set at 4 in Run 4, NBs with sizes of about 80 nm became dominant in the backwash solution. Comparison of the size distributions of NBs with and without NaClO under the acidic condition (Figure 6.3-3 (a) and Figure 6.3-4 (a)) suggested that the presence of NaClO affected the size distribution of NBs under the acidic condition: the presence of NaClO made the size distribution of NBs more uniform. When the pH of the mixture of NBs and NaClO was reduced to 4, most of the NBs became smaller. Therefore, it was expected that NBs could enter the micropores more easily during backwashing in Run 4 and that a synergetic effect of NBs and NaClO was likely to be observed. The

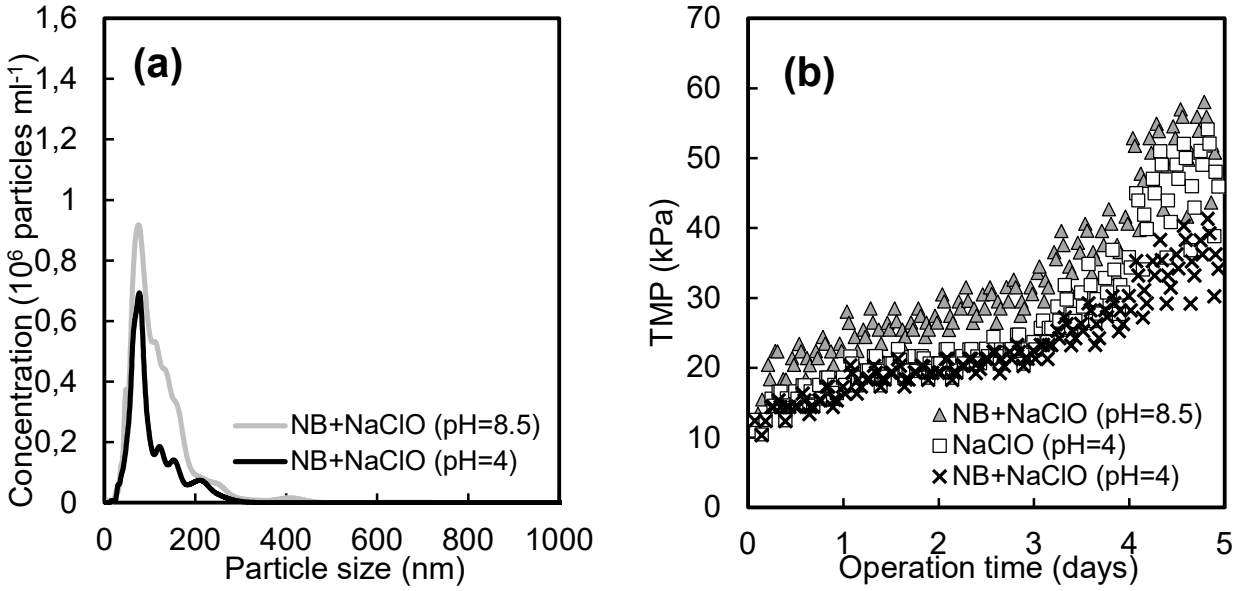

Figure 6.3-4: Average size distribution of NBs used for backwashing in Run 4 (a) and increases in TMP observed in Run 4.

increases in TMP observed with backwashing using the mixture of NBs and NaClO (pH=4) was the slowest among the three MBRs in Run 4. Differences in the particle size distribution of NBs mixed with NaClO (pH=8.5) and NaClO (pH=4) were mostly found in the size range of >100 nm (the size of the micropores of the membrane). Those large NBs present under the condition of pH of 8.5 could neither enter the micropores nor enhance the cleaning efficiency. It should be noted that backwashing with the mixture of NBs and NaClO (pH=4) was more effective than that with NaClO (pH=4), indicating that the addition of NBs to the NaClO solution was beneficial for the enhancement of backwashing efficiency under the acidic condition. Hence, the results obtained in Run 4 suggest that backwashing with the mixture of NBs and NaClO at pH of 4 exhibited synergistic effects of NaClO and NBs.

As mentioned before (section 6.3.3), high oxidation potential of NaClO under acidic conditions is well recognized. In contrast, the mechanisms by which NBs can mitigate fouling in backwashing have not been fully clarified. It has been reported that ROS

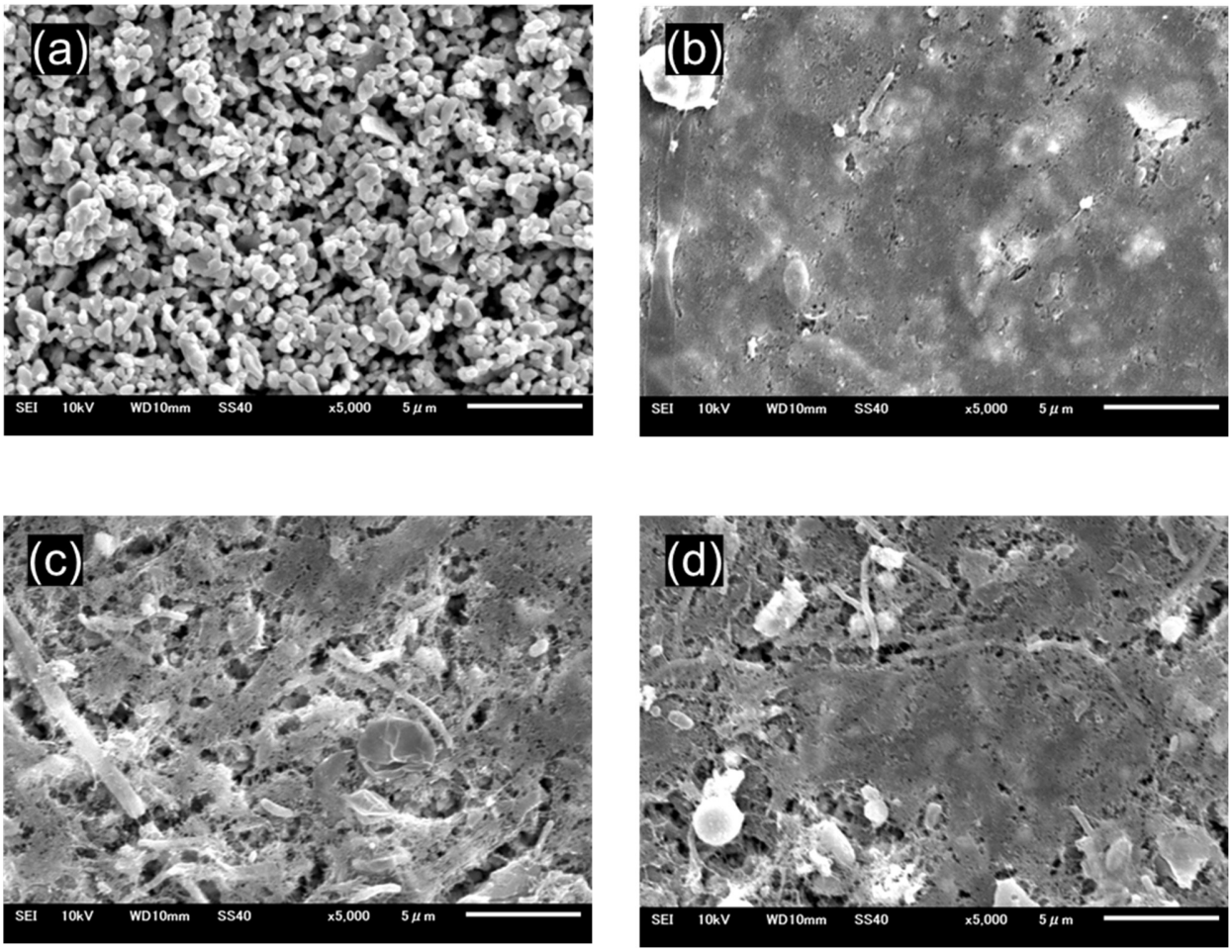

Figure 6.3-5: SEM images of new and fouled membrane samples taken at the termination of Run 4. (a) New membrane, (b) NaClO (pH=4), (c) NBs+NaClO (pH=4), (d) NBs+NaClO (pH=8.5).

are generated from NBs through their destabilization and bursting [14]. Since NBs are less stable under lower pH conditions [15], the generation of ROS from NBs might be enhanced under acidic conditions, and the ROS might contribute to the high cleaning efficiency shown in Figure 6.3-4. However, analysis of the fouling layer by FT-IR analysis did not suggest the generation of ROS by NBs and subsequent oxidation of foulants in Run 4: The FT-IR data (Appendix Fig. B3) showed that there were no differences among the spectra of the fouling layer samples taken from the three MBRs operated in Run 4. It is hypothesized, though, that NBs penetrate the membrane pores during backwashing and loosen the structure of the fouling layer on

the surfaces of the membranes, thus alleviating membrane fouling. SEM images (Figure 6.3-5) of the fouled membranes used in Run 4 support this postulation. The morphology of the fouling layer was more porous when the membrane was backwashed with the acidic mixture of NBs and NaClO (Figure 6.3-5 (c)).

6.4 Impact of pH on the properties of nanobubbles and nanobubble backwashing

Figure 6.4-1 shows the mean size and zeta potential of NBs mixed with NaClO (50 ppm) at different pH values. The size and zeta potential of NBs significantly changed when pH was elevated to 12. In contrast, the characteristics of NBs and NBs mixed with NaClO did not vary greatly when the pH was set at 4 or 8.5, as shown in Figure 6.4-1. The size of NBs under the high alkaline condition was much larger than the membrane's pore size. When the pH of the NB water was set at 12 and the NB water was used for backwashing, most of the NBs could not intrude into the membrane pores and could not make contact with the fouling layer, leading to a poor cleaning efficiency

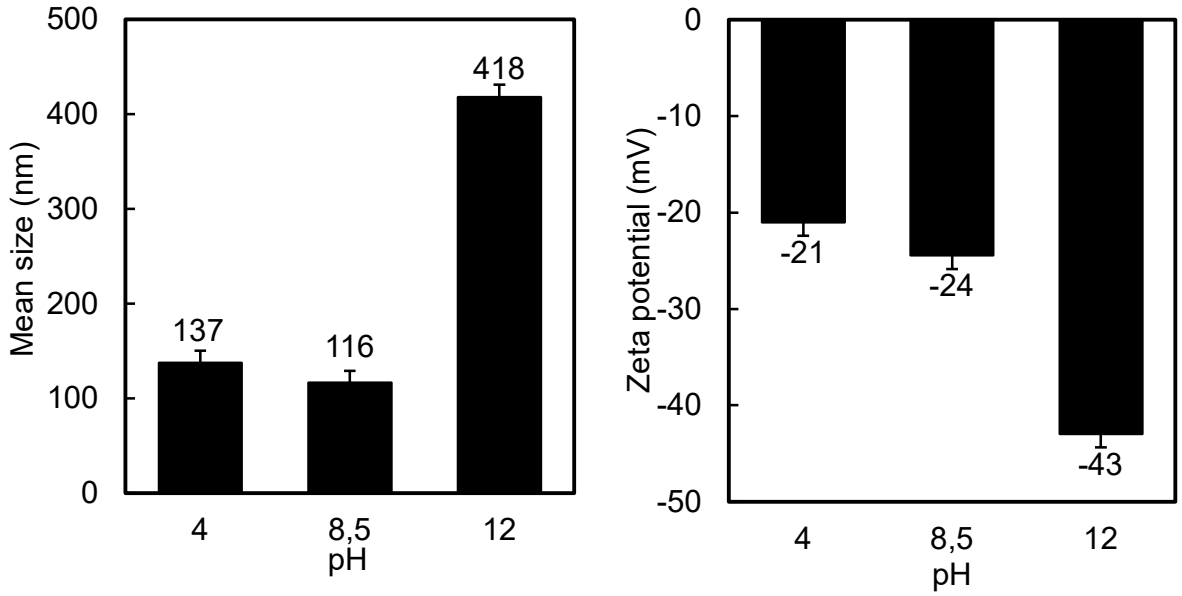

Figure 6.4-1: Mean size and zeta potential of NBs mixed with NaClO (50 ppm) under different pH values.

of NBs mixed with NaClO at pH of 12 as observed in Run 2 (Figure 6.3-2). Although it was not clearly shown that there was a significant difference in the averaged size of NBs between pH of 4 and pH of 8.5 (Figure 6.4-1), the size distributions of NBs at pH of 4 and 8.5 (Figure 6.3-4 (a)) suggests that small NBs were present under acidic conditions: large NBs (>100 nm) disappeared at pH of 4. It should be noted that the analytical instrument used for NB measurements in this study was not good at detecting of particles with sizes of less than 50 nm. It was postulated that those small NBs entered the microstructure of the fouling layer and subsequently made the fouling layer porous (Figure 6.3-5). Also, the absolute value of the zeta potentials of NBs at a pH of 4 was slightly smaller than that at a pH of 8.5. This might also have contributed to the better cleaning efficiency of the backwashing with the mixture of NBs and NaClO at pH of 4 than that at pH of 8.5 in Run 4. Electrostatic repulsion between NBs and the fouling layer, which is supposed to be negatively charged, might be alleviated more at pH of 4 than at pH of 8.5. Attachments of NBs onto the fouling layers might be promoted at pH of 4.

6.5 Summary

In this chapter, a study on the mixture of NBs and NaClO used for backwashing of MBRs treating municipal wastewater was presented. There was a synergetic effect between NBs and NaClO on backwashing of membranes: the mixture of NBs and NaClO exhibited better backwashing efficiencies than did backwashing with either NBs or NaClO. By using the mixture for backwashing of MBRs, fouling in MBRs can be more efficiently controlled than that with CEB. It was thought that NBs used in the backwashing made the structure of the fouling layer loose, which enhanced the cleaning effect of NaClO that was co-present in the backwash solution. However, it was demonstrated in this study that the synergetic effect of the mixture of NBs and NaClO on backwashing efficiency was highly dependent on pH. The alkaline solution (pH 12) facilitated agglomeration of NBs and did not allow resulting large NBs to

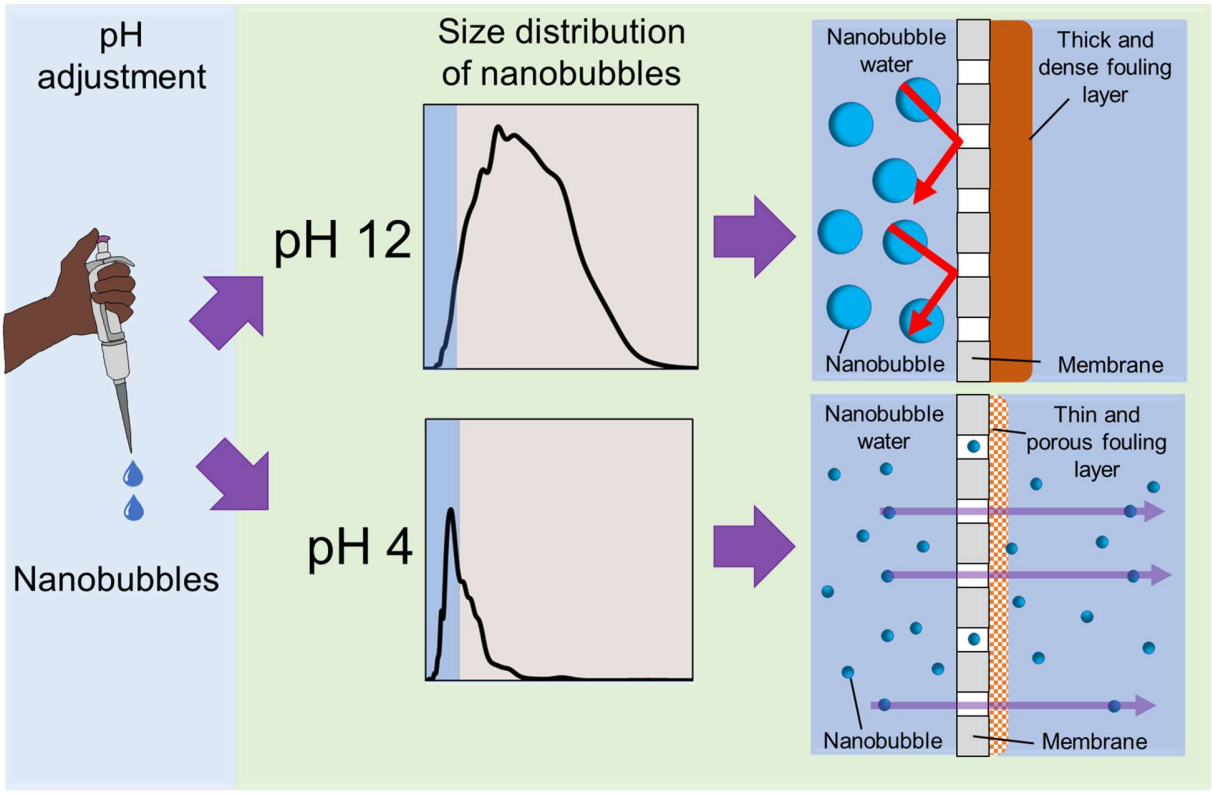

Figure 6.5-1: Proposed mechanism of fouling mitigation of NBs under different pH

enter the micropores of the membrane. No synergetic effects were seen under the condition of pH of 12. At pH of 8.5 or 4, synergetic effects were obvious. At pH of 4, the mixture of NBs and NaClO showed very high backwash efficiency, probably due to the high oxidation power of NaClO and favorable properties of NBs (e.g., size distribution) under an acidic condition. Since the mechanism of cleaning with NBs under different pH conditions is not fully comprehended, a proposed mechanism is suggested () based on the previous discussion.

The key elements to efficiently clean the membrane used in this study (e.g., ceramic flat-sheet membrane, granular scouring and NBs) have already been commercialized and industrialized. Therefore, large-scale application of the cleaning examined in this study is certainly feasible. It was shown in this study that an acid significantly enhanced the cleaning effect of NBB for MBRs. However, that does not mean that the acid used is the best chemical agent to enhance the synergistic effects. It is very likely

that other chemicals would further enhance the cleaning effects of NBB, and that should be investigated in a future study. Therefore, there is plenty of room for enhancement of the synergistic effects of NBs and chemicals. The long-term performance of NBB under optimized conditions should be investigated in future studies.

REFERENCES

[1] S. Dong, E.S. Kim, A. Alpatova, H. Noguchi, Y. Liu, M. Gamal El-Din, Treatment of oil sands process-affected water by submerged ceramic membrane microfiltration system, Sep Purif Technol 138 (2014) 198–209. https://doi.org/10.1016/J.SEPPUR.2014.10.017.

[2] H. Sakamoto, A. Hafuka, T. Tsuchiya, K. Kimura, Intensive routine cleaning for mitigation of fouling in flat-sheet ceramic membranes used for drinking water production: Unique characteristics of resulting foulants, Sep Purif Technol 301 (2022). https://doi.org/10.1016/j.seppur.2022.121950.

[3] S.J. Judd, The status of industrial and municipal effluent treatment with membrane bioreactor technology, Chemical Engineering Journal 305 (2016) 37–45. https://doi.org/10.1016/j.cej.2015.08.141.

[4] Y. Ninomiya, K. Kimura, T. Sato, T. Kakuda, M. Kaneda, A. Hafuka, T. Tsuchiya, High-flux operation of MBRs with ceramic flat-sheet membranes made possible by intensive membrane cleaning: Tests with real domestic wastewater under low-temperature conditions, Water Res 181 (2020) 115881. https://doi.org/10.1016/j.watres.2020.115881.

[5] T. Kurita, K. Kimura, Y. Watanabe, The influence of granular materials on the operation and membrane fouling characteristics of submerged MBRs, J Memb Sci 469 (2014) 292–299. https://doi.org/10.1016/j.memsci.2014.05.057.

[6] R.B. Baird, A.D. Eaton, E.W. Rice, Standard methods for the examination of water and wastewater, 2017.

[7] H. Fernandes, S. Kiuchi, T. Kakuda, A. Hafuka, T. Tsuchiya, Y. Matsui, K. Kimura, Fouling mitigation in membrane bioreactors by nanobubble-assisted backwashing, Journal of Water Process Engineering 53 (2023) 103860. https://doi.org/10.1016/J.JWPE.2023.103860.

[8] S.R.P. Shariati, B. Bonakdarpour, N. Zare, F.Z. Ashtiani, The effect of hydraulic retention time on the performance and fouling characteristics of membrane sequencing batch reactors used for the treatment of synthetic petroleum refinery wastewater, Bioresour Technol 102 (2011) 7692–7699. https://doi.org/10.1016/J.BIORTECH.2011.05.065.

[9] H. Hazrati, A.H. Moghaddam, M. Rostamizadeh, The influence of hydraulic retention time on cake layer specifications in the membrane bioreactor: Experimental and artificial neural network modeling, J Environ Chem Eng 5 (2017) 3005–3013. https://doi.org/10.1016/j.jece.2017.05.050.

[10] R.R.E. Artz, S.J. Chapman, A.H. Jean Robertson, J.M. Potts, F. Laggoun-Défarge, S. Gogo, L. Comont, J.R. Disnar, A.J. Francez, FTIR spectroscopy can be used as a screening tool for organic matter quality in regenerating cutover peatlands, Soil Biol Biochem 40 (2008) 515–527. https://doi.org/10.1016/J.SOILBIO.2007.09.019.

[11] A.J. Jadhav, M. Barigou, On the clustering of bulk nanobubbles and their colloidal stability, J Colloid Interface Sci 601 (2021) 816–824. https://doi.org/10.1016/j.jcis.2021.05.154.

[12] X. Wang, J. Ma, Z. Wang, H. Chen, M. Liu, Z. Wu, Reinvestigation of membrane cleaning mechanisms using NaOCl: Role of reagent diffusion, J Memb Sci 550 (2018) 278–285. https://doi.org/10.1016/j.memsci.2017.12.083.

[13] S. Fukuzaki, Mechanisms of Actions of Sodium Hypochlorite in Cleaning and Disinfection Processes, Biocontrol Sci 11 (2006) 147–157. https://doi.org/10.4265/BIO.11.147.

[14] J. Wu, K. Zhang, C. Cen, X. Wu, R. Mao, Y. Zheng, Role of bulk nanobubbles in removing organic pollutants in wastewater treatment, AMB Express 2021 11:1 11 (2021) 1–13. https://doi.org/10.1186/S13568-021-01254-0.

[15] M. Soyluoglu, D. Kim, Y. Zaker, T. Karanfil, Stability of Oxygen Nanobubbles under Freshwater Conditions, Water Res 206 (2021) 117749. https://doi.org/10.1016/J.WATRES.2021.117749.

CHAPTER 7: COST OF BACKWASHING SOLUTIONS

7.1 Cost computations

In this chapter an assessment of the costs for generating NBs, HC-NBs, and the backwashing solutions used in previous chapters will be made. The price of all chemicals used in the computation of the costs were according to the manufacturers. The cost for the delivery of the chemicals and for the acquisition of the NB generators were not considered in the calculations. Rather, only the cost for the preparation of the chemical solutions and the generation of the NB waters were considered. The cost of electricity is 29,8 JPY kWh^{-1}, while the power requirements the NB and HC-NB generators is 1.2 kW and 1.5 kW, respectively. It takes 10 min to produce 10 L and 1 L of water containing NBs generated by the NB and HC-NB generators, respectively. In Sapporo city, 1 liter of tap water cost 1,45 yen. It costs 1,65-yen L^{-1} to adjust the concentration of NaClO solution to 50 ppm, 0,077 and 0,125 -yen L^{-1} to adjust the pH of backwashing solutions to 12 and 4, respectively. The cost of NBs is calculated as shown in the equation 15:

$$C_{NB} = C_{TW} + \frac{E_{NB} \times T_{NB}}{V_{NB}} \times C_E \quad (15)$$

Where:

C_{NB} is the cost of NBW or HC-NBW generation (yen L^{-1})

C_{TW} is the cost of tap water (yen L^{-1})

E_{NB} is the energy requirement for the generation of NBW or HC-NBW (kW)

T_{NB} is the duration of NBW or HC-NBW generation (h)

V_{NB} is the volume of NBW or HC-NBW per generation (L)

C_E is the cost of energy (yen kWh^{-1})

The cost of all other solutions used in this study are show below, in equations 16 to 21.

$$C_{NaClO8.5} = C_{TW} + C_{NaClO} \quad (16)$$

$$C_{NaClO12} = C_{TW} + C_{NaClO} + C_{pH12} \quad (17)$$

$$C_{NaClO4} = C_{TW} + C_{NaClO} + C_{pH4} \quad (18)$$

$$C_{NB+NaClO8.5} = C_{NB} + C_{NaClO} \quad (19)$$

$$C_{NB+NaClO12} = C_{NB} + C_{NaClO} + C_{pH12} \quad (20)$$

$$C_{NB+NaClO4} = C_{NB} + C_{NaClO} + C_{pH4} \quad (21)$$

Where:

$C_{NaClO8.5}$ is the cost of NaClO at pH 8.5

$C_{NaClO12}$ is the cost of NaClO at pH 12

C_{NaClO4} is the cost of NaClO at pH 4

$C_{NB+NaClO8.5}$ is the cost of NB+NaClO at pH 8.5

$C_{NB+NaClO12}$ is the cost of NB+NaClO at pH 12

$C_{NB+NaClO4}$ is the cost of NB+NaClO at pH 4

Table 7.1-1 summarizes the cost for the production of each backwashing solution used in this study.

Table 7.1-1: Cost of production of backwashing solution.

Backwashing solution	Cost (yen L^{-1})
Tap water (C_{TW})	1,452
NBW (C_{NB})	2,048
NBW (pH=4)	3,625
HC-NBW (C_{NB})	8,902
NaClO (pH=8.5) ($C_{NaClO8.5}$)	3,108
NaClO (pH=12) ($C_{NaClO12}$)	3,185
NaClO (pH=4) (C_{NaClO4})	3,233
NB+NaClO (pH=8.5) ($C_{NB+NaClO8.5}$)	3,704
NB+NaClO (pH=12) ($C_{NB+NaClO12}$)	3,781
NB+NaClO (pH=4) ($C_{NB+NaClO4}$)	3,829
**NaClO (C_{NaClO})	1,650
*NaOH (pH=12) (C_{pH12})	0,007
*HCl (pH=4) (C_{pH4})	0,125

7.2 Discussion

Tap water is the cheapest to acquire, as it is readily available in the municipal water supply system. The cost for generating NBW is the cheapest among all the other backwashing solutions. NBB can be a cheap and environmentally friendly solution for membrane cleaning in MBRs. On the other hand, the cost of generating HC-NBW is the highest among all the backwashing solutions used in this study. More efficient high concentration nanobubble generators are needed. The energy demand to generate 1 L of the HC-NBW doesn't compensate the improvement in cleaning

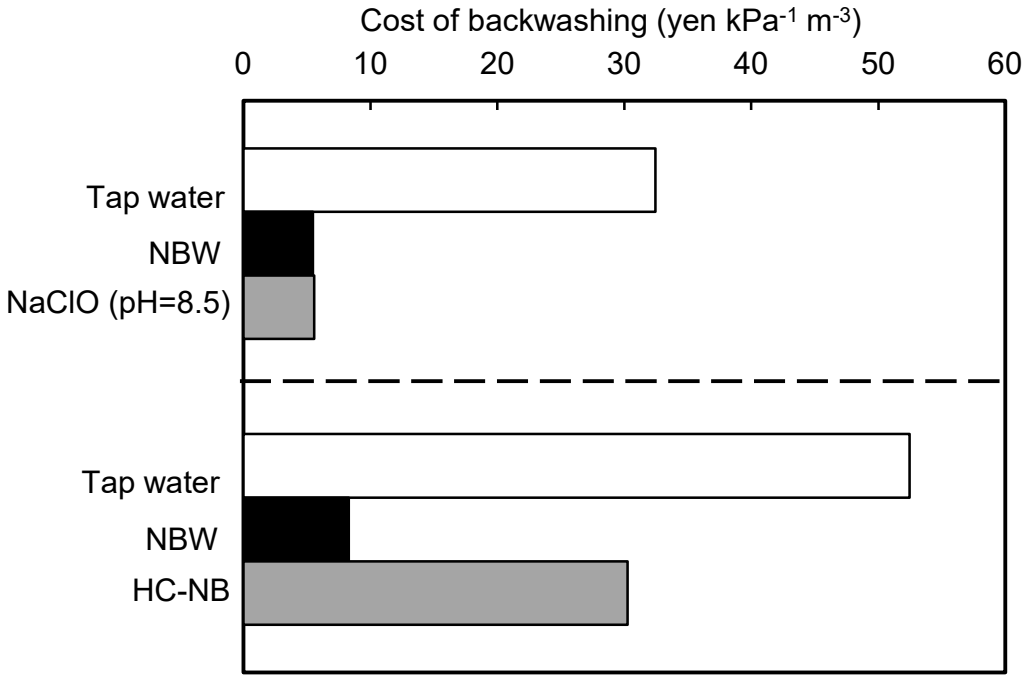

Figure 7.2-1: Cost of application of backwashing solutions used in experiments chapter 4.

efficiency. On the other hand, if studies on the optimal concentration of NBs for maximized cleaning efficiency, as well more efficient HC-NB generators are investigated, the use of HC-NBW can be feasible.

Figure 7.2-1 and Figure 7.2-2 show plots of the costs of backwashing per unit kPa of pressure reduced per cubic meter of treated water, in experiments described in chapters 4 and 5, respectively. In Figure 7.2-1 the backwashing solutions used in each experiment are compared to conventional hydraulic backwashing with tap water. As shown by the plots and Table 7.1-1, although tap water is cheaper than the other backwashing solutions, due to its insufficient cleaning properties, it becomes less cost-effective than the other counterparts. NBW, although not as efficient as NaClO (50 ppm), brings about a comparable cost effectiveness related to tap water, when compared to NaClO. Hence, Although CEB with NaClO is more efficient than NBB in mitigating fouling, due to the low cost of NB generation and high efficiency of NBB,

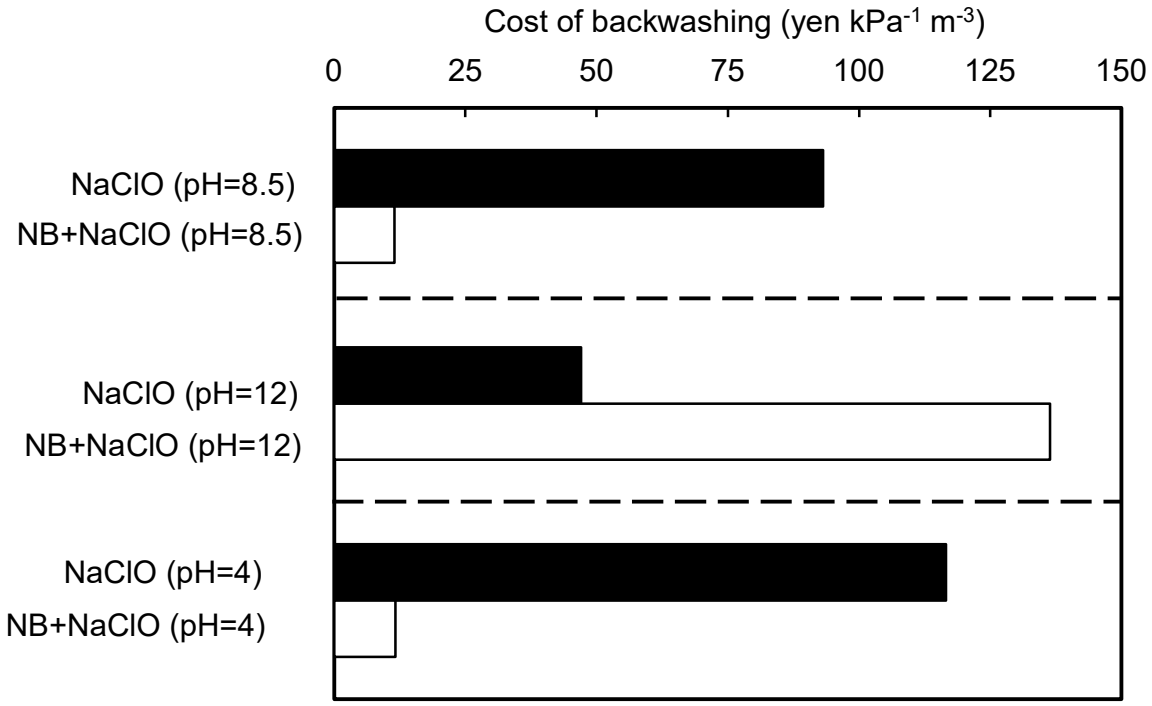

Figure 7.2-2: Cost of application of backwashing solutions used in experiments of chapter 5.

NBB becomes comparably cost efficient for the mitigation of fouling in MBR. Considering the environmental impact and adverse effect of NaClO on the microorganism in the mixed liquor suspension of MBRs, NBB is a cheaper and cleaner alternative. The same cannot be said about HC-NBW because it is very expensive. HC-NBW is still more cost-effective than tap water, due to the large number of NBs contributing for fouling mitigation. However, due to the high cost of generating HC-NBs, HC-NBB is not as cost-effective as NBB.

In Figure 7.2-2 the mixtures of NBs and NaClO at different pH are compared to their respective counterparts used as control experiments. Although adding NBs to NaClO solution represents an extra cost, the improvement in the cleaning properties by the synergy may justify or not using mixed solutions in backwashing of membrane used in MBR.s. In the case of Run 1 (pH=8.5), it compensates to add NBs to NaClO solutions due to its low cost and significant improvement in cleaning. The same cannot be said of NB+NaClO (pH=12) since no significant synergy were detected at high pH.

The mixture of NBs and NaClO at alkaline conditions is not recommended due to the low cost-effectiveness. However, the mixture of NBs and NaClO at low pH becomes more cost-effective than NaClO alone. Although it is more expensive to prepare NB+NaClO solutions then it is to prepared NaClO at pH 4, the significant improvement in cleaning efficiency at acidic conditions makes NB+NaClO more cost-effective. Hence, the synergy of NBs and NaClO at acidic conditions is so positive that it becomes significantly more cost-effective.

CHAPTER 8: CONCLUSIONS AND RECOMENDATIONS

Nanobubble-assisted backwashing (NBB) was applied in MBRs to mitigate membrane fouling for the first time. A series of experiments encompassing the operation of bench-scale MBRs in parallel were conducted. NBB was compared to chemically enhanced backwashing (CEB) and hydraulic backwashing with tap water (TWB). The cleaning efficiency of NBB was enhanced by the synergy with NaClO. The characteristics and effect of NBs on sludge were assessed. Finally, the cost of the backwashing solutions used in this study were compared.

It was shown that NBB is more effective than TWB, but not as effective as CEB. Adding NBs in the backwashing solution of fouled membranes used for MBRs was beneficial due to their properties. Although the mechanisms of NBB efficiency could not be fully elucidated, it could be confirmed that the size of NBs plays a crucial role in contributing for the cleaning efficiency of nanobubble water. Large NBs could not penetrate the membrane pores and contact the fouling layer on the surface of the membranes. However, smaller NBs easily passed through the membrane channels and changed the structure of the fouling layers. It was postulated that NBs made the structure of the fouling layer more porous and easily removed by the mechanical scouring of granules. The pH of the backwashing solution is an important factor affecting the efficiency of NBB. The properties of NBs, as well as their cleaning effect, changes according to pH. In this study, it was observed that the cleaning properties

of NBs were more evident at low pH, such as 4. On the other hand, NBs under the pH of 12 didn't showcase any cleaning efficiency. It is worth noting that the experiments of NBs under different pH were conducted in synergy with a 50 ppm NaClO solution. The synergy of NBs and NaClO was very evident at low pH, but inexistent at high pH. The changes in the fouling layer brought out by small NBs and the well know oxidation powers of NaClO worked synergistically to improve the cleaning efficiency. No significant changes in the properties of the mixed-liquor suspension in the bench-scale MBRs used in this study were observed. The nanobubble water (NBW) produced in the experiments is cheaper and as cost effective as a 50 ppm NaClO solution. However, high-concentration NB water (HC-NBW) is the most expensive of all solutions used. Although the mixtures of NBs and NaClO at pH 4 or 8,5 are very expensive to prepare, the significant improvement in cleaning efficiency, due to their positive synergy is makes them very cost-effective. The same cannot be said of the mixture of NBs and NaClO at the pH of 12.

The following general conclusion can be made, according to the goals set in this study:

1. Fouling mitigation was accomplished by the application of NBB; NBB is superior to TWB but inferior, and at times equal, to CEB;
2. The effect of NBs on the microbial activity in MBRs was indirectly assessed. No confirmation of a negative effect of NBs on the microbial activity could be made.
3. The efficiency of NBB could be enhanced the by the synergy with NaClO. The synergy was more significant at low pH;
4. The cost-effectiveness of the use on NB-based backwashing was assessed. NBB is comparable to CEB. Adding NBs to a NaClO solution at pH 4 or 8,5 significantly improved the cleaning efficiency and is more cost-effective;

The present work is a novel study on the mitigation of fouling in MBRs. NBs were applied for backwashing in MBRs for the first time, and a contribution to current attempts to mitigate membrane fouling and widen the use of MBRs was made. However, this study is not exhaustive, leaving a way for further studies. A limitation of this work is the lack of confirmed mechanisms of NB cleaning in backwashing of

membranes. Although hypotheses were presented, there is still need for confirmation of possible mechanisms. Due to time limitations and constraints, it was not possible to fully elucidate the mechanism. Future studies could also focus on investigating the effect of other properties of NBs (zeta potential, bursting, etc), optimizing the backwashing conditions of NBB, synergy with other cleaning methods (Ultrasound, other chemicals, etc), and the usage of NBs containing other gases (O_2, O_3, etc).

APPENDIX A

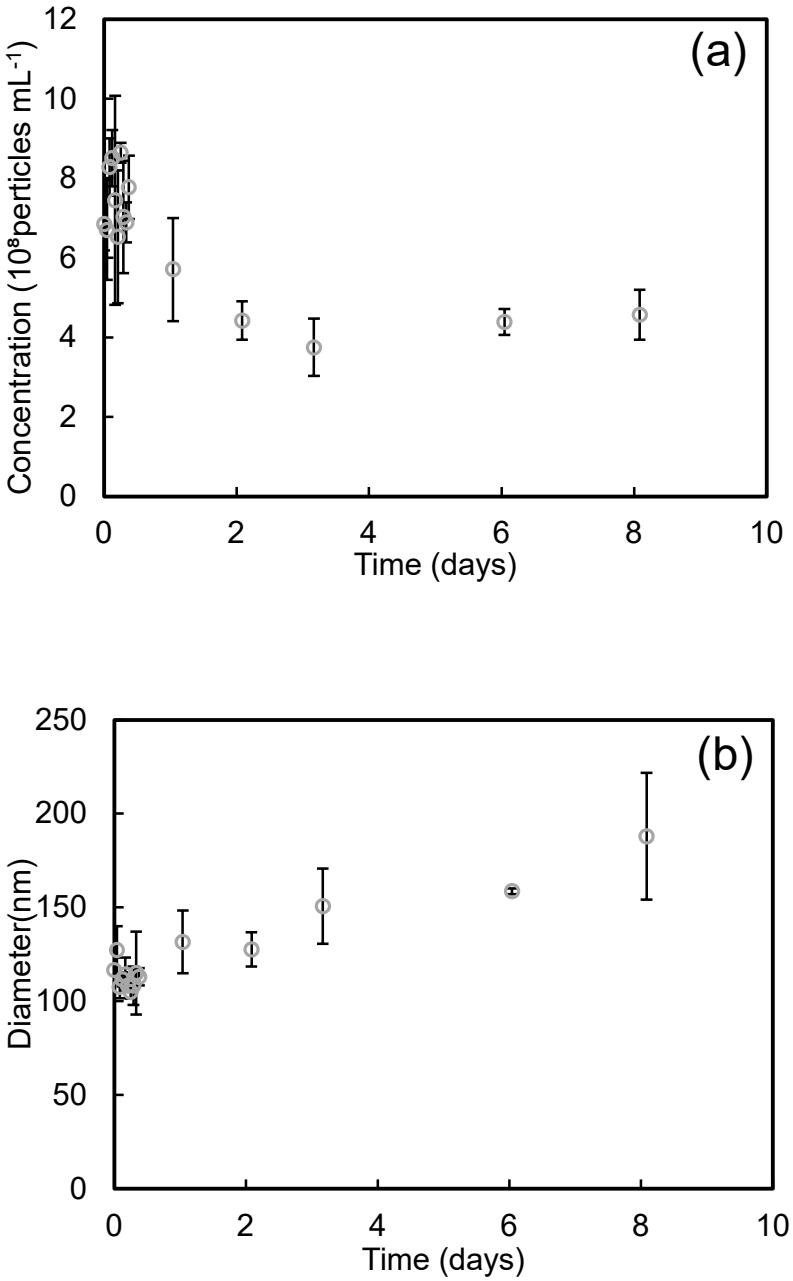

Fig. A1. Long term stability of NBs. Fig. S1 (a): Concentration of NBs. Fig. S1 (b): Mean diameter of NBs.

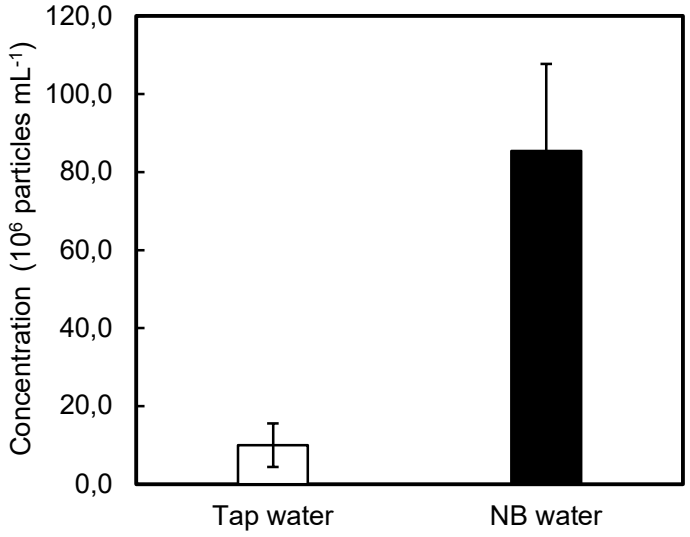

Fig. A2. Measurement of particle concentration before (Tap water) and after (NB water) NB generation.

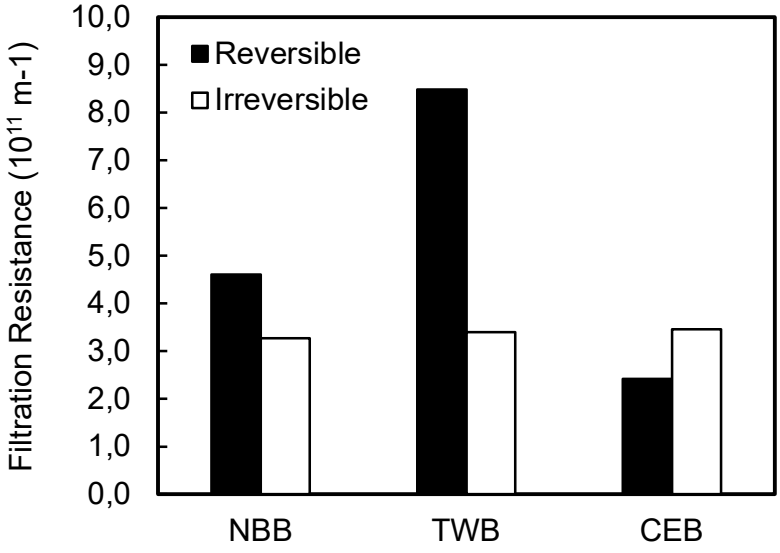

Fig. A3. Distributions of membrane filtration resistances at the termination of Run 2.

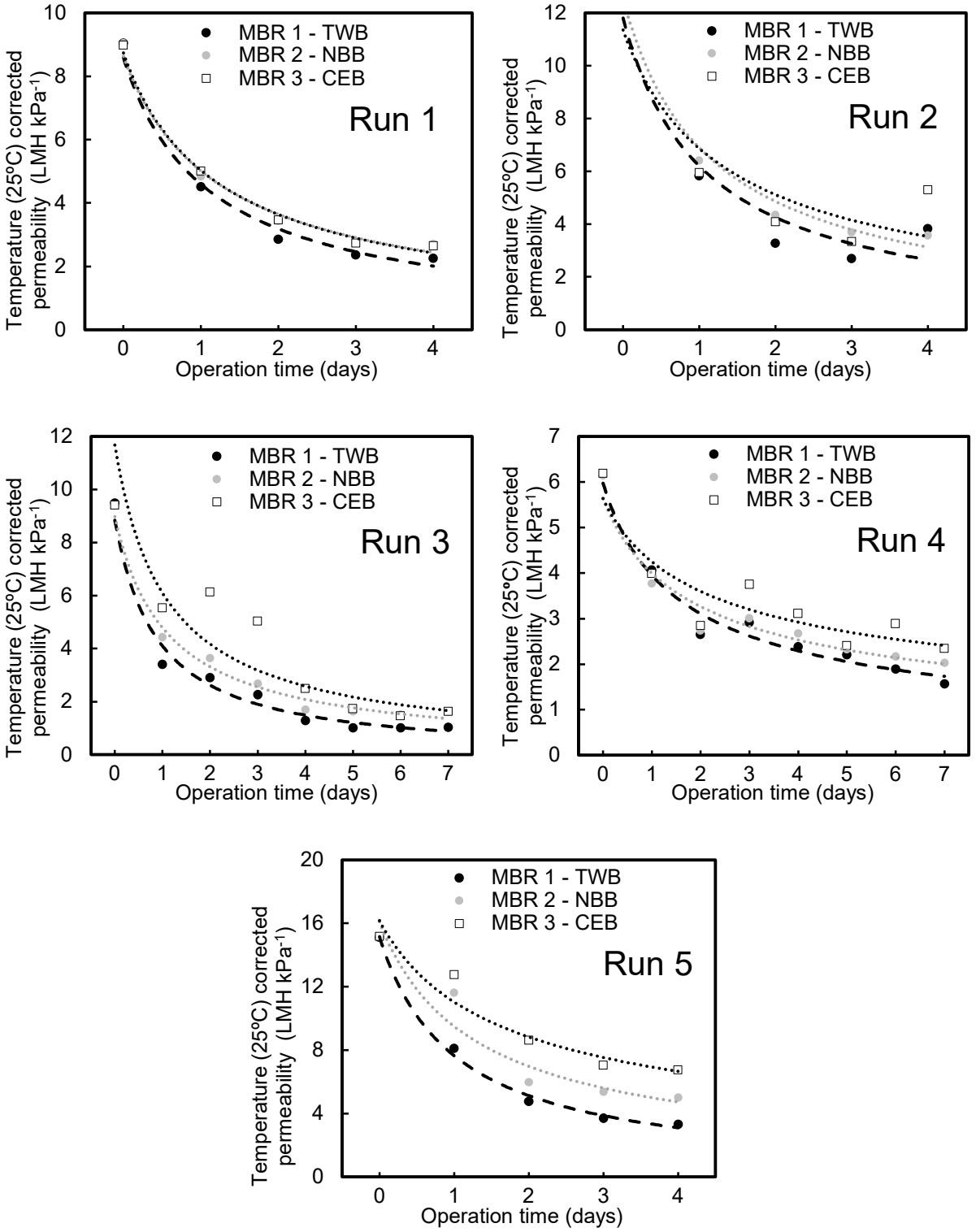

Fig. A4. Decreases in temperature-corrected permeability observed in Runs 1-5. Permeate fluxes: Run 1 (60 LMH), Runs 2-4 (50 LMH), Run 5 (80 LMH).

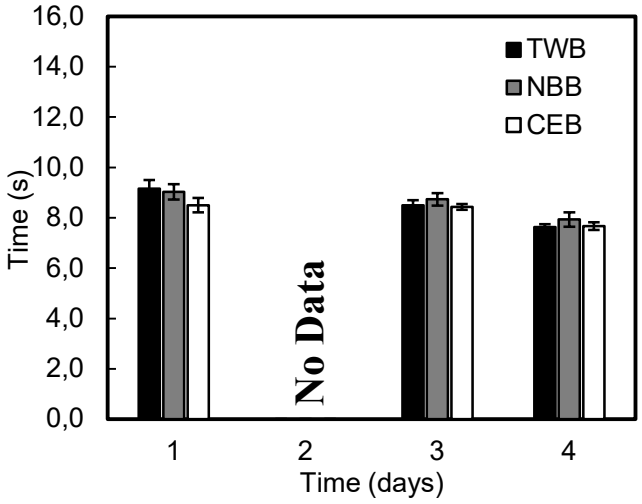

Fig. A5. Capillary suction times of sludge samples collected at the termination of the experiments.

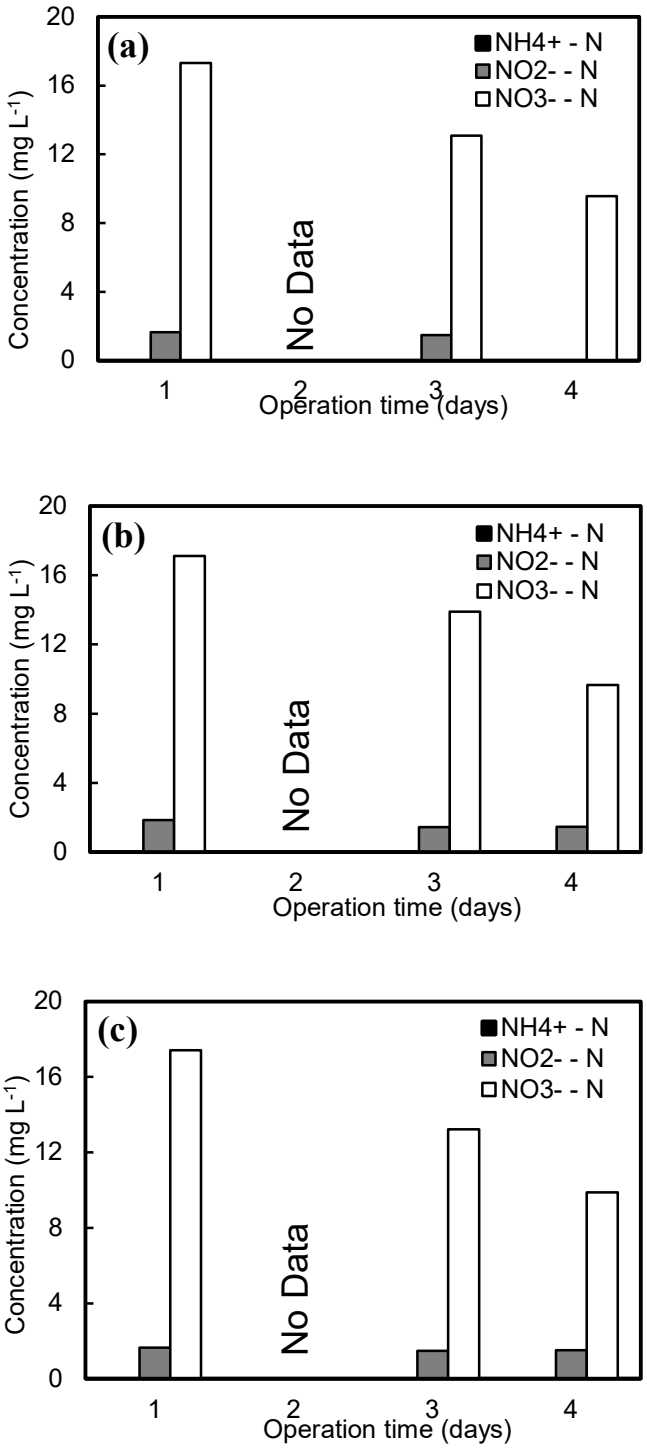

Fig. A6. Concentrations of nitrogen species in the permeate water samples. Fig. S4 (a): CEB. Fig. S4 (b): NBB. Fig. S4 (c): TWB.

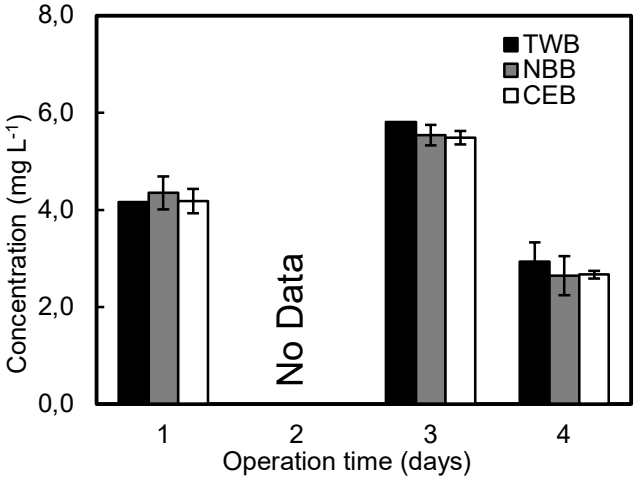

Fig. A7. TOC concentration in the permeate obtained in Run 5.

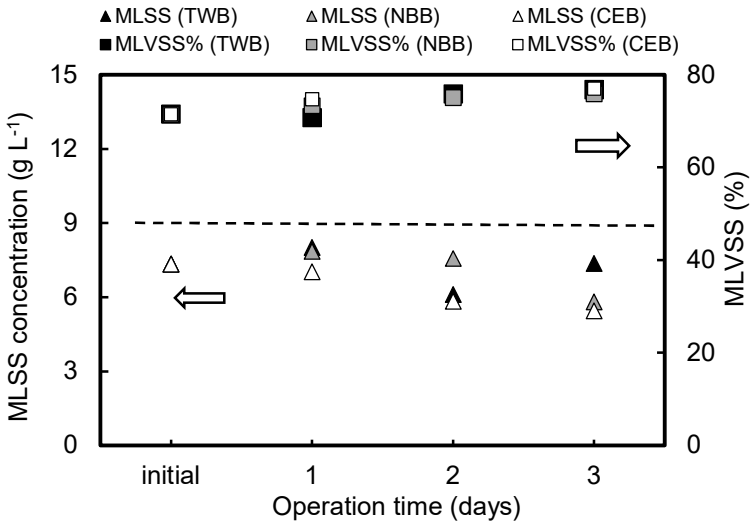

Fig. A8. MLSS concentration and MLVSS percentage of the sludge samples.

(a)

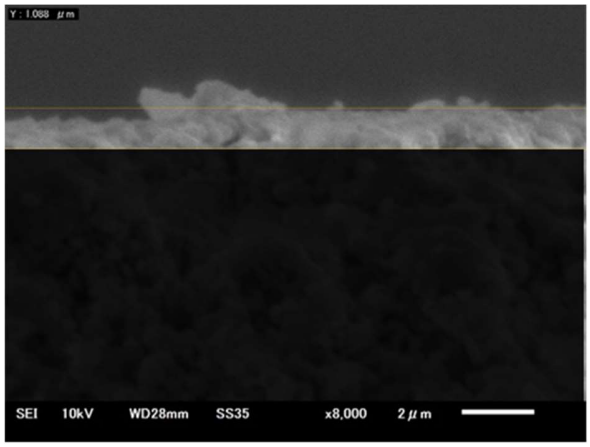
SEI 10kV WD28mm SS35 x8,000 2 μm

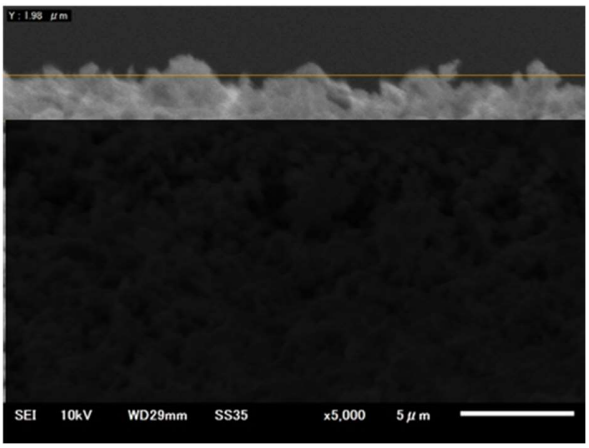
SEI 10kV WD29mm SS35 x5,000 5 μm

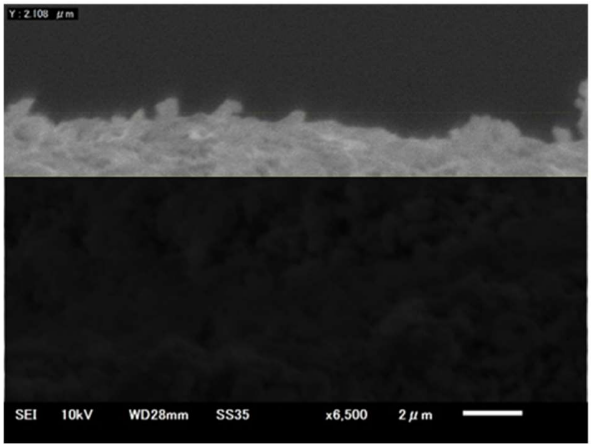
SEI 10kV WD28mm SS35 x6,500 2 μm

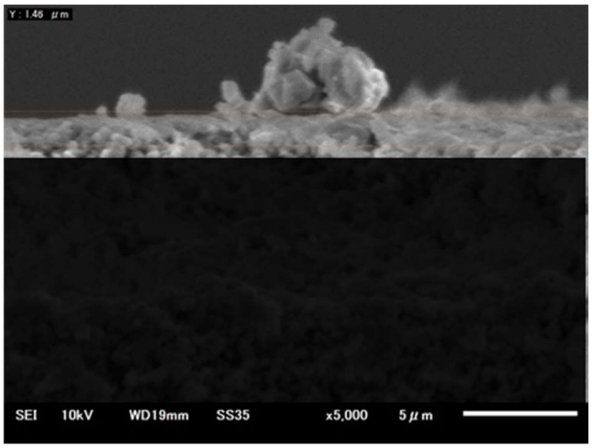
SEI 10kV WD19mm SS35 x5,000 5 μm

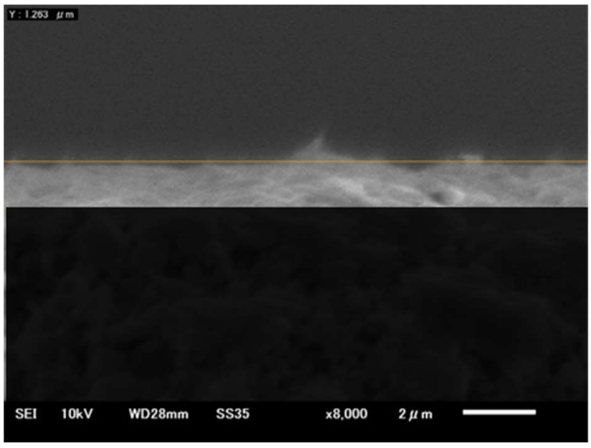
SEI 10kV WD28mm SS35 x8,000 2 μm

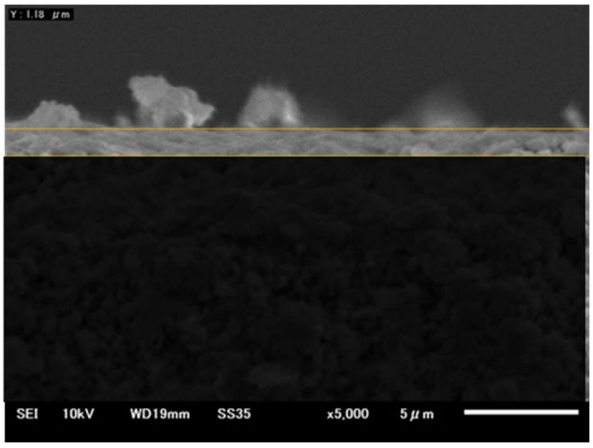
SEI 10kV WD19mm SS35 x5,000 5 μm

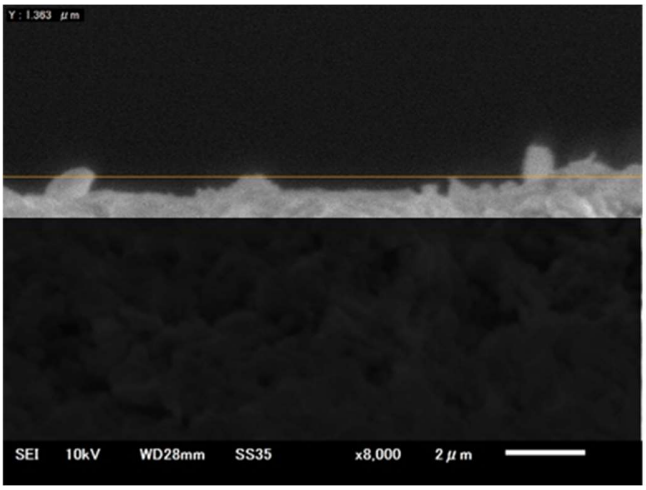
Y : 1.363 μm
SEI 10kV WD28mm SS35 x8,000 2 μm

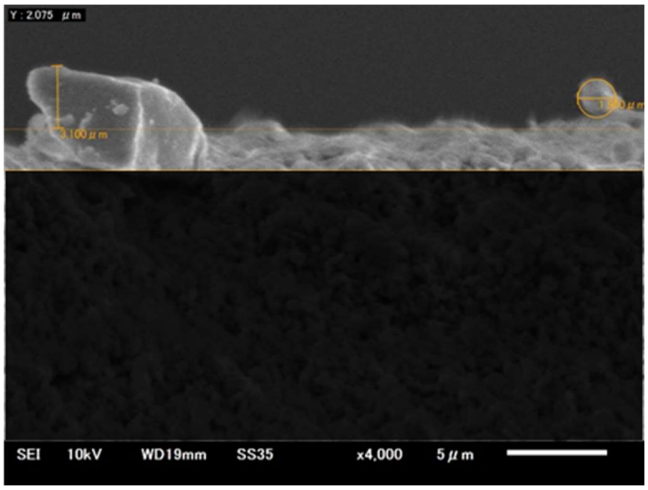
Y : 2.075 μm
SEI 10kV WD19mm SS35 x4,000 5 μm

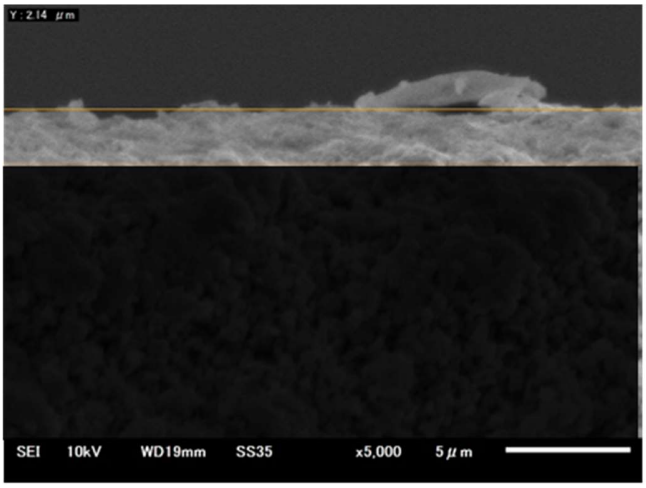
Y : 2.14 μm
SEI 10kV WD19mm SS35 x5,000 5 μm

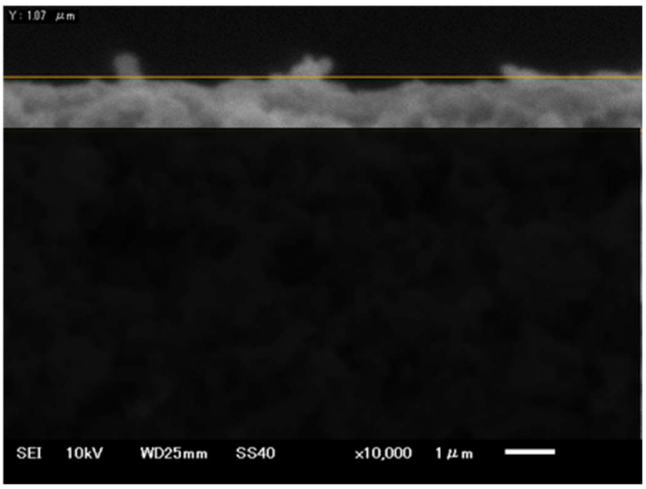
Y : 1.07 μm
SEI 10kV WD25mm SS40 x10,000 1 μm

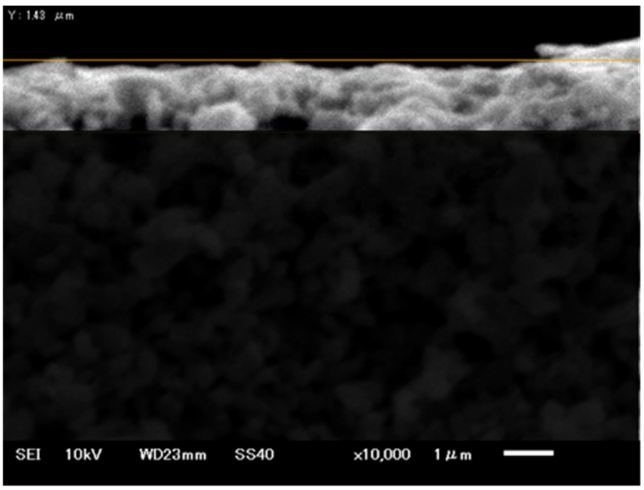
Y : 1.43 μm
SEI 10kV WD23mm SS40 x10,000 1 μm

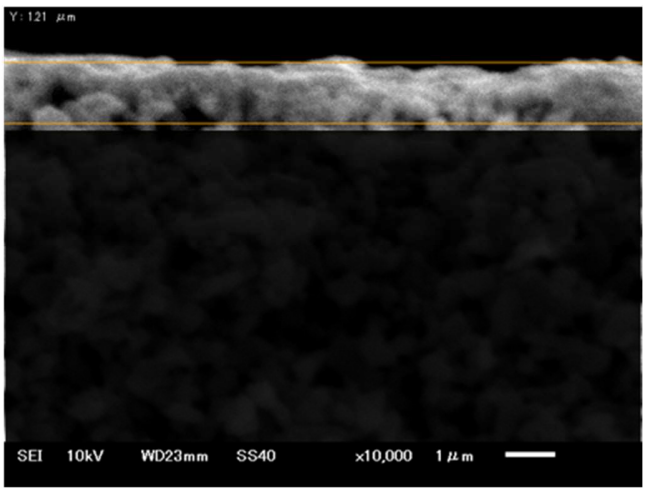
Y : 1.21 μm
SEI 10kV WD23mm SS40 x10,000 1 μm

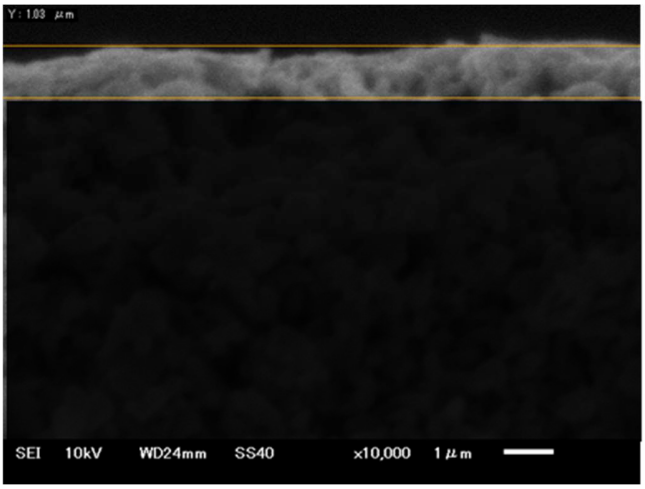
Y : 1.03 μm
SEI 10kV WD24mm SS40 ×10,000 1 μm

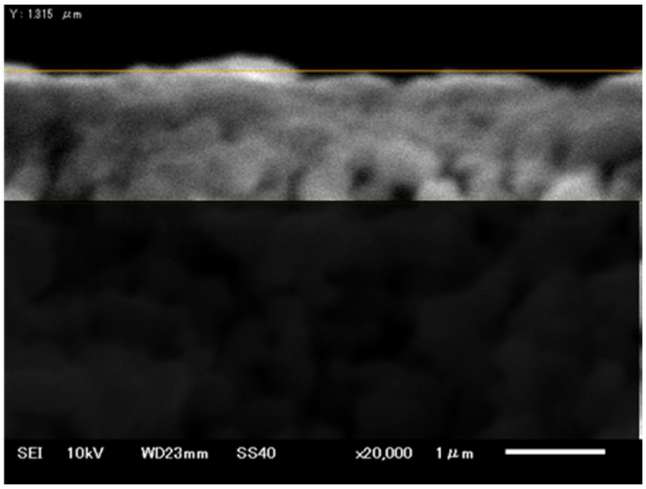
Y : 1.315 μm
SEI 10kV WD23mm SS40 ×20,000 1 μm

(b)

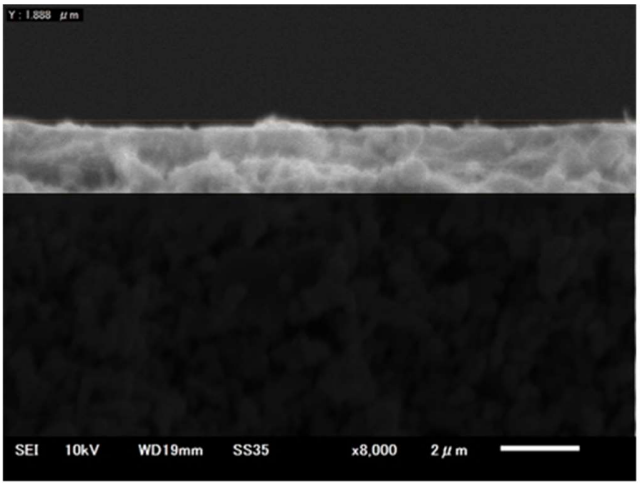
Y : 1.888 μm
SEI 10kV WD19mm SS35 ×8,000 2 μm

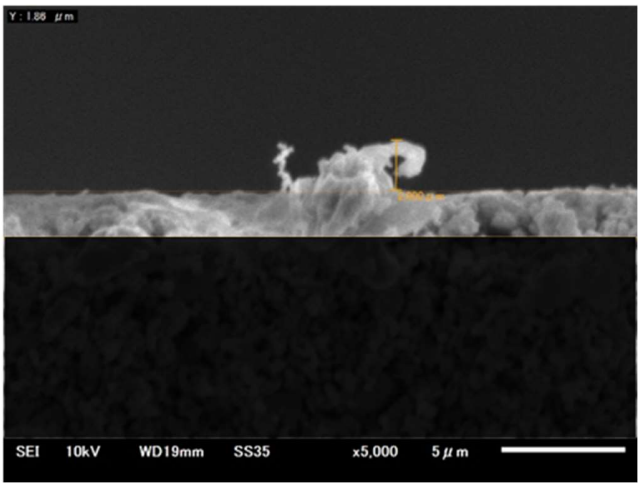
Y : 1.86 μm
SEI 10kV WD19mm SS35 ×5,000 5 μm

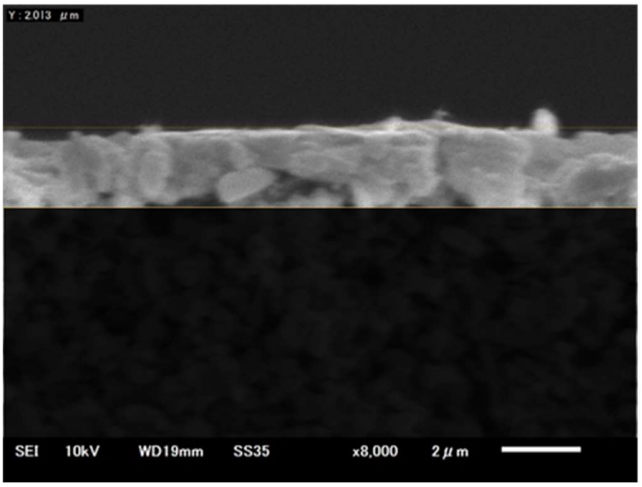
Y : 2.013 μm
SEI 10kV WD19mm SS35 ×8,000 2 μm

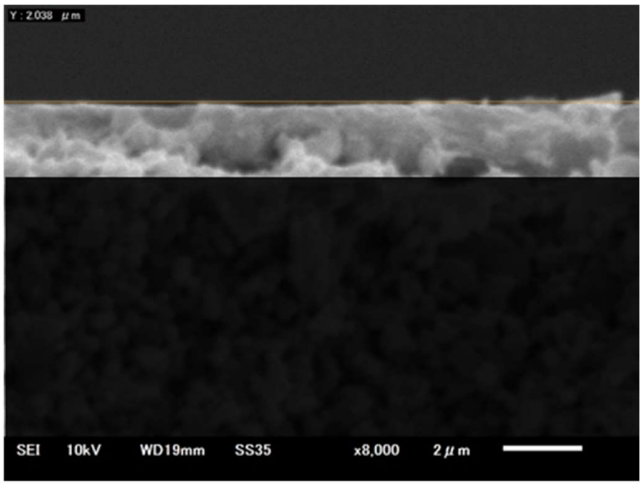
Y : 2.038 μm
SEI 10kV WD19mm SS35 ×8,000 2 μm

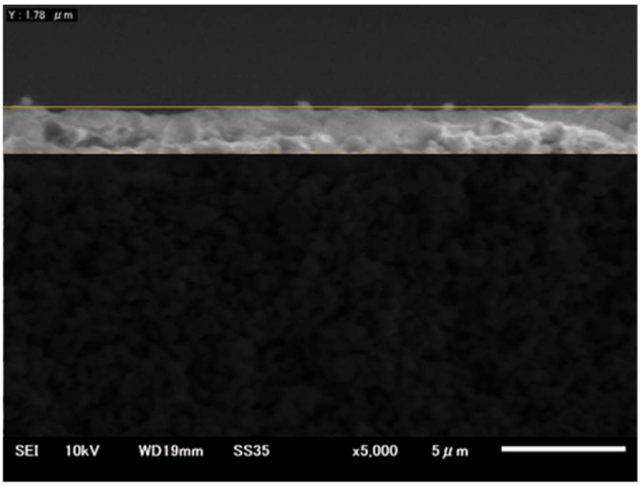
Y : 1.78 μm
SEI 10kV WD19mm SS35 x5,000 5 μm

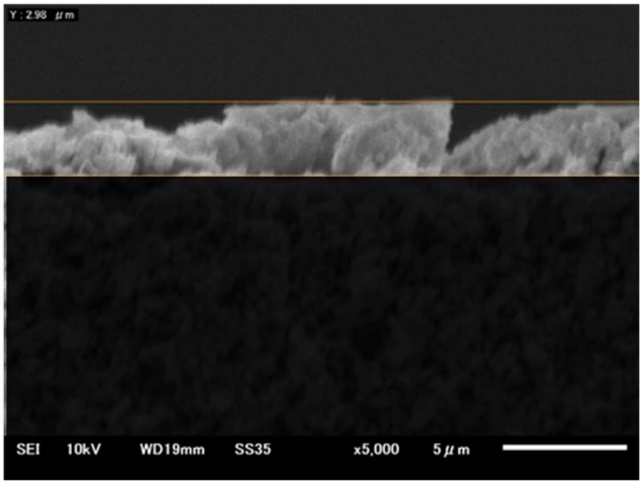
Y : 2.98 μm
SEI 10kV WD19mm SS35 x5,000 5 μm

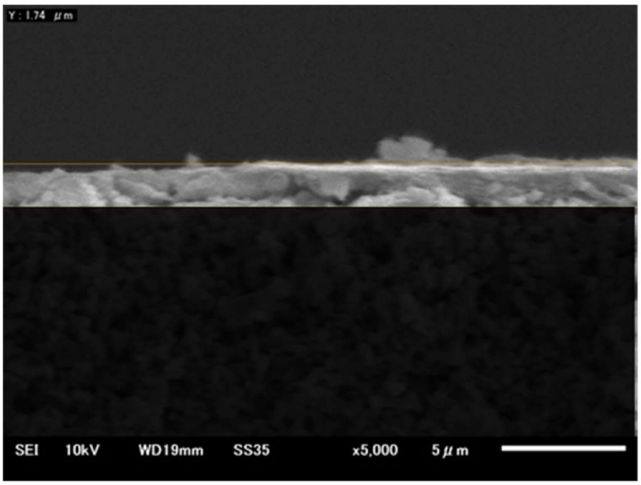
Y : 1.74 μm
SEI 10kV WD19mm SS35 x5,000 5 μm

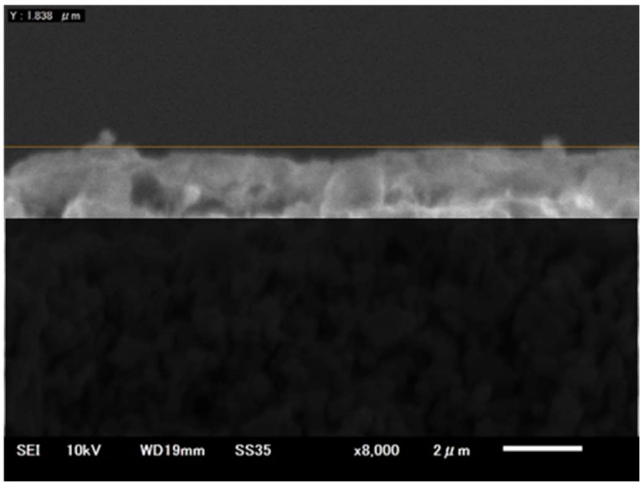
Y : 1.838 μm
SEI 10kV WD19mm SS35 x8,000 2 μm

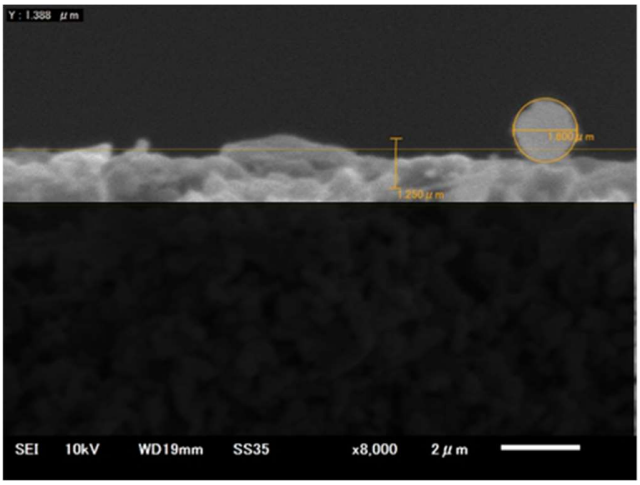
Y : 1.388 μm
SEI 10kV WD19mm SS35 x8,000 2 μm

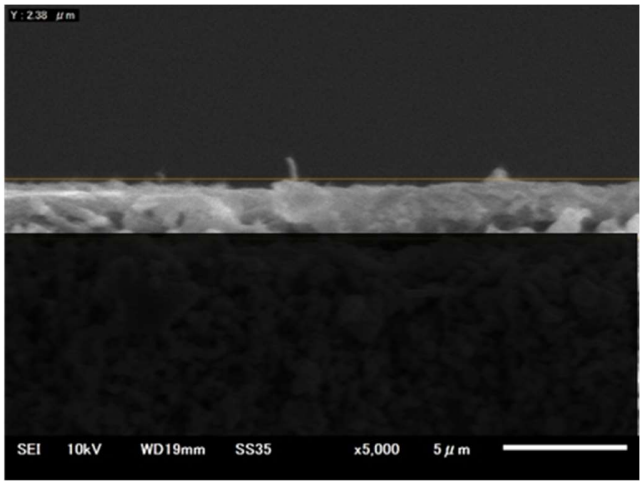
Y : 2.38 μm
SEI 10kV WD19mm SS35 x5,000 5 μm

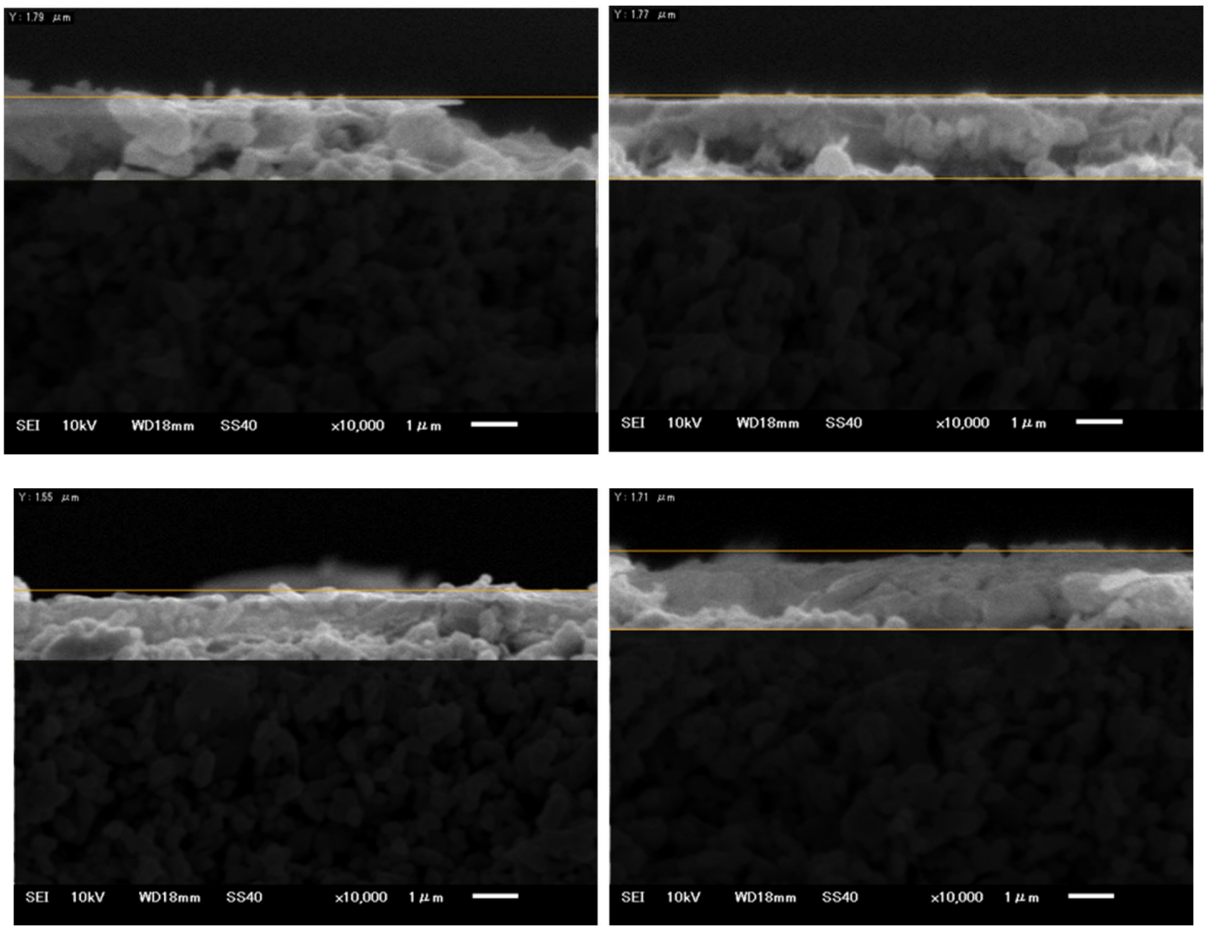

Fig. A9. SEM images of fouled membranes backwashed by NBB (a) and TWB (b).

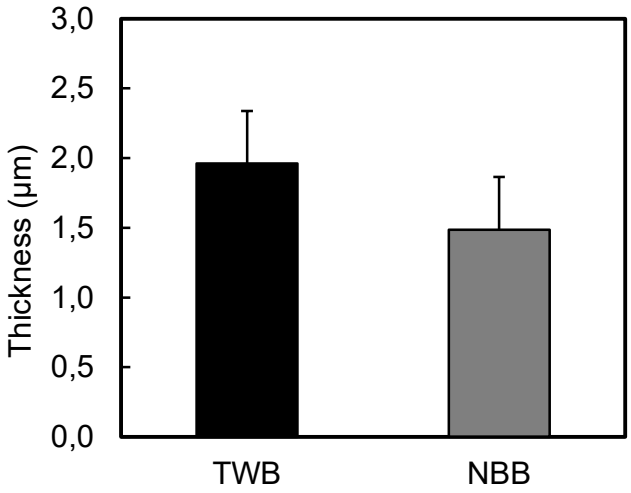

Fig. A10. Fouling layer thicknesses of a new membrane and fouled membranes backwashed by TWB and NBB

Table A1. F-Test Two-Sample for Variances. Thickness of the fouling layers on membranes cleaned by TWB and NBB

	NBB	*TWB*
Mean	1.4868	1.933529412
Variance	0.1541916	0.14968489
Observations	15	17
df	14	16
F	1.030107984	
P(F<=f) one-tail	0.472896342	
F Critical one-tail	2.373318231	

Table A2. t-Test: Two-Sample Assuming Equal Variances. Thickness of the fouling layers on membranes cleaned by TWB and NBB

	TWB	*NBB*
Mean	1.933529412	1.4868
Variance	0.14968489	0.154192
Observations	17	15
Pooled Variance	0.151788021	
Hypothesized Mean Difference	0	
df	30	
t Stat	3.236837508	
P(T<=t) one-tail	0.001472355	
t Critical one-tail	1.697260887	
P(T<=t) two-tail	0.002944711	
t Critical two-tail	2.042272456	

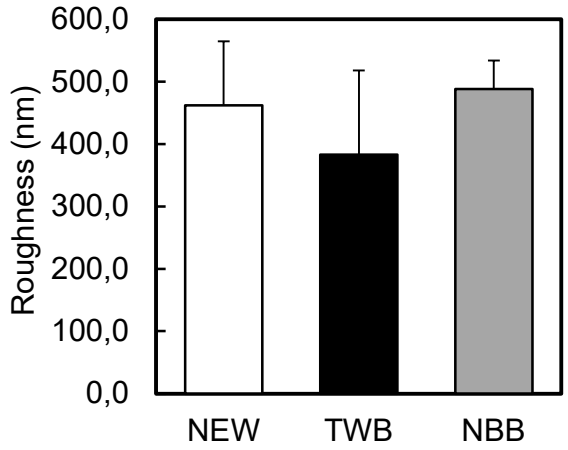

Fig. A11. Surface roughness of each membrane sample taken at the termination of the experiments.

APPENDIX B

Table B1: Experimental conditions in Runs 1-4.

	MBR	Temperature (°C)	MLSS (g L^{-1})	pH	CST (s^{-1})	TOC Removal (%)	T-N Removal (%)	Influent	
								TOC	T-N
Run 1 (Winter)	NaClO (pH=8.5)	12.0±0.5	7.9±0.3	7.0±0.2	10.1±0.3	74.7±6.8	35.4±6.8	19.1±8.2	27.1±10.8
	NB+NaClO (pH=8.5)	12.0±0.6	8.1±0.4	7.0±0.2	10.1±0.4	76.7±8.8	40.0±9.3		
	NB (pH=7)	11.7±0.5	8.0±0.5	6.9±0.2	10.1±0.3	75.0±10.5	40.7±9.3		
Run 2 (Winter)	NaClO (pH=12)	10.5±0.2	7.6±0.5	7.2±0.2	15.6±2.6	74.7±1.7	40.3±6.9	18.3±0.9	26.1±3.8
	NB+NaClO (pH=12)	10.6±0.2	7.5±0.6	7.2±0.2	15.0±2.1	74.3±1.4	40.2±9.6		
	NB+NaClO (pH=8.5)	10.5±0.4	7.5±0.7	7.2±0.2	14.8±2.1	75.3±1.9	42.4±8.0		
Run 3 (Autumn)	NaClO (pH=4)	21.1±0.1	5.9±0.4	6.3±0.3	10.6*	79.8±13.3	#	29.2±19.4	19.6±16.1
	NB (pH=4)	20.9±0.1	5.8±0.2	6.7±0.3	12.8*	81.6±11.1	#		
	HCl (pH=4)	20.5±0.2	5.6±0.1	6.4±0.4	11.8*	81.7±6.3	#		
Run 4 (Winter)	NaClO (pH=4)	9.9±0.4	7.7±0.3	6.9±0.1	12.3±1.4	80.5±3.6	37.1±11.6	25.5±9.9	24.5±1.9
	NB+NaClO (pH=4)	8.3±3.6	8.0±0.4	6.9±0.1	12.5±1.2	80.5±3.0	35.6±3.9		
	NB+NaClO (pH=8.5)	9.7±0.4	7.5±0.5	6.9±0.1	12.8±1.0	81.5±3.1	35.9±4.8		

1

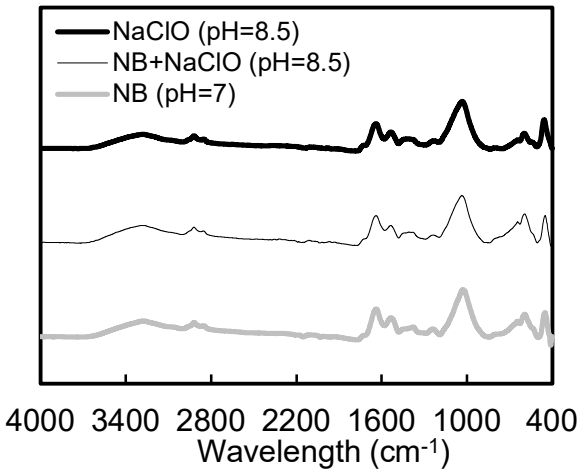

Fig. B2. FT-IR spectra of gel layer samples on the membrane surface collected at the termination of Run 1.

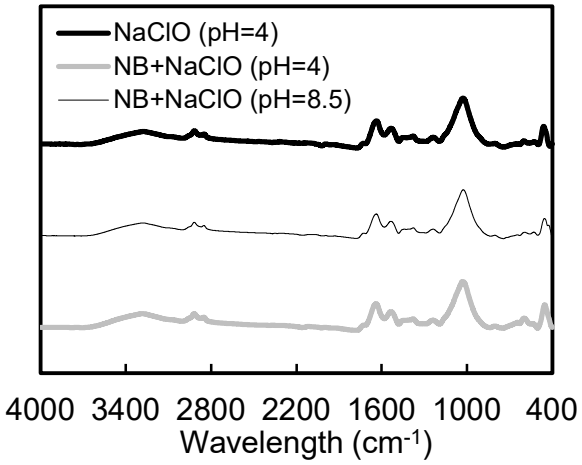

Fig. B3. FT-IR spectra of gel layer samples on the membrane surface collected at the termination of Run 4.